UNIMORE
UNIVERSITÀ DEGLI STUDI DI MODENA E REGGIO EMILIA

UNIVERSITÀ DEGLI STUDI
DI MODENA E REGGIO EMILIA

PhD programme in
Clinical and experimental medicine (CEM)
– Medicina clinica e sperimentale

Ciclo XXXVIII

Preclinical characterization of platelet-based therapies for oncological and regenerative applications

Candidate: Gaia Gavioli

Supervisor: Dr. Lucia Merolle

Co-Supervisor: Prof. Stefano Luminari

PhD School Coordinator: Prof. Marco Vinceti

SUMMARY

Abstract

Platelets are small, anucleate cell fragments derived from megakaryocytes in the bone marrow and playing a pivotal role in multiple pathophysiological processes, including coagulation, wound healing, immune modulation and cancer progression. Clinically, platelet transfusions are routinely employed to control bleeding and manage thrombocytopenia, particularly in oncology patients. To address the limitations of room temperature storage, platelet cryopreservation has been adopted as an alternative strategy; however, this approach is not without challenges. The freeze-thaw process induces platelet activation, leading to the release of significant quantities of growth factors and extracellular vesicles, alongside alterations in their coagulation profile. However, beyond their well-established function in haemostasis and coagulation, platelets also play a pivotal role in wound healing. Their regenerative potential is largely attributed to the diverse array of growth factors and cytokines stored within their α-granules. As such, platelet concentrates have become a cornerstone of regenerative medicine, widely used to support tissue repair and accelerate healing processes. Platelet-Rich Plasma (PRP) is the most commonly utilised platelet-derived product, with broad clinical applications including the treatment of chronic wounds, musculoskeletal injuries, oral and maxillofacial surgeries, and various dermatological conditions.

This thesis presents a comprehensive investigation into the multifaceted roles of platelets across diverse biomedical contexts. The study first examined the coagulative functionality of platelets following cryopreservation, with particular emphasis on how variations in thawing time influence platelet viability, activation state, and their capacity to support clot formation. The post-thaw biological activity of these platelets was further evaluated by analysing their influence on cancer cell behaviour *in vitro*, providing insights into potential alterations in tumour–platelet interactions after cryostorage. Beyond their haemostatic role, the regenerative potential of platelets was explored through their secretion of bioactive molecules that promote wound healing and tissue repair. Given the widespread clinical use of platelet-rich plasma (PRP) for managing various wound types, this work also investigated how differences in PRP preparation and application methods influence the regenerative responses of key skin cell populations, such as fibroblasts and keratinocytes. The primary aim of this work was to investigate the impact of cryopreservation on the biochemical and functional characteristics of apheresis cryopreserved platelets, in order to optimize transfusion timing and assess their effects on cancer cell behaviour *in vitro*. This analysis was intended to elucidate their potential utility as a transfusion resource for onco-haematological patients. The secondary objective was to characterize and compare the regenerative capabilities of buffy coat–derived (BC) and apheresis-derived (Aphe) platelet-rich plasma (PRP) preparations. Together, these findings are expected to offer significant contributions toward refining transfusion practices and expanding the

therapeutic applications of platelet products, thereby promoting their integration into personalized strategies for haemostasis and tissue regeneration.

1 INTRODUCTION

1.1 Platelets

Platelets, also known as thrombocytes, are small, anucleated, disc-shaped blood cells measuring 2-4μm in diameter[1]. Their average number is typically between 150 and 350 × 10^3 platelets/μl of blood and they have an *in vivo* half-life of about 5-7 days[2], after which they are removed from circulation by the spleen and liver[3]. Normally, platelets fluctuate in the blood stream close to the vessel walls as a non-thrombogenic cells and, after being activated, they change shape and develop pseudopodia. This process also involves platelets' granules and platelet derived extracellular vesicles (P-EVs) release. Platelet are mostly known for the critical role they play in maintaining haemostasis but, because of their secretory nature, they are involved in different pathophysiological processes such as wound healing, inflammation and cancer progression.

1.2 Platelets structure

Platelets consist of different area that can be conceptually divided in peripheral zone, sol-gel zone, organelle zone and canalicular systems[4] (see Figure 1). The peripheral zone presents a lipid bilayer on which surface platelet expose specific molecules and receptors that define their interactions. Right under, there is a submembrane area containing an intricate system of actin filaments important for the shape changing and translocation of receptors on platelet surface after activation. The sol-gel-zone is a transparent and viscous matrix containing microtubules and microfilament important for the maintaining of the discoid shape. After activation, actin filaments stretch the microtubules moving platelet granules to the centre of the cells before their secretion. These granules define the nature of platelets as secretory cells and are confined in which is called the organelle zone. There are three main types of platelet secretory organelles that will be described in the next chapter: α-granules, δ-granules (also called dense-granules), and lysosomes. The canalicular system consist of a dense tubular system and surface-connected open canalicular system. The latter is an internal protrusion of the surface membrane that absolve the important function of transporting granular contents from platelet centre to the peripheral zone for them to be released after activation[5]. These systems are also important during clot formation, after platelet adhesion to the vessel they provide membrane parts needed for platelet change of shape and protrusion formation[6]. The dense tubular system is separated from the open canalicular system and is a residuum of megakaryocyte's endoplasmic reticulum kept during thrombopoiesis[7].

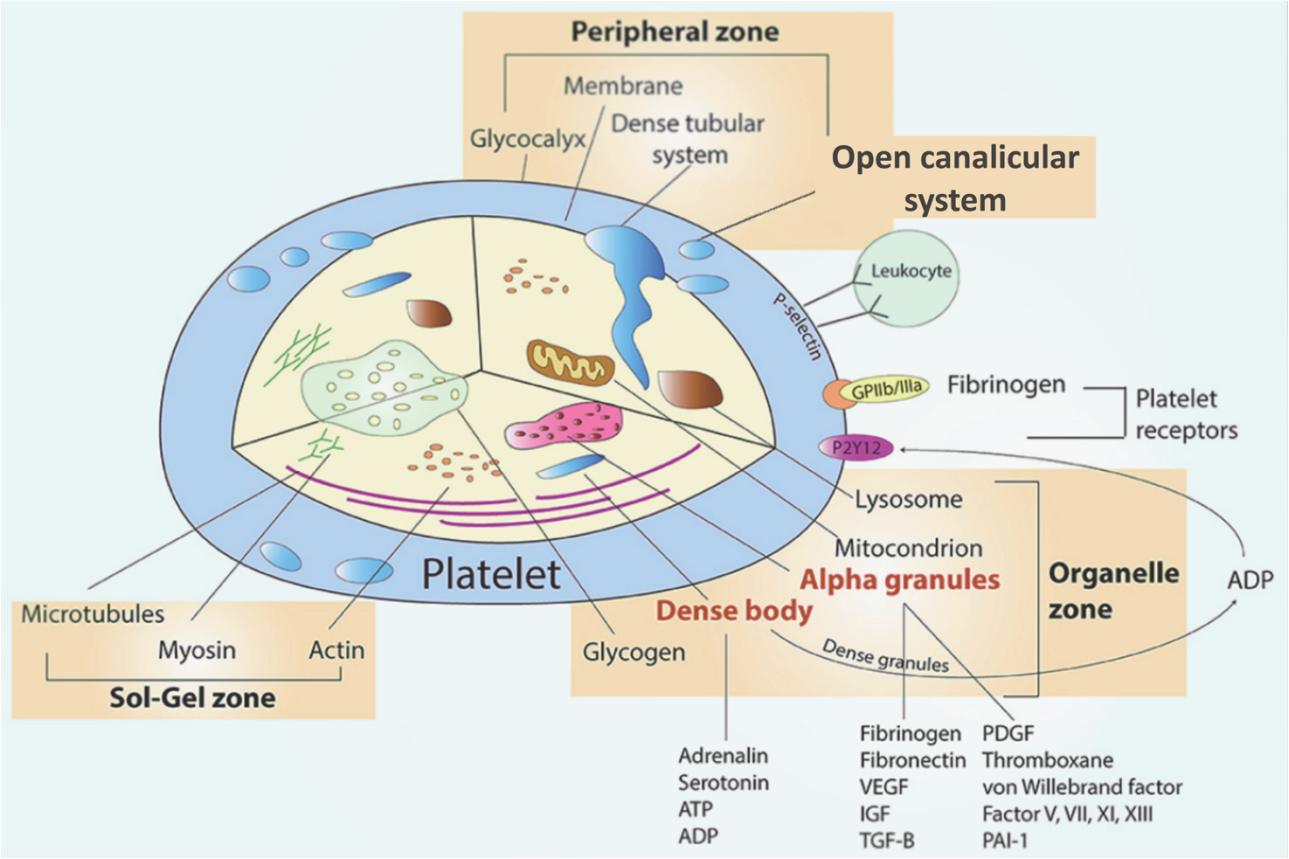

Figure 1. Overview of Platelet Structure. The image illustrates the internal composition of a platelet, highlighting the peripheral zone, sol-gel zone, and organelle zone and the open canalicular system. Image from Ostrowska et al[8].

1.3 Platelets as secretory cells

As anticipated before, platelets contain different type of granules that are released by exocytosis defining platelet nature as secretory cells. These granules are defined by their morphology, molecules content, development process and exocytosis.

1.3.1 α-granules

The most abundant granules are α-granules, approximately 80 vesicles of about 200-500nm in diameter in each mature platelet[9]. Most of the molecules released by platelet derive from α-granules and are inherited from megakaryocyte during thrombopoiesis (for example coagulation factor V (FV), thrombospondin, P-selectin (CD62), Von Willebrand Factor (VWF))[10]. However, platelets has the peculiar capacity to take up molecules from the environment via endocytic pathways and store them into these granules[11]. Most of the molecules found in α-granules are coagulation factors, adhesive molecules, growth factors, angiogenic and immune mediators.[12,13] A variety of protein types have been identified encompassing both surface proteins and soluble proteins. After platelet activation and

granule release, membrane associated proteins are transported on the platelet surface, while soluble proteins are released into the environment. The majority of membrane bound proteins are already settled on platelet surface during the resting phase[13] while others like P-selectin are only expressed after activation. P-selectin, in fact, is commonly used as a specific platelet activation marker in flow cytometric analysis[14]. Following platelet activation, fibrinogen and VWF are released from α-granules to promote platelet-platelet and platelet-endothelial cell interactions. In addition, also fibrinogen and collagen receptors support platelet adhesion[15,16]. α-granules are also known to mediate the interaction between platelets and immune system by releasing pro and anti-inflammatory molecules, immune modulating factors inducing chemokine secretion and the recruitment and activation of inflammatory cells[17,18]. It has been demonstrated that soluble complement regulators such as Factor H[19,20] and C1 inhibitor[21,22] are also stored in α-granules. As slightly anticipated, platelets play a role in cancer progression releasing proangiogenic factors from α-granules such as vascular endothelial growth factor (VEGF), platelet derived growth factor (PDGF), transforming growth factor (TGF-β), epidemic growth factors (EGF), endothelial cell growth factor (ECGF) and insulin-like growth factor (IGF)[23] but also inhibitors of angiogenesis like thrombospondin-1, CXCL4, angiostatin and endostatin[24]. The assumption is that different pro and anti-angiogenic factors are released agonist specifically[25]. By the secretion of these mitogenic factors, α-granules also play an important role in wound healing.[26,27]

1.3.2 δ-granules (or dense granules)

Normally, each platelet contains only 3 to 8 δ-granules with a diameter of 200-300nm[28]. They contain serotonin, calcium, magnesium, pyrophosphate, potassium, histamine[29]. Elevated concentrations of adenosine triphosphate (ATP) and adenosine diphosphate (ADP)[28], which play a crucial role in platelet activation, have also been found. ADP and serotonin function as potent platelet agonists at the site of vascular injury, thereby promoting the recruitment of circulating platelets[30]. Other than haemostasis and thrombosis, δ-granules participate in platelet aggregation and clot formation by releasing serotonin[31] which also support neutrophils recruit to inflammation site[32].

1.3.3 Lysosomes

Human platelet also contain up to 2 lysosomes, which role remains still largely unknown[4]. They bear protein degrading enzymes such as cathepsins, elastase, and collagenase; carbohydrate degrading enzymes such as glucosidase and galactosidase; and acid phosphatase as phosphate ester cleaving enzyme[7].

1.3.4 Granule release

Different mechanisms of secretion have been described. After platelet activation, platelet shape changes and granules can accumulate in the centre of the cell fusing with one another[33] before fusing with the open canalicular system and realising their content into it and then to the extracellular space[34]. Differently, granules can directly fuse themselves with the plasma membrane realising their content to the extracellular space[33]. Both of these mechanisms are mediated by Soluble N-ethylmaleimide-sensitive factor attachment protein receptors (SNAREs) on platelet granules, vesicular SNAREs (vSNAREs) and target SNAREs (tSNAREs), associated with the plasma membrane and the open canalicular system, mediating the fusion of platelet granules with the different structures involved[35]. The function of SNAREs in platelet granule secretion is subject to regulation by chaperone proteins, in particular the N-ethylmaleimide sensitive fusion protein (NSF), a Mg2þ-dependent ATPase[36,37].

1.4 Thrombopoiesis

Platelet production process[38] is known as thrombopoiesis and is comprised of three distinct stages: differentiation of hematopoietic stem cells into megakaryocytes, endomitosis with polyploid megakaryocytes formation, and platelet release[39] (see Figure 2). This process is of significant importance in ensuring the stability of platelet count. Its dysregulation leads to the development of platelet-related disorders such as thrombocytopenia (low platelet count), which can cause excessive bleeding and bruising. This condition can result from bone marrow disorders, chemotherapy or immune disorders. Conversely, elevated platelet counts (thrombocytosis) increase the risk of abnormal clot formation, which can result in stroke or heart attack.

Megakaryocytes, the precursor of platelets[40], originate from haematopoietic stem cells (HSC) in the bone marrow [41]. Thrombopoietin is the key regulator of thrombopoiesis, controlling each stage of the process[42]. This hormone is primarily produced by the liver in response to the interaction between interleukin-6 (IL-6) and GPIbα, the VWF platelet receptor, stimulating platelet production during systemic inflammation. Its signaling is mediated through the thrombopoietin receptor (c-MPL), which is expressed from HSCs to platelets[39]. Upon receiving the thrombopoietin signal, megakaryocytes initiate endomitosis, undergoing multiple cycles of DNA replication without cell division and resulting in enlarged cytoplasmic body and polyploidy[43,44]. During this process, the cell cycle remains incomplete, with mitosis repeatedly halting in late anaphase. This disruption affects both karyokinesis (nuclear division) and cytokinesis (cytoplasmic division), preventing full cell separation. Alongside endomitosis, platelet-specific granules are synthesized and accumulated, they will be the mediators of platelet functions, as anticipated before. After migrating to the vascular niche,

mature polyploid megakaryocytes extend long, branching pro-platelets into the sinusoidal blood vessels of the bone marrow, under the influence of β1-tubulin[45–47]. During this process, microtubules facilitate the transport of granules containing platelet-specific proteins into the developing pro-platelets[48] which are outgrowths of cells that consist of vesicles linked by cytoplasmic bridges. Once released in the vascular space, they undergo a rapid and spontaneous transformation into pre-platelets at first and then, within the lungs, into mature platelets circulating in the bloodstream[49] and ready to fulfil their functions.

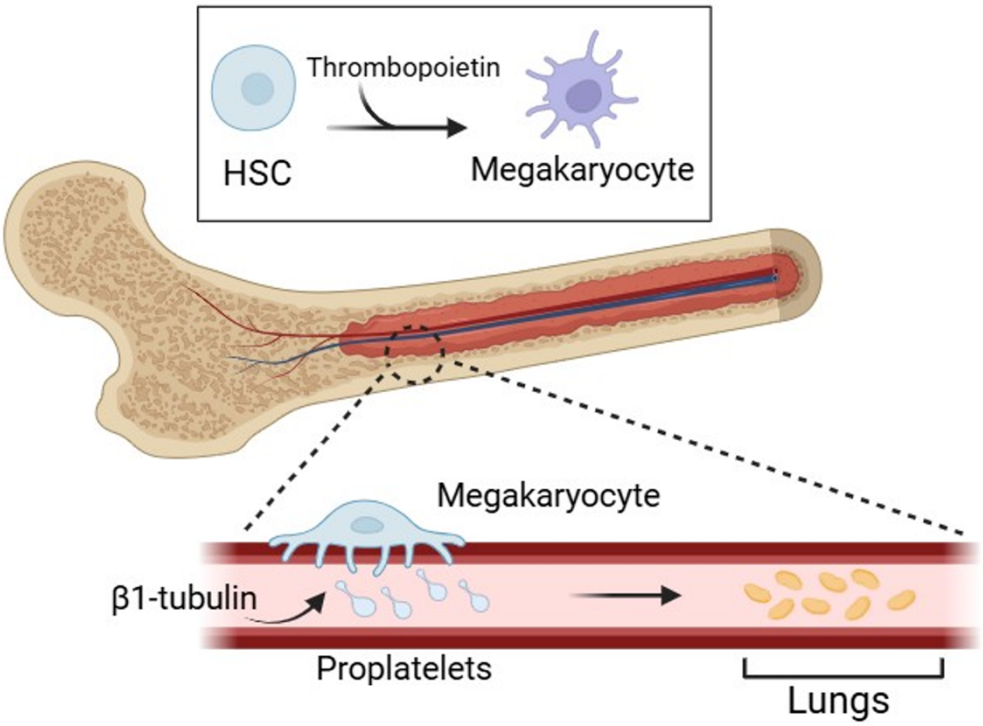

Figure 2. Thrombopoiesis schematic illustration. Image created with Biorender.

1.5 Platelet in haemostasis and thrombosis

Haemostasis is defined as a complex process that ensures the maintenance of blood flow under physiological conditions and prevents significant blood loss after vascular injury. This process necessitates the intricate interplay of numerous physiological pathways, encompassing blood vessels and endothelial cells, platelets and coagulation factors and inhibitors.

Under normal conditions, blood components flow unhinged through the circulatory system. The endothelial barrier releases non-thrombogenic factors that inhibit platelet activation, such as heparan sulphate which activates antithrombin and thrombomodulin, both coagulation inhibitors[50]. On the contrary, the subendothelial layer is highly thrombogenic: it contains different factors involved in platelet adhesion such as collagen, VWF, laminin, thrombospondin and vitronectin[51]. Following trauma or during inflammation, disruption of the vascular endothelium leads to the release of VWF

and collagen, along with the exposure of tissue factor (TF) on the surface of endothelial cells. Concurrently, platelets become activated and undergo a morphological transformation, adopting an irregular shape and extending numerous pseudopodia. This structural change increases their surface area, thereby enhancing platelet–platelet interactions and promoting the formation of a larger and more stable platelet plug. During this activation process, platelets also release the contents of their intracellular granules into the circulation, contributing further to haemostatic and inflammatory responses.

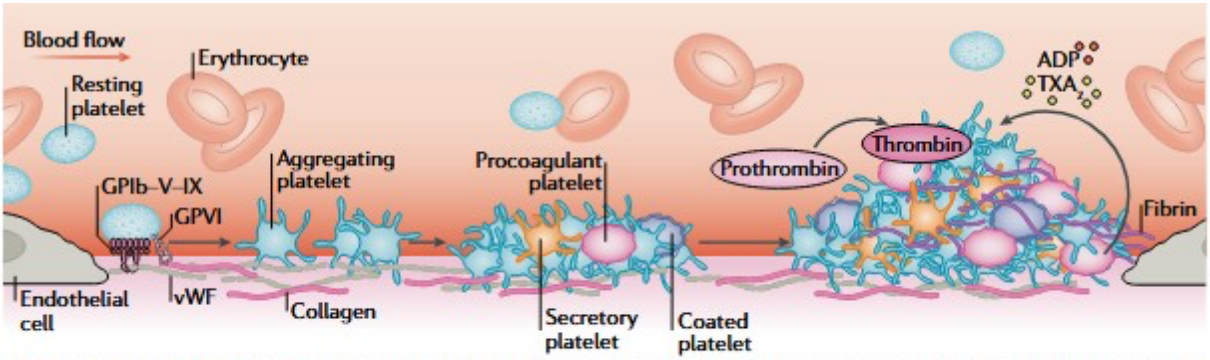

Figure 3. Schematic diagram depicting the various phases of thrombus formation. Image from Paola E. J. van der Meijden et al[1].

Usually, the coagulation pathway is classified into extrinsic, intrinsic and common pathways. This model is useful for the interpretation of *in vitro* coagulation tests (such as prothrombin time (PT) or activated partial thromboplastin time (aPTT)) but does not take into consideration the key role played in the coagulation process by the endothelial cell surface and it does not predict which patients are at risk of bleeding or thrombosis[52]. Hoffman et al.[53] conceptualized the cell-based model of haemostasis in the early 00‘, incorporating the cellular contribution to the coagulation process. Since then, the classical pathway model has been superseded by this model, which proposes that coagulation occurs on different surfaces and takes place over three distinct yet concurrent stages: initiation, amplification, and propagation.

1.5.1 The cell-based model: Initiation

The primary event that characterizes *in vivo* coagulation is the exposure of TF[54] on endothelial cells surface after vessel injury. With the binding of factor VIIa (FVIIa), the forming TF:FVIIa complex catalyses the activation of factor IX (FIX) and X (FX)[55]. Activated FX, then, will transform a tiny amount of prothrombin in thrombin, one of the strongest platelet activators. At this point, however, the thrombin produced is not enough to sustain the coagulation process and clot fibrinogen[56] but, it will activate factor VIII (FVIII), V (FV) and XI (FXI)[57] in a positive feedback leading to the amplification of the signal[52].

1.5.2 The cell-based model: Amplification

The amplification stage takes places on platelet surface. Using GP1a/VI[52] and GP1b/V/IX[58,59] receptors, platelets adhere respectively to collagen and VWF on the subendothelial tissue, exposed to blood after being injured. This interaction strengthens platelet adhesion to the site of injury and, together with the production of thrombin during the initiation stage, increases platelet activation. Degranulation of activated platelet contributes to the release of procoagulant material, including FVIII and FIX. Moreover, ADP, serotonin and thromboxane A2 will activate other platelets amplifying the signal and inducing the release of FV from α-granules.

1.5.3 The cell-based model: Propagation

The extensive production of thrombin is based on the formation of two complexes on platelet surface: FVIIIa:FIXa (intrinsic tenase) and FVa:FXa (prothrombinase)[59]. In combination with calcium ions[52] released from δ-granules, these complexes assure the catalysation of prothrombin in thrombin leading to a massive production of the latter (thrombin burst)[59]. Thrombin generated during these stages catalyzes the conversion of soluble fibrinogen into insoluble fibrin. The resulting fibrin strands are deposited at the site of injury, reinforcing the initial platelet plug and stabilizing it into a mature fibrin clot, using the αIIβIII receptor to bind platelet[60].

Stalker et al[61]. have proposed a novel model of thrombus structure, demonstrating that two distinct platelet populations are present in a growing thrombus *in vivo*. The platelet population is comprised of a 'core' of more stable and activated P-selectin-expressing platelets, and a more fragile 'shell' of less activated, P-selectin-negative platelets. While the formation of the core appears to rely heavily on thrombin and contact-dependent activation, the recruitment of platelets to the shell is critically dependent on ADP signalling[61].

1.5.4 Anticoagulation mechanisms

Following the resolution of vascular injury, it is essential to restore normal blood flow, which requires the removal of the fibrin clot. This is achieved through fibrinolysis, an enzymatic process that is activated in parallel with coagulation to limit excessive clot formation. Dysregulation of fibrinolysis can result in either a predisposition to bleeding or the development of thromboembolic events[51]. Upon vascular injury, tissue plasminogen activator (t-PA) and urokinase are released into the circulation, promoting the conversion of plasminogen to plasmin[62]. Plasmin subsequently degrades fibrin into fibrin degradation products (FDPs)[59] which serve as clinical markers for assessing fibrinolytic activity[63]. The main regulators of fibrinolysis are plasminogen activator inhibitor-1 (PAI-1)[64] and α2-antiplasmin[52].

Additional critical mechanisms regulating haemostasis involve inhibitors of coagulation factors that act directly on the coagulation cascade. Antithrombin (AT), a serine protease inhibitor, suppresses thrombin activity and its generation by targeting FIX and FX[65]. The activity of AT is significantly enhanced upon binding to heparan sulphate present on the endothelial cell surface[66]. Another key regulator is the tissue factor pathway inhibitor (TFPI), which attenuates thrombin generation during the initiation phase by inhibiting of FX, FVII, and TF[67]. Furthermore, protein C, also a serine protease, inactivates FV and FVIII during the propagation phase of coagulation, with protein S and phospholipids serving as essential cofactors. Activation of the protein C pathway is initiated by the interaction of thrombin with thrombomodulin on the endothelial surface[51].

1.5.5 Clotting Tests

The most widely utilized coagulation assays include prothrombin time (PT), activated partial thromboplastin time (aPTT), thrombin time (TT) and fibrinogen levels. PT assesses the time required for clot formation following the addition of tissue factor to recalcified citrated plasma. The assay entails the introduction of thromboplastin into the patient's plasma sample, with clot formation serving as the endpoint. PT is commonly employed as a screening test to identify deficiencies in coagulation factors, including fibrinogen and factors II, V, VII, and X[68]. To address inter-laboratory variability due to differences in thromboplastin reagent sensitivity, the World Health Organization (WHO) introduced the International Normalized Ratio (INR) as a standardized measure[69]. aPTT is a coagulation screening test used for monitoring unfractionated heparin (UFH) therapy, used in emergency to inhibit clot formation. The test is affected by the levels of different factors, such as FVIII, IX, X, XI, XII, II and fibrinogen[68] and by numerous pre-analytic and analytic variables unrelated to the anticoagulant effect of UFH, further strengthen existing evidence of the limitation of this test[70]. TT assesses the conversion of fibrinogen to fibrin by introducing exogenous thrombin into platelet-depleted plasma. Finally, measuring fibrinogen levels can help investigate prolonged aPTT or PT. Fibrinogen levels are commonly determined using two methods: the Clauss fibrinogen assay, which measures the time required for clot formation, and PT-derived fibrinogen, which estimates fibrinogen concentration based on prothrombin time[52].

However, as these tests are performed on plasma, they fail to fully replicate the complexity of *in vivo* haemostasis. This limitation has driven growing interest in the use of whole blood assays that assess viscoelastic properties, offering a more comprehensive and physiologically relevant evaluation. Such tests include thromboelastography (TEG) and, its modern modification, rotational thromboelastometry (ROTEM). These encompass the entire haemostatic process, from initiation of clot formation to clot propagation and clot lysis[71]. Although both technologies offer comparable information regarding the kinetics and strength of clot formation, their results are not directly

interchangeable due to differences in their operational principles[72]. In the TEG system, a cylindrical cup containing a 340µL whole blood sample rotates around a stationary pin suspended by a torsion wire. In contrast, the ROTEM system features a stationary cup, while the pin is suspended on a ball-bearing mechanism and oscillates within the blood sample. In both systems, clot formation is assessed by applying a rotational force to the blood sample, generating a specific tracing (thromboelastograms) from which various parameters are derived, each described using distinct nomenclature[73], as summarized in Table 1. ROTEM also allows to run different assays simultaneously: EXTEM, evaluation of common extrinsic pathway functionality using tissue factor as activator; INTEM, intrinsic pathway detection using ellagic acid as activator; FIBTEM, fibrinogen test using cytochalasin-D as platelet inhibitor detecting fibrinogen contribution to clot formation[74]; APTEM, test hyperfibrinolysis using aprotinin inhibitor[75].

TEG	**ROTEM**	**Description**
R (Reaction rate)	CT (Clotting Time)	Time it takes to the clot to reach 2mm amplitude (s)
K (Kinetics time)	CFT (Clot Formation Time)	Time necessary for clot amplitude to reach 20mm (s)
Angle	Alpha	Kinetic of clot development (°)
MA (Maximum Amplitude)	MCF (Maximum Clot Firmness)	Peak amplitude of the clot (maximum strength, mm)
A10	A5, 10 and 20	Clot amplitude 5, 10 and 20min after CT (mm)
LY30 and 60	LI30	Percent reduction 30 and 60 min after MA (TEG) or percent reduction in MCF after 30 min from CT (ROTEM, mm)
LY	ML (Maximum Lysis)	Total lysis (mm)

Table 1. Nomenclature of parameters described in thromboelastograms obtained with TEG and ROTEM systems[73].

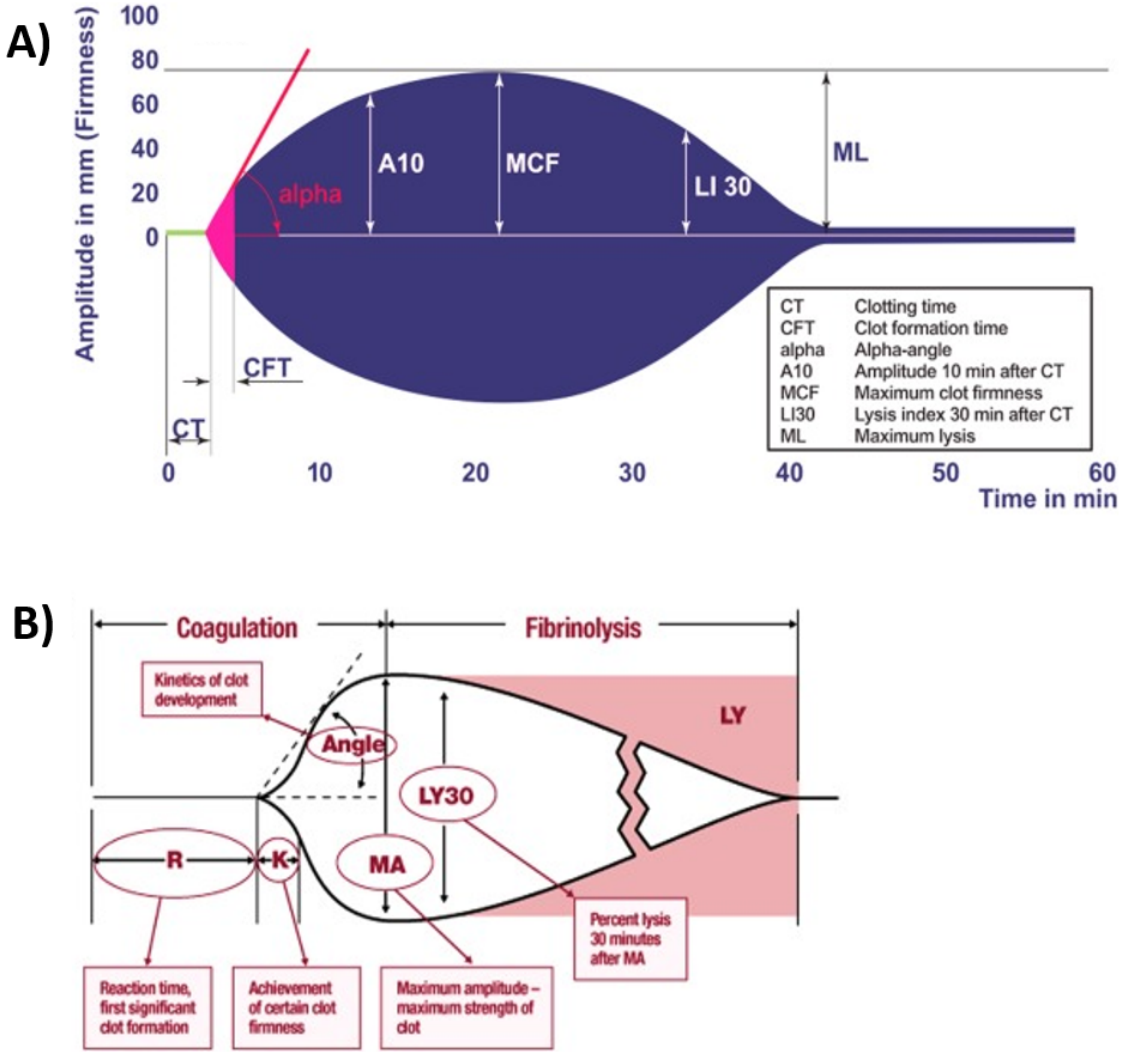

Figure 4. Example of A) ROTEM and B) TEG tracing output, showing clot initiation, propagation, stabilization and lysis. See Table 1 for nomenclature explanation. Image from Whiting et al[73].

1.5.6 Bleeding and thrombotic disorders

Disruptions in any part of the haemostatic pathway can lead to either haemorrhagic or thrombotic complications, depending on the specific abnormality involved. Haemophilia is a genetic bleeding disorder characterised by impaired blood clotting due to the deficiency or absence of certain clotting factors. Haemophilia A, the most common type, is linked to a deficiency in FVIII, while haemophilia B arises from a deficiency in FIX. Both forms are associated with reduced and delayed thrombin generation, leading to defective clot formation[76]. Haemophilia C, caused by a deficiency of FXI, is much rarer, affecting approximately 1% of the population[51]. Von Willebrand disease (VWD), the

most prevalent inherited bleeding disorder, is characterised by excessive mucocutaneous bleeding, such as frequent nose bleeds, bruising and prolonged bleeding after surgery. It results from quantitative or qualitative defects in the VWF glycoprotein which may include a partial or complete absence of VWF, or abnormalities in the protein structure[77]. Disorders involving abnormalities in fibrinogen are known as dysfibrinogenemias[78]. These can be congenital or acquired and encompass a range of fibrinogen function defects. They are extremely rare disorders with a highly heterogeneous phenotype going from no manifestation (55%) to bleeding (25%) and/or thrombotic events(20%)[78]. As most clotting factors are synthesised in the liver, severe liver disease is often associated with coagulopathy. In addition, as the liver plays a key role in removing activated clotting factors and fibrinolytic products, its dysfunction can increase the risk of developing disseminated intravascular coagulation (DIC)[51].

1.5.7 Platelet elimination from the bloodstream

At the end of their lifespan, or following full activation and incorporation into a forming thrombus, platelets are removed from the circulation. Several mechanisms have been proposed to explain the clearance of activated or ageing platelets from the bloodstream. Similar to other cell types, platelet clearance is partially governed by apoptosis, a programmed cell death process regulated by pro-apoptotic (Bak and Bax) and anti-apoptotic (Bcl-2 family) proteins. It has been demonstrated that double deletion of both Bak and Bax significantly extends platelet lifespan[79], while single deletions indicate that Bak plays the predominant role in this process[80]. In many apoptotic cells and in platelet as well, the translocation of PS from the inner to the outer membrane surface functions as a key molecular signal, marking the cell for recognition and clearance by scavenger receptors on phagocytic cells. PS exposure can occur via two distinct pathways[81,82]: an increase in intracellular Ca^{2+} levels[83] or the activation of apoptotic signalling cascades using Bak and Bax[81]. Mitochondrial damage and outer membrane permeabilization also contribute to platelet clearance, serving as key initiating events in the apoptotic process[84]. In addition, glycans play a critical role in the regulation of platelet clearance as well. Neuraminidases, a class of glycoside hydrolase enzymes, remove sialic acid residues from glycan chains: the loss of terminal sialic acid on the platelet surface has been associated with enhanced platelet clearance[85]. The resulting exposure of β-galactose residues is recognized by the Ashwell-Morell receptor (AMR) on hepatocytes and/or liver macrophages, thereby facilitating the removal of desialylated platelets from circulation[86,87]. Moreover, in pathological conditions, platelet clearance can also be antibody-mediated. In immune thrombocytopenia (ITP), for example, antiplatelet antibodies targeting surface glycoproteins such as GPIIb–IIIa and GPIb–IX promote platelet removal by macrophages and may additionally impair platelet production by targeting megakaryocytes[84,88]. It

has been demonstrated that GPIb–IX complex is also implicated in platelet clearance across other different pathways: from VWF-platelet complexes[89], platelet surface desialylation[90], or ectodomain shedding of GPIalpha during platelet storage[91].

1.6 Platelet disorders

Disorders of platelets can be broadly classified into quantitative and qualitative abnormalities, both of which can significantly impact haemostatic function and lead to either bleeding or thrombotic complications. Quantitative disorders refer to abnormal platelet counts. Thrombocytopenia is defined by a platelet count less than $150x10^3$ platelets/μL[92]. Usually patients showing a platelet count higher than $50x10^3$ platelets/μL are asymptomatic while under $5x10^3$ platelets/μL spontaneous bleeding is common and it is considered a haematologic emergency[93]. The reduction of platelet count can happen because of decreased platelet production, increased platelet consumption and/or sequestration[94]. Conversely, thrombocytosis is characterized by platelet count major than $1x10^6$ platelet/μL[95]. Thrombocytosis can be either reactive, when secondary to inflammation or infection due to elevated endogenous level of IL-6 or other cytokines, or clonal, as seen in chronic myeloproliferative disorders such as essential thrombocythemia[96]. In such cases, the risk of both bleeding and thrombosis increases due to dysfunctional platelet activation and aggregation[96]. Inherited platelet disorders (IPDs) represent a heterogeneous group of rare conditions caused by genetic mutations affecting platelet production and/or function[97]. To date, approximately 60 distinct types of IPDs have been identified, involving molecular defects in nearly 75 different genes[98]. They are characterized by dysfunctional (typically hypofunctional) platelets resulting from abnormalities in membrane receptors, granules, signal transduction pathways, or other components of the platelet biochemical machinery[99]. A hallmark of IPDs is a lifelong predisposition to spontaneous mucocutaneous bleeding, including epistaxis, gingival bleeding, purpura, and menorrhagia, which commonly manifests in childhood. While bleeding is usually mild to moderate, it may become more severe in situations that challenge haemostasis, such as trauma, surgical procedures, drug exposure, or childbirth. In rarer cases, patients may also experience deep or life-threatening bleeding events, such as intracranial haemorrhage or gastrointestinal bleeding[100].

1.7 Platelet role in inflammation and cancer

1.7.1 Platelet's immune receptors

Although the role of platelets in haemostasis has been extensively characterized, emerging evidence underscores their critical involvement in immunity and inflammation. This immunomodulatory capacity is largely mediated by a broad array of preformed factors present on platelet surface and

molecules stored within platelet granules, which are rapidly externalized upon activation. Platelets express numerous innate immune receptors, including Toll-like receptors (TLRs 1–9)[101] and immunoglobulins[102,103]. Functional studies have demonstrated that activation of Toll-like receptors (TLRs) by their respective ligands initiates intracellular signaling cascades, leading to platelet activation and underscoring their active role in host immune defense[101]. Also P-selectin can mediate the adhesion to cell expressing P-selectin glycoprotein ligand-1 (PSGL-1) such as neutrophils, monocytes, leukocytes but also endothelial cells and other platelets[102,104]. In addition to their interactions with leukocytes within the bloodstream, platelets actively facilitate leukocyte adhesion to the endothelium, functioning as key mediators of leukocyte recruitment to sites of tissue injury and inflammation. Following vascular damage, platelets rapidly adhere to the exposed subendothelial matrix, initiating thrombus formation to prevent blood loss. This adhesion begins with a tethering step involving the interaction between the platelet glycoprotein (GP) Ib-IX-V complex and immobilized VWF, followed by firm adhesion mediated by GPVI binding to exposed collagen[105]. Alternatively, platelets can adhere directly to intact endothelial cells. Upon adhesion, they upregulate surface expression of P-selectin, supporting neutrophil recruitment via engagement with neutrophil-expressed PSGL-1[105,106] . Among the key adhesion molecules expressed by platelets are integrins, which mediate binding to intercellular adhesion molecules (ICAMs) and junctional adhesion molecules (JAMs) present on leukocytes, endothelial cells, and components of the extracellular matrix (ECM)[105,106]. To further support interactions with immune and vascular cells, platelets themselves express ICAM-2, JAM-A, JAM-C, and platelet endothelial cell adhesion molecule-1 (PECAM-1)[106]. Further evidence supporting the involvement of platelets in the inflammatory response is the frequent observation of thrombocytopenia in patients with severe bacterial or viral infections[107]. Furthermore, interactions between platelets and leukocytes result in the formation of platelet–leukocyte aggregates (PLAs), which have been identified as specific biomarkers of sepsis[108] . Notably, when mediated by activated platelets, these interactions promote leukocyte activation, leading to neutrophil degranulation[109] and enhanced phagocytic activity[110]. In addition to various soluble mediators, platelets also release large quantities of CD40L, which has been implicated in the induction of reactive oxygen species (ROS), the upregulation of adhesion molecule expression on neutrophils, and the activation of macrophages, cytotoxic T cells and B cells in response to infection[111]. It has also been demonstrated that CD40L is implicated in the upregulation of E-selectin, ICAM-1 and VCAM-1 and the secretion of chemokines by endothelial cells[112].

1.7.2 Platelet as immune cells

Platelets not only modulate immune responses but also actively contribute to pathogen capture and sequestration. They achieve this through multiple mechanisms, including the induction of neutrophil extracellular traps (NETs), the encasement of pathogens within platelet aggregates, and the direct internalization of pathogens. NETs are fibrous webs composed of extracellular DNA filaments decorated with histones, myeloperoxidase (MPO), neutrophil elastase (NE), and other proteolytic enzymes[113,114], which exert potent antimicrobial effects by trapping and degrading invading pathogens[115]. Importantly, their formation appears to occur predominantly following platelet activation[116]. Since the initial discovery of NETs in 1996[117], two distinct forms have been described: classical (suicidal) NETosis, which culminates in neutrophil death, and vital NETosis, in which neutrophils retain viability and most of their functional capacity[118,119]. NETosis is morphologically and mechanistically distinct from apoptosis or necrosis, it is characterized by chromatin decondensation and disorganization of intracellular compartments[120]. Platelets induce NET formation through both direct contact and paracrine signaling. Direct interactions involve platelet P-selectin and glycoprotein Ibα (GPIbα) binding to neutrophil PSGL-1 and Mac-1[116], in parallel, platelet-derived soluble factors, including PF4, RANTES and high-mobility group box 1 (HMGB1)[121], have been implicated in NET induction[122,123]. Beyond promoting NET formation, platelets also recognize and are activated by NETs. Histone H4 within NETs engages platelet Toll-like receptors TLR2 and TLR4, triggering platelet activation[124,125], while both histones H3 and H4 can stimulate the nod-like receptor protein 3 (NLRP3) and caspase-1 cleavage, contributing to thrombus formation[126]. Furthermore, double-stranded DNA in NETs is detected by several platelet receptors, including TLR9, AIM2-like receptors (ALRs)[124], and cyclic GMP-AMP synthase (cGAS)[127], leading to platelet activation[128]. This reciprocal activation between platelets and NETs establishes a feed-forward loop that amplifies the thromboinflammatory response. In fact, NETs have been detected in both venous and arterial thrombi and are implicated in the pathogenesis of deep vein thrombosis, pulmonary embolism, myocardial infarction, and ischemic stroke[114,129–131]. Beyond their role in promoting pathogen entrapment via NETs, platelets contribute directly to host defence by binding and sequestering microorganisms. *In vitro* experiments have revealed that platelets are able to recognize and adhere to certain bacterial clusters, triggering a cascade of aggregation that progressively envelops the pathogens within a dense platelet matrix[132]. This, leading to a reduction in bacterial growth due to the action of antimicrobial peptides released by platelets, such as β-defensins[133]. In addition, platelets are capable of internalizing pathogens, both bacteria and viruses, into engulfing vacuoles which then fuse with platelet α-granules[134]. However, despite this internalization, platelets do not appear to effectively eliminate the captured microbes[134], likely because of their limited capacity for generating oxidative bursts and to

sufficiently acidify the vacuoles to support pathogen killing[135]. As previously mentioned, while platelets are now recognized as key modulators of the inflammatory response, it remains uncertain whether their involvement in immunity is uniformly beneficial to the host since several studies have also associated platelet–leukocyte aggregates with ischemia leading to organ dysfunction, and tissue injury[108,136].

1.7.3 Platelet in cancer

The association between a procoagulant state and cancer was first documented in the 19th century by Armand Trousseau[137], who described the link between malignancy and thrombotic events. This relationship was later substantiated at the molecular level through a series of studies demonstrating that tumour cells can induce platelet aggregation under various experimental conditions[138,139] identifying multiple platelet receptors involved in these interactions[140–144]. More recently, it has become clear that tumour progression is not solely dictated by tumour-intrinsic mechanisms but is profoundly shaped by the surrounding tumour microenvironment (TME)[145,146].

In normal tissues, somatic mutations occur sporadically, and only occasionally confer a selective growth advantage that allows the expansion of mutant clones. When these expanding clones encounter additional oncogenic signals or environmental cues, their proliferation may evade normal regulatory controls, initiating malignant transformation[147]. This multistep process, known as tumorigenesis, involves the progressive accumulation of genetic mutations and epigenetic changes that drive increasingly aggressive cellular phenotypes, including immune evasion, disruption of tissue architecture, and invasive behaviour. Concurrently, the TME evolves from being tumour suppressive to actively supports tumour growth and malignancy[147], with reciprocal crosstalk between tumour cells and their surrounding TME, involving diverse cellular components as well as the immune and coagulation systems[148]. As a matter of fact, thromboembolic disease represents the second leading cause of death among cancer patients[149,150], and thrombocytosis is consistently associated with poor prognosis, hightened risk of metastasis, and increased incidence of thromboembolic events across multiple cancer types[151,152]. One proposed mechanism underlying cancer-associated thrombocytosis is the ability of certain tumour cells to produce thombopoitein (TPO), which promotes megakaryocyte differentiation and platelet biogenesis[153–155]. Elevated plasma TPO levels in patients have also been correlated with increased IL-6 production, with both factors being associated with advanced disease stages and poorer survival outcomes[156]. In addition to thrombocytosis, cancer patients often exhibit elevated levels of CD40, thromboglobulin[157] and platelet derived extracellular vesicles[158]. Various tumour cells type[159] are also capable of inducing platelet activation and aggregation *in vitro*, in part through the expression of cancer cell-resident podoplanin (PDPN)[160]. Moreover, cancer cells can

stimulate endothelial cells to release ECM proteins and TF, further supporting platelet adhesion and promoting thrombus formation[161].

Beyond their role in coagulation, platelets critically contribute to tumour angiogenesis. As tumours reach a certain size, neovascularisation becomes essential to meet escalating demands for oxygen, nutrients, and growth factors[162]. Platelets indirectly promote angiogenesis by stimulating tumour cells to express pro-angiogenic mediators[163], however α-granules remain the major source of angiogenic factors in the TME[164].

Metastasis remains the leading cause of cancer-associated mortality[165]. During this process, invasive tumour cells detach from the primary tumour, enter the bloodstream, and migrate to distant sites where they colonise new tissues and form secondary tumors[143,166]. As tumour cells transit through the vasculature, their metastatic potential is actively supported by platelets: notably, thrombocytopenia and impaired megakaryopoiesis have been linked to reduced metastatic spread[167] while platelet transfusion in thrombocytopenic mice restores the ability of tumour cells to form metastases[168]. Platelets are the first cells to interact with circulating tumour cells in the bloodstream, rapidly forming a protective "cloak" composed of platelets and fibrin or fibrinogen that surrounds tumour cells and shields them from immune surveillance[143,169]

Platelet also facilitate epithelial–mesenchymal transition (EMT), a key program enabling epithelial tumour cells to lose polarity, detach from the basement membrane, and acquire mesenchymal characteristics associated with increased motility and invasiveness[170]. Platelet-derived soluble mediators promote the expression of mesenchymal markers including Snail1, vimentin (VIM), N-cadherin, fibronectin, and matrix metalloproteinase-2 (MMP-2), while downregulating epithelial markers such as E-cadherin and claudin-1[171]. Furthermore, platelets enhance tumour cell extravasation: during the rolling of tumour cells along the endothelium, platelet P-selectin binds to mucins, integrin β3, PSGL-1 fostering interactions among tumour cells, leukocytes, and endothelial cells[172–174]. Upon activation, platelets secrete a range of permeability-enhancing factors, including serotonin, VEGF, platelet-activating factor (PAF), thrombin, ATP/ADP, HGF, and fibrinogen[166,175].

1.7.4 P-EVs

EVs are small membrane-bound vesicles that include exosomes (30–100 nm) and micro-vesicles (100–1,000 nm in diameter)[176]. They are present in virtually all biological fluids, transporting a wide range of biomolecules such as proteins, lipids, and RNAs both on their surface or within their lumen[177]. EVs are released into the extracellular environment by nearly all cell types[178] and in the past decade, they have gained significant attention as potential biomarkers due to their molecular cargo reflecting the phenotype and state of their cell of origin[179]. P-EVs represent the most abundant

population of EVs in human blood, accounting for more than half of the circulating EVs[180] and typically express markers including CD31, CD41, CD42a, P-selectin, PF4, and GPIIb/IIIa besides specific EVs markers (such as tetraspanins CD9,CD63,CD81)[181,182]. P-EVs participate in various biological and pathological processes including inflammation[183] and tumour progression[184], among others. Notably, P-EVs have been demonstrated to enhance angiogenesis and support endothelial integrity following vascular injury[185]. Furthermore, increasing evidences support the involvement of P-EVs in inflammatory processes with elevated circulating P-EV levels associated with various disease states[186–189] and P-EVs facilitating inflammation by transferring platelet adhesion receptors to monocytes and promoting their recruitment[190].

1.8 Platelet use in clinical practice

Platelets are critical in transfusion medicine to prevent and treat bleeding in patients with thrombocytopenia or qualitative platelet dysfunction, while emerging non-transfusion uses in regenerative medicine and oncology are expanding their clinical value. Platelet transfusions are indicated for the prevention and management of bleeding in patients with thrombocytopenia, typically when platelet counts fall below 10×10^9/L for prophylaxis, or below 50×10^9/L in a therapeutic setting when there is active bleeding[191]. Common indications include chemotherapy-induced thrombocytopenia, haematological malignancies, and perioperative bleeding control [192]. Platelets for transfusion are sourced as platelet concentrates either as pooled random donor platelets derived from whole blood donations or as single donor platelets collected by apheresis[192].

Non-transfusional use blood components represent a distinct category of blood-derived products that, unlike conventional blood components administered intravenously for transfusion, are applied in therapeutic, surgical, and regenerative contexts without systemic infusion. Their clinical relevance is based on their ability to deliver bioactive molecules such as growth factors, coagulation proteins, and cytokines, which play critical roles in haemostasis, tissue repair, angiogenesis, and wound healing. Their progressive development reflects a paradigm shift in transfusion medicine, extending the use of blood donations beyond the traditional replacement of deficient components to include novel regenerative and targeted applications[193]. Among the principal non-transfusional blood components PRP remains the most studied and widely applied[194]. It is prepared by centrifugation protocols that concentrate platelets while minimizing leukocyte contamination, yielding a product rich in growth factors[195]. Autologous serum eye drops, derived from a patient's own plasma or others', provide growth factors, vitamins, and other trophic substances for the management of ocular surface disorders, including severe dry eye syndrome and neurotrophic keratitis[196]. Additional plasma-derived fractions, such as cryoprecipitate, are used as raw material for the pharmaceutical production

of clotting factors and albumin[193]. Furthermore, fibrin glue is now routinely employed in surgery to enhance local haemostasis and tissue adhesion, reducing intraoperative bleeding and improving wound closure[197]. The preparation of these products is performed in authorized transfusion medicine services, starting from whole blood donations or apheresis collections. Specific laboratory techniques such as differential centrifugation, filtration, or activation with calcium and thrombin are employed to isolate the desired fractions. As human-derived products, their processing and clinical use are governed by strict regulatory frameworks that ensure traceability, microbiological safety, and standardized quality[193]. Additionally, in oncology, the role of platelets as biomarkers for disease progression, response to therapy, and as potential targets to inhibit tumour–platelet interactions is under investigation, highlighting their importance beyond haemostasis[198].

1.8.1 Platelet concentrates for transfusion use

Platelet concentrates are essential blood products in transfusion medicine, and are indicated both prophylactically and therapeutically to prevent or control bleeding in patients with quantitative or qualitative platelet defects. These situations result in a significant decrease in circulating platelet counts, necessitating platelet concentrates transfusion to restore platelet levels, maintain haemostasis, and prevent bleeding complications[199].The principal clinical uses include prophylactic transfusion to prevent spontaneous bleeding in severe thrombocytopenia (arisen in patients with bone marrow failure or undergoing intensive myelosuppressive chemotherapy)[94], therapeutic transfusion for active bleeding in thrombocytopenic or functionally defective patients, and periprocedural transfusion to reduce bleeding risk for invasive interventions (with thresholds adapted to procedure type and patient risk)[193]. In haematology and oncology practice the majority of platelet transfusions are given to thrombocytopenic patients with haematological malignancies[200,201] or those undergoing hematopoietic stem cell transplantation, where profound, prolonged thrombocytopenia frequently occurs and bleeding risk is high; by contrast, in surgical and critical care settings platelet transfusion is often tailored to the clinical scenario (active bleeding, urgent invasive procedures, or reversal of antiplatelet therapy) rather than used routinely[202]. European best practice guidance emphasizes a restrictive, individualized approach to prophylactic platelet transfusion (a threshold of 10×10^9 platelet/L for stable patients with reversible marrow suppression, with higher thresholds such as 20–50×10^9 platelet/L when additional risk factors are present or for high-bleeding-risk procedures), while therapeutic transfusion is indicated for clinically significant bleeding irrespective of the count[202]. Platelets used for transfusion are sourced from healthy volunteer donors, either through whole blood collection or by apheresis procedures[203]. When derived from whole blood, platelet concentrates are prepared by centrifugation to separate platelet-rich plasma, which is then processed to produce platelet unit, typically pooled from 4–6 donors to achieve a therapeutic adult dose[204]. In contrast,

apheresis platelets are collected directly from a single donor using cell separators, yielding a complete therapeutic dose in a single collection, while minimising donor exposure and thereby reducing risks of alloimmunization and transfusion-transmitted infections[205]. Following collection, platelets are stored in either plasma or platelet additive solution (PAS) and maintained at room temperature (RT, 22–24°C) under continuous gentle agitation in gas- permeable storage bags to preserve their viability and function[206]. During the preparation of platelet concentrates, platelets can undergo a series of metabolic and structural alterations including loss of discoidal shape, pH fluctuations and decreased functionality that continue to accumulate during storage. These changes are collectively termed "platelet storage lesions" (PSL) and are influenced by the type of resuspension medium used[207–209]. PSL development is also associated with reduced *in vivo* platelet recovery, shorter post-transfusion survival, and diminished haemostatic efficacy[210]. To minimise the risk of septic transfusion reactions and prevent platelet aggregation during storage, platelet are stored for a maximum of 5–7 days under continuous gentle agitation[211]; the European Directorate for the Quality of Medicine & Healthcare (EDQM) Blood Guide and national guidelines detail quality standards for collection, storage, bacterial testing, and release criteria for platelet components across Europe[193]. Clinical decision-making about transfusion must balance expected benefit (bleeding prevention or haemorrhage control) against known risks. Acute transfusion reactions include febrile non-haemolytic reactions, allergic reactions, and, rarely, severe anaphylaxis; transfusion-associated circulatory overload (TACO) and transfusion-related acute lung injury (TRALI) are recognized, life-threatening complications that require immediate management[212]. Immunologic complications include alloimmunization against HLA or platelet-specific antigens, which can produce refractoriness to subsequent platelet transfusions manifested by poor post-transfusion platelet count increments[213]; strategies to reduce alloimmunization and manage refractoriness include universal leukoreduction, ABO-compatible platelet selection, HLA/HPA matching, use of cross-matched platelets, and in some cases the use of immunomodulatory therapies or matched single-donor apheresis units[214]. Pathogen-reduction technologies can further reduce infectious risk but may alter some platelet functional parameters and add cost; European guidance discusses the role of such technologies in blood services, balancing safety gains and operational considerations[193]. When immune refractoriness is confirmed, provision of HLA-matched or cross-matched platelets is recommended also including leukoreduction of platelet products, the use of HLA-matched platelets, and pathogen reduction technologies, which additionally enhance transfusion safety by reducing infectious risks[213]. European guidance and national transfusion services outline workflows for investigation, notification to transfusion laboratories, and availability of matched products, and emphasize preventive strategies such as universal leukoreduction and minimization of donor exposure in chronically transfused patients[193].

1.8.2 Platelet cryopreservation

Storing platelets at RT poses significant logistical and clinical challenges, including a limited shelf-life of typically 5–7 days[211], increased risk of bacterial contamination, and reliance on continuous donor availability, a factor that can be critically impacted during emergencies, such as the SARS-CoV-2 pandemic[215]. These limitations have driven the advancement of platelet cryopreservation as a viable alternative to RT storage. Platelet cryopreservation was originally developed to address the urgent need for effective platelet storage in military and war-time scenarios, ensuring a reliable supply during combat situations where fresh platelet availability was limited[216]. This method typically involves freezing platelets at −80 °C with cryoprotectants such as dimethyl sulfoxide (DMSO), which preserves cellular integrity during freeze-thaw cycle[217,218]. Platelets can be stored under these conditions for up to one year, or for periods exceeding one year at ≤−150 °C in the vapor phase of liquid nitrogen, as recommended by European (EU) Guidelines[193]. While a universally accepted maximum storage duration for cryopreserved platelets (Cryo-PLT) at −80 °C has not yet been established, emerging evidence suggests that their shelf-life could be extended to 5–12 years under controlled conditions[216]. Clinically, cryopreserved platelets have demonstrated efficacy in managing bleeding in various contexts, including trauma, surgery, and hematologic disorders[219,220], providing a critical resource for emergency transfusions when conventional platelet products are unavailable. Both RT-stored and cryopreserved platelets undergo storage lesion accumulation, leading to metabolic and functional alterations; however, Cryo-PLT are associated with reduced bacterial contamination risks due to storage at low temperatures[221,222]. The use of Cryo-PLT is primarily limited by the need to achieve at least 50% platelet recovery post-thaw compared to pre-freezing counts and by a short post-thaw shelf-life of only 6 hours hours[223,224], their shorter circulation time in fact may limit their use in prophylactic transfusions requiring sustained platelet counts. While the use of Cryo-PLT in actively bleeding patients is well-supported[225], their application in prophylactic transfusions for thrombocytopenic oncology patients remains controversial. Concerns include reduced functionality and lower transfusion efficacy, as well as Cryo-PLT exhibiting increased activation upon thawing, leading to morphological changes and extensive release of bioactive molecules from α-granules[226]. These molecules, including growth factors and cytokines, are implicated in modulating the tumour microenvironment, promoting cell proliferation, angiogenesis, and EMT[171,227], as already discussed. Additional concerns regarding the prophylactic use of Cryo-PLT in cancer patients include their potential pro-thrombotic effects, particularly relevant given that cancer patients already exhibit a heightened baseline risk of thrombosis due to their underlying disease[227,228]. The selection of appropriate cryoprotective agents (CPAs) is critical for minimizing platelet damage during freezing and thawing, directly impacting post-thaw viability and function[229].

CPAs can be broadly classified as intracellular or extracellular, based on their membrane permeability and mechanisms of action. Intracellular cryoprotectants penetrate cell membranes to mitigate intracellular ice formation and stabilize cellular structures during cryopreservation, while extracellular cryoprotectants act by modulating the extracellular environment, osmotically counteracting the effects of ice formation and preventing excessive cellular dehydration[230]. Among CPAs, dimetilsulfoxyde (DMSO) is the most widely used for the cryopreservation of cells, including blood components, tissues, and stem cells, both in *in vitro* research and clinical applications such as autologous hematopoietic stem cell transplantation. DMSO exhibits excellent intracellular cryoprotective properties; however, its cytotoxicity necessitates precise concentration optimization and careful handling to balance efficacy with safety[231]. Despite the established utility of DMSO-based cryopreservation, current clinical practices face challenges including cellular damage during freezing and thawing, leading to impaired platelet function and reduced transfusion efficacy. Addressing these limitations is crucial for advancing platelet transfusion practices, making the development of improved cryopreservation strategies a key focus of current research efforts[219]. For example, Johnson et. al.[232] recently developed a simplified platelet cryopreservation protocol that eliminates centrifugation steps and employs a reduced DMSO concentration (3%), resulting in improved post-thaw platelet quality, evidenced by higher GPIbα expression and reduced degranulation. To overcome the limitations associated with traditional cryopreservation and DMSO toxicity, alternative cryoprotectants are actively being investigated[233].

1.8.3 Platelet concentrates in wound healing

The wound healing process involves the dynamic recruitment and activation of multiple cell types, including immune cells, fibroblasts, and endothelial cells. Among the key mediators of this process, platelets play a pivotal role in coordinating tissue repair: platelets actively drive wound healing by releasing a wide array of bioactive molecules, including growth factors (GFs), cytokines, chemokines, and extracellular vesicles[23,31]. Building on these biological principles, platelet-rich plasma (PRP) has emerged as a therapeutic preparation that concentrates platelets and their associated growth factors within a small plasma volume, providing a bioactive microenvironment that can accelerate tissue repair and regeneration[234]. Despite its promise, PRP is not a uniform product but rather a family of preparations whose biological activity varies substantially depending on methodological differences. The Dohan Ehrenfest classification distinguishes PRP formulations according to leukocyte content and fibrin architecture: pure platelet-rich plasma (P-PRP, referred to as simply PRP in this text), leukocyte- and platelet-rich plasma (L-PRP), pure platelet-rich fibrin (P-PRF), and leukocyte- and platelet-rich fibrin (L-PRF)[235]. These subtypes are not interchangeable, as P-PRP is generally

preferred in intra-articular applications where minimizing inflammation is desirable, whereas L-PRP may exert additional catabolic effects useful in chronic tendinopathies, and PRF products provide a fibrin scaffold that enables a slow release of growth factors and cellular migration in oral and maxillofacial surgery[236]. Preparation protocols also introduce variability. Single-spin centrifugation separates red blood cells from plasma but yields variable platelet enrichment, while double-spin techniques add a second centrifugation step to achieve higher platelet concentration and remove platelet-poor plasma[237]. Even within the same PRP subgroup, numerous variables can influence the quality and efficacy of the product. These variables include the method of platelet collection (e.g., buffy coat or platelet apheresis) as well as differences in the phlebotomy protocol, freeze-thawing processes and activation techniques. Patient-specific variables including age, comorbidities, and baseline platelet count also influence PRP quality, meaning that two samples prepared under similar conditions may differ considerably in regenerative potential[238]. The absence of standardized protocols, individual donor variability, and the heterogeneity of preparation methods can result in significant variations in PRP composition, ultimately leading to unpredictable treatment outcomes[239,240]. To address these limitations, allogeneic PRP products have been proposed, offering greater standardization in donor selection and preparation processes. While autologous PRP remains the most widely used in clinical practice and research, its collection can pose additional challenges, especially in critically ill or elderly patients, and patient-specific factors can negatively impact the quality of the PRP obtained[241]. In this context, the use of platelet concentrates prepared by blood banks under Good Manufacturing Practice (GMP) conditions may provide PRP with more consistent and well-defined compositions, ensuring minimal contamination with erythrocytes and leukocytes while maintaining higher reproducibility and safety for clinical applications[242]. Among allogeneic products, buffy coat-derived PRP (BC PRP) is prepared by pooling platelets from 4–5 donors, reducing inter-individual variability. However, pooling platelets also increases the risk of transmitting infections, prions, and inducing allogeneic immune reactions[242,243]. In contrast, apheresis-derived PRP (Aphe PRP) is obtained through a more complex and invasive collection process, which limits the pool of eligible and willing donors[215]. To date, in routine clinical practice PRP is often substituted by more standardized alternatives. For musculoskeletal disorders, corticosteroid injections remain widely used due to their rapid analgesic effects, despite concerns over potential cartilage damage with repeated administration[244]. Hyaluronic acid injections are also commonly applied in knee osteoarthritis, supported by regulatory approval and longer clinical track records. In chronic wound care, negative pressure wound therapy, advanced dressings, and topical growth factor gels remain first-line approaches. In addition, autologous conditioned serum (ACS), which is enriched in anti-inflammatory cytokines such as interleukin-1 receptor antagonist, has been developed as another

orthobiologic alternative[245]. PRP has emerged as a promising therapeutic option in regenerative medicine, with diverse applications across dermatology[246,247], maxillofacial surgery[248], orthopedic surgery[249], ocular surface disorders[250] and selective autoimmune conditions[251]. In dermatology, the application of PRP for alopecia, acne, scarring, and skin rejuvenation is gaining considerable interest, with novel indications, including radiodermatitis and rheumatological skin conditions, recently proposed and under investigation[243,252,253]. Crucially, PRP has demonstrated efficacy in the management of chronic and non-healing wounds, providing a valuable adjunct in wound care strategies[246,254]. This therapeutic use is increasingly recognized by the scientific community[255] and is reflected in emerging clinical[193], positioning PRP as a validated and evolving treatment option for complex wound management. The growth factors and cytokines released from PRP promote revascularisation of damaged tissue by inducing endothelial cells reorganization into new blood vessels, while simultaneously activating fibroblasts to enhance fibrogenesis, restore the extracellular matrix, and stimulate keratinocyte proliferation and migration[256,257]. Extensive literature supports the safety and clinical efficacy of PRP for treating non-healing wounds of various aetiologies, particularly diabetic ulcers, where accelerated and more complete wound closure has been consistently observed[246,254,258]. *In vitro* studies further demonstrate that PRP significantly enhances the migratory capacity and proliferation rates of mesenchymal stem cells and fibroblasts[259], key contributors to effective wound healing. Despite these promising findings, the widespread clinical adoption of PRP in chronic wound management remains limited by the heterogeneity of PRP preparation and administration protocols, which are often inconsistent or insufficiently described across studies, underscoring the urgent need for protocol standardization in clinical practice[241,260,261].

1.9 Aim of the thesis

The aim of this thesis is to characterize platelet concentrates and their clinical application in both oncology and regenerative medicine. Although platelet concentrates are widely used for transfusion, limitations related to their short shelf-life, bacterial contamination and storage are being addressed through cryopreservation strategies. However, despite extensive characterization of Cryo-PLT[219,226,262], only a limited number of time points after thawing have been evaluated, primarily for BC-PRP[263], and the effects of Cryo-PLT on cancer cell proliferation and migration remain unclear. Identifying optimal transfusion timing and understanding the effect of Cryo-PLT supernatants are essential to reducing transfusion-related risks in cancer patients.

Therefore, this work first aimed, through a multidisciplinary approach, to investigate how the time after thawing influences the biochemical and functional characteristics of apheresis Cryo-PLT to optimize transfusion timing and to evaluate their effects on cancer cell behaviour *in vitro*, thereby

clarifying their potential as a transfusion resource for onco-haematological patients. Characterization included flow cytometric analysis of platelet activation (via CD62P exposure), platelet recovery assessment, and coagulation capacity analysis using ROTEM, complemented by Fourier Transform Infrared (FTIR) spectroscopy to evaluate cryopreservation-induced changes in lipid and protein structures within the platelet membrane.

As second objective, this thesis aimed to characterize and compare the wound healing and regenerative potential of BC and Aphe PRP products, in both liquid and gel forms, as previous studies had not directly evaluated their differences nor the impact of PRP activation and gel formation on its functionality. The release kinetics of GFs and EVs from PRPs was assessed over a 7-days period and, using *in vitro* models of human keratinocytes, fibroblasts and microvascular endothelial cells, PRPs effect was examined on cellular processes critical to tissue regeneration.

Collectively, these findings will contribute valuable insights for improving transfusion strategies and expanding the therapeutic use of platelet products, supporting their integration into personalized approaches for bleeding prevention and tissue regeneration in clinical practice.

1.10 New perspectives

P-EVs are the most abundant EV subset in human circulation[180,264] and express PS on their surface, providing a highly procoagulant platform that is 50–100 times more active than platelets themselves in supporting thrombin generation and fibrin formation[265]. P-EVs also carry immunomodulatory mediators, including PF4 and HMGB1, facilitating the crosstalk between coagulation and inflammation and supporting the formation of NETs, central in immunothrombosis[266].

Given the growing interest in P-EVs as potential biomarkers and disease mediators in immunothrombosis and oncology-related thrombosis, understanding how anticoagulants impact their measurement and functional interactions with monocytes is essential. P-EVs interaction with immune cells is particularly relevant and has already been investigated in citrate blood in which P-EVs preferentially bind to monocytes (and granulocytes), while exhibiting minimal association with lymphocytes[267]. This preferential binding is further nuanced within monocyte subsets: intermediate monocytes (CD14+/CD16+) display the highest affinity for P-EVs, followed by classical and non-classical monocytes, with storage conditions amplifying these interactions[267]. Since the effect of anticoagulant has been only investigated on EVs[268], this preliminary data were obtained using flow cytometry to explore the differential effects of citrate and EDTA specifically on P-EV–monocyte interactions with the future aim to investigate P-EV-driven mechanisms in coagulation, immune regulation, and oncology-related thrombosis. This approach will enable clearer interpretation of P-EV functional assays and biomarker studies, reducing variability due to pre-analytical factors and ensuring the translational relevance of P-EV research in precision medicine.

2 MATERIAL AND METHODS

This section is structured in three parts.

The first part focuses on the biochemical characterization of cryopreserved platelets and the evaluation of their effects in co-culture with tumour cells. The second part addresses the PRPs' characterization and the evaluation of their capacity to promote tissue regeneration, while the third part is focused on the determination of the anticoagulant effect on P-EVs interaction with monocytes subpopulations.

2.1 Characterization of cryopreserved platelets and development of an optimized cryopreservation solution

Platelet apheresis sample collection was conducted in two distinct phases. In the first phase, donors were recruited to obtain platelet samples for characterization and to evaluate their effects on tumour cells *in vitro*. In the second phase, a separate recruitment was carried out to collect additional apheresis samples for cryopreservation using different cryoprotective solutions, with the objective of identifying the most effective formulation.

2.1.1 Study design and platelets collection

The study was carried out by the Transfusion Medicine Unit of the Azienda USL-IRCCS di Reggio Emilia, approved on 17 December 2020 (protocol number 2020/0149618) and emended on 26 July 2021 (protocol number 2021/0094053) by the Institutional Board Review (Reggio Emilia Ethics Committee).

Five platelet donors were recruited by the Transfusion Medicine Unit at "Casa del Dono" in Reggio Emilia (Italy). All recruited donors signed an informed consent according to the Declaration of Helsinki. Platelet apheresis was performed using an automated blood collection system (Mobile Collection System MCS+, Haemonetics Corp., Boston, MA, USA), according to the manufacturer's instructions. Acid Citrate Dextrose Solution A (ACD-A, Haemonetics Corp., USA) was used as anticoagulant and plasma combined with platelet additive solution (T-PAS+, Terumo) were added in a 30:70 ratios. Following collection, platelet units were irradiated with at a dose of 35 Gy (Raycell) before cryopreservation, in compliance with Italian regulations[269].

PLT units (n = 5) were cryopreserved without the use of a controlled freezing rate protocol within 24 hours from collection according to Valeri et al[270]. Briefly, a sterile solution of 25% DMSO (Sigma Aldrich) in 0.9% Sodium Chloride (NaCl, Baxter) was added to each PLT unit to achieve a DMSO final concentration of 6%. Next, the PLT units were equally divided into three satellite 300 mL PVC made Teruflex® bags (Terumo) and subjected to centrifugation at 1349 g for 10 minutes at 20°C using Rotixa 50 RS (Hettich Zentrifugen). After removing the supernatant, a PLT pellet of

approximately 10 mL ± 1,9 was stored at −80°C using the MDF-U5386S freezer (Sanyo). Cryo-PLT were stored for a mean of 200 ± 30 days before analyses.

Each satellite Cryo-PLT units was thawed at 37°C in water bath and then reconstituted with 70 mL T-PAS (Terumo). For each donation, donor plasma was also collected separately. Experimental plan is reported in Figure 5.

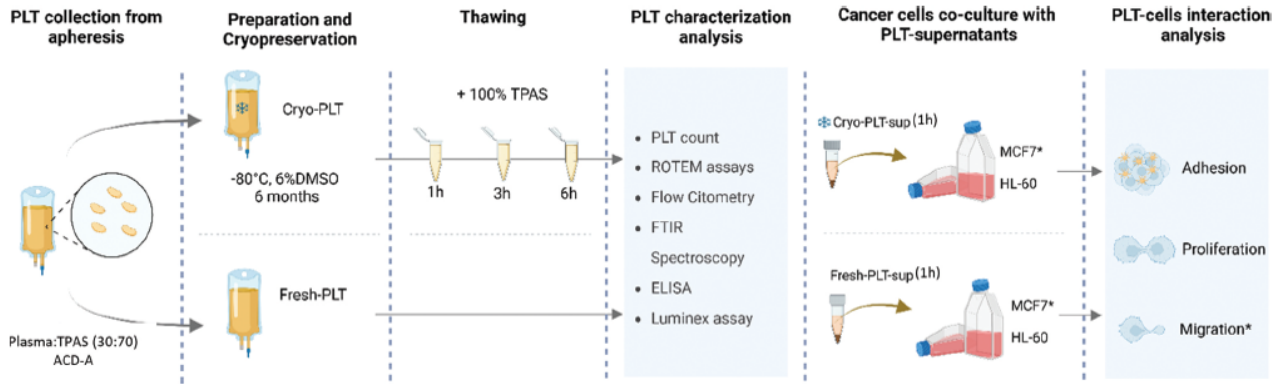

Figure 5. **Schematic illustration of experimental design**. Image created with Biorender.

2.1.2 Platelet characterization

All characterization analyses were conducted on both fresh (control samples, T0) and thawed platelet products. Fresh-PLT were stored at 22–24°C under constant agitation for a maximum of 5 days. Thawed, reconstituted platelets were maintained at 22–24°C under agitation, aliquotes (15 mL) were collected at 1, 3 and 6 hours post-thaw for subsequent analysis. Additionally, Fresh-PLT (5×10^6/mL) activated with thrombin (0.5 U/mL) for 10 minutes at 37°C (Midi CO2 Incubator, ThermoScientific) were used as positive control.

2.1.3 Platelet counts and ROTEM assay

PLT counts were performed on both Fresh and Cryo-PLT immediately after thawing using an automated blood cell counter (XS-1000i analyzer, Sysmex). Post-thaw platelet recovery was calculated according to the following formula[271]:

$$Recovery(\%) = \frac{Cryo - PLTplateletcount}{Fresh - PLTplateletcount}\ x\ 100$$

Platelet clot viscoelastic parameters were assessed on Fresh-PLT and thawed Cryo-PLT using thromboelastometry on a ROTEM® delta system (Werfen, Milano, Italy). A volume of 350 µL of platelet concentrate was diluted with 150 µL of autologous plasma. Intrinsic, extrinsic and contact-mediated coagulation pathways were evaluated using INTEM, EXTEM and NATEM assays respectively, according to the manufacturer's instructions. The following thromboelastometric

parameters were recorded: Clotting Time (CT, sec) representing the time until clot formation begins; Clot Formation Time (CFT, sec) as the time from CT until the clot reaches an amplitude of 20 mm; A20 (mm) indicating the clot amplitude 20 minutes after CT; Maximum Clot Firmness (MCF, mm), corresponding to the maximum amplitude achieved during clot formation.

2.1.4 Flow-cytometry

Surface receptors, activation markers (P-selectin, CD62P) and phosphatidylserine (PS) expression were analyzed using a FACSLyrics flow cytometer (BD, Bioscience). Unless otherwise specified, all reagents were sourced from BD Biosciences. Glycoproteins expression was carried out adding 20 µL of anti- CD41a-PE, anti-CD42b-FITC, anti-CD62P-APC and 5 µL of anti- CD61-PerPC to 100 µL of platelets (5×10^6/mL). Samples were incubated at RT in the dark for 15 minutes and then 400 µL of PBS (EuroClone) was added before acquisition. PS exposure was assessed using AnnexinV-FITC. In brief, samples were diluted in PBS to a final concentration of 200.000 platelet/mL, centrifuged at 1500 g for 5 minutes and resuspended in 200 µL of Annexin V Binding Buffer. 5 µL of Annexin V-FITC were added to 100 µL of samples, incubated in the dark for 15 minutes and then resuspended in 400 µL of Annexin V Binding Buffer for flow cytometer analysis. Platelet microparticles were enumerated using the customized EVs kit for flow cytometry (BD Biosciences, #626267, Custom Kit)[272] according to manufacturer's instruction. A reagent mix was prepared for each sample as follows: 94 µL of 0.22 µm-filtered PBS, 0.5 µL of Lipophilic Cationic Dye, 0.5 µL of FITC-conjugated phalloidin, 5 µL of CD41a-PE and centrifuged at 22.000 g for 15 minutes (Centrifuge 5424, Eppendorf). The mix was added to 100 µL of PLT (150.000/µL) previously dispensed into a TrueCount™ Tube (BD). After 45 minutes of incubation (RT, in the dark), 1 mL of filtered PBS was added and vortexed (ZX3, Velp Scientifica) immediately before the acquisition.

2.1.5 FTIR spectroscopy

FTIR spectroscopy was performed at the SISSI-Bio beamline[273] at Elettra Sincrotrone Trieste, in order to assess protein and lipid structure of both Fresh and Cryo-PLT. Platelet samples were diluted 1:10 with 0.9% NaCl and fixed with 0.5% PFA (Promega) for 15 min, at RT. Samples were then centrifuged for 5 min at 1500 g (Centrifuge 5424, Eppendorf), resuspended in 500 µL of 0.9% NaCl and left at 4° C (Recorder fridge, Medical Project) until the analysis. Samples were deposited onto a CaF2 window, 1 mm thick and 13 mm in diameter, dried inside a laminar flow biological hood and then measured. The measurements were carried out using a Bruker Hyperion 3000 IR/VIS microscope coupled to an in-vacuum interferometer VERTEX70V (Bruker Optics – Billerica MA, US) with a single-point MCT (Mercury Cadmium Telluride) detector. The microscope apertures were closed at 50 × 50 microns in order to select small groups of platelet. A total of 1366 spectra were

collected. Each spectrum is the average of 256 scans, at 2 cm−1 of spectral resolution, with a scanner velocity of 40 kHz. After the recording, spectra were corrected for the atmospheric water vapor and CO2 with a routine embedded in OPUS 8.5 SP1 (Bruker Optics – Billerica, MA – US) and imported in QUASAR (http://quasar.codes)[274]. With the modules present in this software, data were baseline corrected, 2nd degree derivative was calculated using Savitzky-Golay filter (31 point of smoothing and 3rd degree polynomial function) and normalized with Standard Vector Normalization (SVN). Using the baseline corrected absorbance spectral data the following spectral ratio were calculated:

- C=O/Lipids (Area 1760–1700 cm−1/Area 3000–2800 cm−1)
- C=O/Amide I (Area 1760–1700 cm−1/Area 1715–1590 cm−1)
- CH2/CH3 (Area 2860–2840 cm−1/Area 2945–2910 cm−1)
- NucAcids/Amide I (Area 1278–1200 cm−1/Area 1715–1590 cm−1)

Results were then imported in Origin (Pro)2022 (Origin Lab Corporation, Northampton, MA, USA) and the averages were compared using an ANOVA, according to the class of interest, being it time (Fresh, 1 h, 3 h and 6 h) or activation status. A Principal Component Analysis (PCA) was performed on 2nd derivative normalized spectral data considering the ranges between 3200 and 2800 cm−1 and 1800 and 900 cm−1.

2.1.6 ELISA and Luminex assays

The concentration of TGF-β (pg/mL) was quantified using an ELISA kit (Transforming growth factor beta ELISA Kit, R&D system, Biotechne), following the manufacturer's instructions. Each measure was performed on platelet supernatant and tested in triplicate against a standard curve. Samples in 96-well plates were read at 450 nm (Glomax® Discover Microplate Reader, Promega, Madison, WI, USA).

Luminex technology (Bio-Plex Pro Human Cytokine Screening Panel Kit, BIORAD) was employed to evaluate the concentration of RANTES, PDGFB and FGF (pg/ml) in platelet supernatants. To obtain 1hour platelet supernatants, both fresh and thawed platelet samples were centrifuged at 1500 g for 20 minutes at 10°C. Subsequently, a second centrifugation at 10 000 × g for 5 minutes was performed to obtain platelet-free supernatant. After, the pellet was resuspended in a fresh resuspension solution and subjected to another round of centrifugation to measure the delta release at 3 hours after thawing. This identical procedure was repeated for the subsequent time point of 6 hours after thawing. All supernatants were stored at −80°C with 1:200 protease inhibitor cocktail (Abcam, MA, USA) until further analysis. Measurements were performed following the manufacturer's instructions and assessed in triplicate against a standard curve. Samples were read in 96-well plates

with Bio-Plex MAGPIX® Multiplex Reader (Luminex XMAP Technology, BIORAD, Hercules, CA, USA).

2.1.7 Cell culture and cell proliferation analysis

The human breast cancer cell line MCF-7 was selected as *in vitro* model to mimic solid tumors[275,276]. MCF-7 were cultured in low glucose Dulbecco's modified Eagle's medium (DMEM Low Glc, EuroClone) supplemented by 10% fetal bovine serum (FBS, EuroClone), 1% L-Glutamine (EuroClone) and 1% Penicillin-Streptomycin (Pen-Strep, Sigma Aldrich). Complete growth medium was refreshed 2–3 times per week and cell confluency was maintained below 80% confluency in T75 flasks (CytoOne). The human myeloid leukemia cell line HL-60 was cultured in RPMI 1640 medium (EuroClone) added with 10% FBS (EuroClone) and 1% Pen-Strep (Sigma Aldrich).

Platelet samples (1×10^6/mL) were centrifuged twice at 10 000 g for 5 minutes (Centrifuge 5424, Eppendorf) to obtain Fresh-PLT supernatant (Fresh-PLT) and Cryo-PLT supernatant (Cryo-PLT).

Cell viability of MCF-7 and HL-60 was measured by WST-1 cell proliferation assay (Cell Proliferation Reagent WST-1, Merck). Experimental conditions are detailed in Table 2. MCF-7 and HL-60 cells were seeded at a concentration of 15 000 cells/ cm^2 and 30 000 cells/mL respectively, into 96well-plates (EuroClone). After 24 hours, cell culture media were replaced with the conditioned media listed in Table 2. Cell proliferation was assessed after 24, 48 and 72 hours of incubation (Midi CO2 Incubator, ThermoScientific) by addingWST-1 to the wells for 2 h at 37°C (Midi CO2 Incubator, ThermoScientific) followed by absorbance measurement at 450 nm using a GloMax Discover microplate reader (Promega).

	Sample	Culture Condition
1	Positive control (normal proliferation)	10% FBS
2	Negative control (slow proliferation)	0.1% FBS
3	Treatment with Fresh-PLT	0.1% FBS + 5% Fresh-PLT
4	Treatment with Cryo-PLT	0.1% FBS + 5% Cryo-PLT

Table 2. Experimental culture conditions.

2.1.8 Cell migration and cells-platelet adhesion assay

Wound healing assay was performed to monitor MCF-7 migration. MCF-7 cells were seeded in culture medium at a concentration of 75 000 cells/cm^2 and allowed to grow for 24 h to reach approximately 100% confluence. Then, the medium was removed and a linear wound was generated in the monolayer with a sterile 10 µL plastic pipette tip (ClearLine, Dominique Dutscher). Wells were washed twice with PBS to eliminate cellular debris and new medium was added following the

conditions indicated in Table 2. Digital images of cells' clear area were acquired right after wound generation (0 h) and at 24, 48, and 72 h at 4X magnification. Image analysis was conducted using ImageJ[277] software and wound closure was calculated as a percentage, with results expressed as the mean of five replicates for each condition.

Platelets-cells adhesion assay was performed as previously described[278]. Briefly, MCF-7 and HL-60 cells were resuspended at the concentration of 1×10^6 cells/mL in culture medium containing 1 mM $CaCl_2$ and 0.1% FBS. Subsequently, 2×10^5 cells/ mL cells were incubated in agitation with 2×10^8 platelets/mL for 30 min at 37°C. Staining with anti-CD41a-PE antibody (BD Biosciences) was performed to discriminate platelets from cancer cells (30 min at RT, in the dark) before flow cytometric analysis (FACSLyrics system, BD Biosciences). MCF-7 and HL-60 cells resuspended in PBS were used as negative controls (CTRL).

2.1.9 Statistics

Statistical analysis was performed using GraphPad (Prism 8.4.2, GraphPad Software, San Diego, CA, USA). One- way or two-way ANOVA with multiple comparisons test or Benjamini correction were performed to assess difference among samples. A P-value of <.05 was considered statistically significant. Flow cytometry data were analyzed with FacSuite Software (BD Biosciences).

2.2 Comparison of different PRPs effect on wound healing in vitro

2.2.1 Study design, platelet collection and PRP preparation

The study was conducted by the Transfusion Medicine Unit of the Azienda USL-IRCCS di Reggio Emilia in collaboration with the Unit of Clinical Immunology, Allergy and Advanced Biotechnologies and approved by the Institutional Board Review on 12 May 2022 (Reggio Emilia Ethics Committee, protocol number 2022/0062204), all recruited donors signed an informed consent according to the Declaration of Helsinki.

Platelet concentrates were collected by apheresis with an automated blood collection system (Mobile Collection System MCS+, Haemonetics Corp., Boston, MA, USA)[241] in anticoagulant ACD-A (40 ml of Acid Citrate Dextrose Solution A, ACD-A, Haemonetics, Italy) and plasma (160 ml). Prior to PRP preparation platelets were further diluted in plasma (200 ml of platelet concentrate + 150 ml of Plasma.VPlateletConcentrate:VPlasma=4:3) (Figure 6A). Leukodepleted Aphe PRP was obtained pooling together platelet concentrates from 4 different donors. Aliquots obtained from the pool were stored at -80 °C and used after a single freeze–thaw cycle. BC were obtained from separation of whole blood donations with Compomat G4 separator (Fresenius Kabi Medicare, Italy), as previously described[204]. Each BC was diluted in a solution having the same composition used for platelets from apheresis (ACD-A and plasma). 4 different diluted BC were combined in a Transfer bag (Transfer

bag BB*T200BM, Terumo, Italy) and centrifuged using a specific kit (TACSI PL kit, Terumo, Italy) in order to obtain a platelet concentrate. In the final step the platelet concentrate was diluted in plasma with the same ratio used for platelet concentrate from apheresis (Figure 6B). The pooled platelet concentrates were aliquoted and stored at -80°C to be used as Apheresis and BC derived PRPs after a single freeze–thaw cycle within one year. PRPs from Apheresis and BC were prepared to achieve the same final platelet count. This was verified prior to storage on both Apheresis and BC platelet concentrates, resulting in a platelet count of $580x10^3/\mu l$.

2.2.2 PRP preparation for in vitro experiments

In our experimental conditions, we investigated the release bioactive factors from PRPs and their effects on different cellular models. To this end, liquid and gel PRPs were prepared in 6-well Transwell for releasate collection experiments and in 24-well Transwell for cell culture experiments, respectively (Figure 6C) (6-well Cell Culture Inserts 0.4µm PET clear, 24-well Cell Culture Inserts 0.4 µm PET clear, cellQART, Germany). Aphe liquid, BC liquid, Aphe gel and BC gel PRPs were prepared as following in order to compare products with an equal final volume. Liquid PRPs were obtained by diluting PRPs with PBS (EuroClone, Italy) at a 3:1 ratio. Gel PRPs were prepared by activating platelets with thrombin and Calcium Gluconate. Briefly, PRPs were mixed at a 3:1 ratio with a solution of calcium gluconate (Galenica Senese, Industria Farmaceutica, Italy), thrombin (Homologous thrombin is a product of blood routinely obtained at Transfusion Medicine Unit of the AUSL-IRCCS of Reggio Emilia[252]) and PBS to achieve complete platelet activation and clot formation. The final concentration of calcium gluconate was 7.7 mg/ml while thrombin was diluted 6.5 times before use. For release experiments conducted in 6-well plates, 2 mL of PRPs were used per Transwell insert, while for cell culture experiments in 24-well plates, 0.4 mL of PRPs were used per insert. Experimental conditions are summarized in figure 6C.

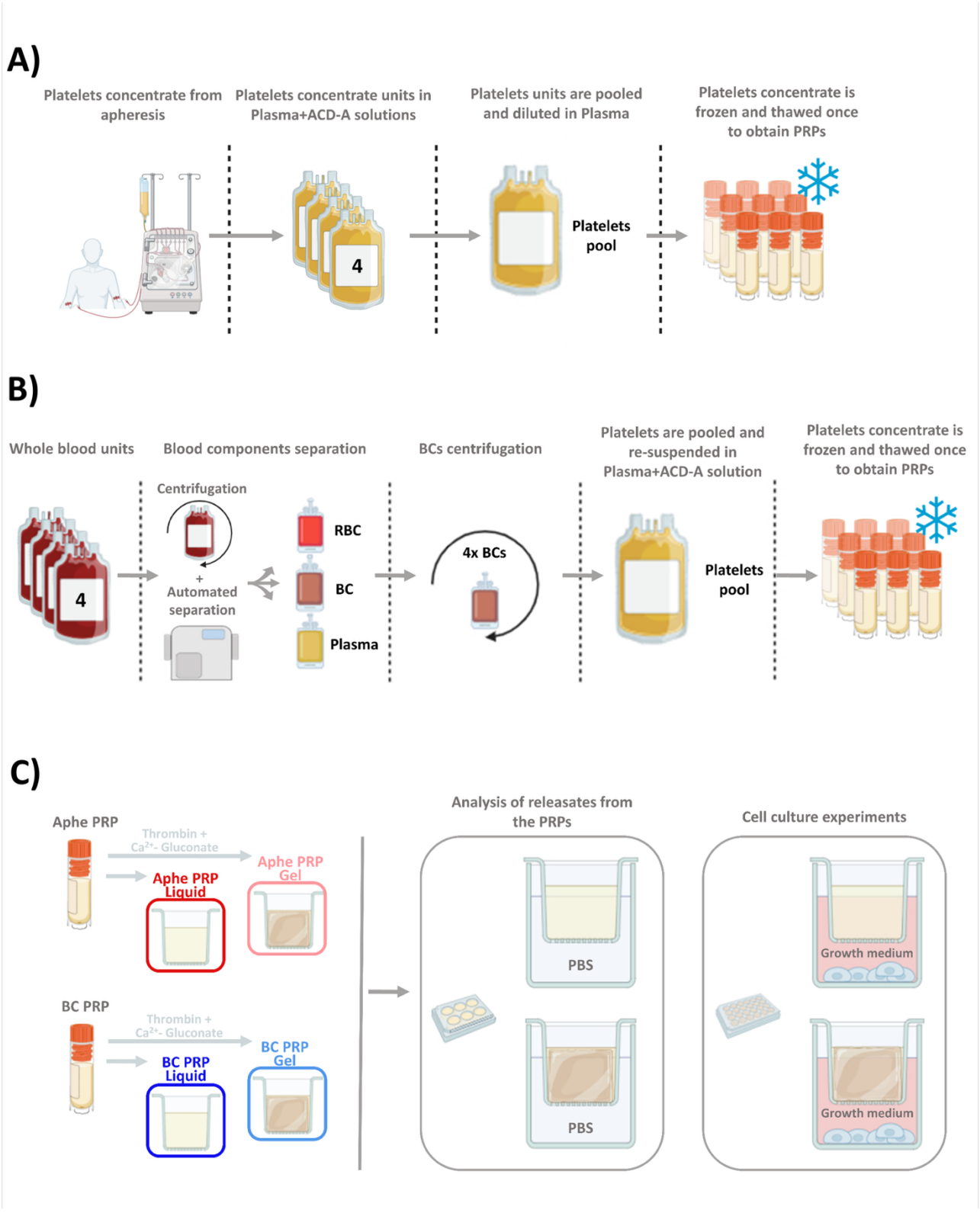

Figure 6. Schematic representation of: A) Procedure to obtain PRPs from a pool of platelet concentrate form Apheresis. B) Procedure to obtain PRPs from a pool of platelet concentrate from Buffy-Coat. C) Experimental setting for releasate biochemical characterization and cell culture experiments. Image created with Biorender.

2.2.3 Characterization of GFs and EVs released by PRPs

To evaluate the concentration of GFs and EVs released by PRPs (PRPs' releasate), liquid and gel PRPs were prepared in the upper chamber of 6-well Transwells as previously described, while 3 mL of filtered PBS were added to the lower chamber. PRPs' releasates were collected from the lower chamber every 24 hours over a period of 7 consecutive days. At each time point, the Transwell was transferred to a new well containing the same amount of PBS to allow the collection of the GFs and EVs released during the preceding 24-hour period (Figure 7 C). The experiment was performed in duplicate, resulting in approximately 6 mL of releasate collected per sample at each time point. Following collection, protease inhibitor cocktail 1:200 (Abcam, USA) was added to each sample and the releasates were stored at -20°C until further analysis.

GFs concentration, including EGF, CTGF, TGF-β1, PDGF-AA, PDGF-AB and FGF2, were measured in Aphe PRP, BC PRP and in PRP releasates at multiple time points (1-7 days). TGF-β1, PDGF-AB, and CTGF samples were concentrated (dilution factors for the different conditions ranged between 2.8 and 3.3) using Amicon Ultra-15 Centrifugal Filters (Sigma-Aldrich, USA) prior to GFs determination. ELISA assays were employed for quantification, following manufacturer protocols. Specifically, the assays used for the quantification of EGF, PDGF-AB, PDGF-AA were purchased from Sigma-Aldrich (USA). Data were collected using the GloMax® Discover Microplate Reader (Promega, USA). Concentrations were normalized according to concentration factors (measured values were multiplied for the dilution factor). The assays used for the quantification of TGF-β1, FGF2 (FGF basic/FGF2/bFGF) were purchased from R&D Systems (USA). The assay used for the quantification of CTGF was purchased from Abcam (UK, Human CTGF SimpleStep ELISA kit). Data were collected with the FLUOstar OMEGA instrument. (BMG LABTECH, Germany).

EVs released from PRPs were quantified in the releasates at each time point using a FACSLyrics flow cytometer (BD Bioscience, USA). EVs analysis was performed with the customized EV kit for flow cytometry (Custom Kit #626267 BD Biosciences, USA) as previously described[272]. Calcium concentrations in the releasates were measured using a Calcium Microplate Assay Kit (Biorbyt, USA), according to manufacturers' instructions. Citrate levels were quantified at T0 in both Aphe PRP and BC PRP using a colorimetric assay (MAK057 Citrate Assay Kit, Sigma-Aldrich, USA), in accordance with the manufacturer's guidelines.

2.2.4 Cell cultures

BJ cell line (human fibroblasts) was cultured at 37°C in high glucose Dulbecco's modified Eagle's medium (DMEM High Glc, EuroClone, Italy) supplemented by 10% fetal bovine serum (FBS, EuroClone, Italy) and 1% Penicillin-Streptomycin (Pen-Strep, Sigma Aldrich, USA). Cells were

detached 1 or 2 times per week keeping the confluence approximately under 90% in T75 flasks (CytoOne, Italy), growth medium was renewed 1-2 times a week. For PRPs experiments, BJ cells were seeded and, after 24 hours, cultured for additional 24, 48 and 72 hours in presence or absence of TGF-β (TGF-β1, GF345, Millipore, Germany) at 10 ng/mL, prior to PRP treatment. The 72 h TGF-β treatment was selected and used for most of the experiments, as described in the Results section.
HaCaT cell line (human keratinocytes) was cultured at 37°C in DMEM High Glucose (EuroClone, Italy) supplemented by 10% fetal bovine serum (FBS, EuroClone, Italy) and 1% Penicillin-Streptomycin (Pen-Strep, Sigma Aldrich, USA). Cells were detached twice a week and kept at approximately 80% confluence in T75 flasks, with growth medium renewed 2-3 times per week. HaCaT cells were cultured and seeded in standard DMEM, at 24h from seeding DMEM was replaced by fresh standard DMEM or DMEM Low Ca2+ (Gibco, USA), in order to obtain HaCaT with differentiated and basal phenotype respectively and treated with PRPs.
Human Dermal Microvascular Endothelial Cells cell line (HDMEC, Cat.No.C-12212 PromoCell,Germany), were cultured in the Endothelial Cell Basal Medium MV (Cat.No.C-22220, PromoCell, Germany) supplemented with the Endothelial Cell Growth Medium MV SupplementPack (Cat.No.C-39220, PromoCell, Germany) at 37°C, 5% CO2. Cells were detached with Trypsin 0.025% - EDTA 0.25 mM (Thermo Fisher Scientific, USA). Trypsin was neutralized using PBS + 10 % FBS and cells centrifuged at 220 g for 5 minutes. HDMEC cells were seeded and, after 24 hours, cultured for additional 72 hours with the addition of PRPs. Heparin 2U/mL (Millipore, Germany) was added to the cell culture medium together with PRPs for all the experimental conditions and for cellular types in order to avoid fibrin activation. Treatment of PRP was evaluated in the presence of 0.1% FBS or Fetal Calf Serum (FCS).

2.2.5 Cell proliferation

Cell viability was measured using WST-1 cell proliferation assay (Cell Proliferation Reagent WST-1, Merck, Germany). Proliferation was assessed by adding WST-1 (1:20 in 300µl medium) to the cells for 4 hours at 37°C. Fluorescence was measured at 450 nm (GloMax Discover).
To investigate PRPs effect on cell viability BJ were seeded into a 24 well-plates (Euroclone, Italy) at a concentration of 3.000 cells/cm^2, HaCaT at a concentration of 30.000 cells/cm^2 and HDMEC at a concentration of 10.000 cells/cm^2. Proliferation was assessed after 72 hours of treatment.

2.2.6 Scratch assay and cell circularity

To assess cell migration, cells were allowed to grow to reach approximately 90% confluence. The medium was then removed and a linear wound was generated in HaCaT (seeded at 80.000 cells/cm^2), BJ (seeded at 17.000 cells/cm^2) and HDMEC (seeded at 60.000 cells/cm^2) monolayer using a sterile

10µl pipette tip (ClearLine, Dominique Dutscher, France) for HaCaT and BJ while a 1.000µl pipette tip (TipOne Filter Tips, Starlab, Italy) was used for HDMEC, because of their higher migration capacity. Wells were washed twice with PBS (EuroClone, Italy) to remove cellular debris, after that, fresh medium and PRPs treatment were added. Scratch was assessed at 48, 72 for BJ and HaCaT cells and at 64hours for HDMEC. Digital images of the wound area were acquired and the data were analyzed using ImageJ software[277]. Results were expressed either as the percentage of wound closure or as the number of migrated cells. For HaCaT cells and HDMEC cells, migration capacity was quantified by calculating the percentage of wound area closure, as the monolayer migrated as a compact front. Differently, for BJ cells, migration capacity was assessed by counting the number of individual cells that migrated into the wound area.

To assess cellular shape changes, cell circularity was measured at the same time points of the scratch assay. Digital images at 20X (BJ, HaCaT) or 4X (HDMEC) magnification were acquired and then analysed with ImageJ software. The area and perimeter of approximately 15 cells per condition across replicates were considered. Circularity was calculated, as a mean value of the replicates, using the following formula[279,280]:

$$Circularity: \frac{4\ x\ \pi\ x\ area}{perimeter^2}$$

2.2.7 Quantitative polymerase chain reactions (qPCR)

BJ, HaCaT and HDMEC were analysed for gene expression, all cell types were treated as described in the Results section prior to gene expression analysis. Cell culture conditions were the same described in the Cell Proliferation paragraph of the Material and Methods. RNA samples were isolated from BJ and HaCaT cells pellet with the Monarch® Total RNA Miniprep Kit (New England Biolabs, USA) following manufacturer's instruction. cDNA was obtained by reverse-transcribing the same amount of total RNA (200 ng) using the RevertAid RT Kit (Thermo Fisher Scientific, USA). Regarding HDMEC, RNA was extracted from the cells with the Quick DNA/RNA MicroPrep Plus kit (ZymoResearch, USA). The NanoDrop instrument (Thermo Scientific, USA) was used for RNA quantification. For gene expression, 45 ng of RNA were reverse transcribed with the PrimeScrip RT Reagent Kit with gDNA Eraser (Takara, Japan). For the real-time PCR, the following QuantiTect Primer Assay from QIAGEN (USA) were used: selectin E (SELE, QT00015358 - Hs_SELE_1_SG), von Willebrand factor (VWF, QT00051975 - Hs_VWF_1_SG), collagen type I alpha-2 (COL1A2, QT00072058 - Hs_COL1A2_1_SG). qPCR was performed on cDNA samples by using the GoTaq® qPCR Master Mix (Promega, USA), the reactions were carried out on the CFX Duet Real-Time PCR System (BioRad, USA). The other primers for qPCR were purchased from Eurofins (Italy) and their sequences are listed in the Table SD3. GAPDH was used for normalization.

2.2.8 Statistics

Statistical analysis was performed using GraphPad (Prism 8.4.2, GraphPad Software, USA) and Microsoft Excel 2010 (USA). One-way ANOVA with multiple comparisons test or two-tailed Student's t test were performed to assess differences among samples. Data were presented as mean ± standard deviation (SD). A P-value of <0.05 was considered statistically significant.

2.3 Anticoagulant-Dependent Interaction of Platelet EVs with Monocytes

2.3.1 Flow cytometry analysis

Whole blood samples were collected in vacutainer using 9mL Citrate-Vacuettes (Greiner Bio-one) and 6mL EDTA Vacutainer (BD), with respectively citrate and EDTA as anticoagulants. CD66b-APC (Beckman Coulter) was used as granulocyte marker, CD45-PB (Beckman Coulter) as leukocyte marker, CD14-PE (Beckman Coulter) and CD16-PC5 (Beckman Coulter) as monocyte markers. Lactadherin-FITC (LA, HTI) and CD41-PC7 (Beckman Coulter) were used as a marker of PS exposing P-EVs. A mix of antibodies was prepared as follows: 5µl of CD14-PE, CD16-PC5, CD66b-APC, CD45-PB, 1µl of CD41-PC7 and 3µl of LA-FITC were mixed and centrifuged at 18 000g for 10min at 4°C to pellet possible aggregates. The mix (24µl) was added to 200µl whole blood, from both citrate and EDTA samples, in a 2mL Protein LoBind tube (Eppendorf) and then incubated for 15min at RT in the dark. Subsequently, 1.8mL of diluted Lysis Buffer (1:10=BD FACS Lysing Solution:Aqua Bidest "Fresenius") were added to the stained whole blood samples. The samples were then incubated for 10min at RT in the dark and then centrifuged at 500g for 5min to pellet lysed cells. The supernatant was discarded and the pellet washed with 900µl of sterile filtered (0.1µm filters) $DPBS^{-/-}$ (w/o Ca^{++} and Mg^{++}, GIBCO) and transferred into a 1.5mL LoBind tube (Eppendorf). Samples were centrifuged again at 500g for 5min and the pellet was resuspended in 500ul of $DPBS^{-/-}$. Samples were analyzed using flow cytometry (Beckman Coulter CytoFlex LX) immediately after collection and after 3.5hours of gentle agitation at RT to assess changes in P-EVs to monocyte interactions and blood stability. CD66b/SSC-H was used to identify granulocytes and exclude them from the analysis. CD14/CD45 was used to visualize both leukocytes and monocytes, which then were gated by C14/CD16 into different monocytes subset: classical ($CD14^{++}/CD16^{-}$, CM), intermediate ($CD14^{++}/CD16^{+}$, IM) and non-classical ($CD14^{+}CD16^{++}$, NCM). Within monocytes subset gates, LA and CD41 were used to identify P-EVs to monocytes interactions.

3 RESULTS

This section follows the same structure as Material and Methods.

3.1 Characterization of cryopreserved platelets and development of an optimized cryopreservation solution

3.1.1 Cryopreservation affects coagulation capacity and activation profile of Cryo-PLT vs. Fresh-PLT

To evaluate platelets recovery after cryopreservation, we compared platelet counts before freezing and after reconstitution of the thawed units in T-PAS as the resuspension medium. The mean platelet count in fresh samples was 1206 ± 160 × 10^3/ µL while post-thaw it was 983 ± 189 × 10^3/µL, corresponding to a recovery rate of 81%. We then assessed the haemostatic activity of Fresh- and Cryo-PLT resuspended in T-PAS after 1, 3 and 6 hours post-thawing using ROTEM delta parameters (CT, CFT, MCF).

All ROTEM parameters were significantly impaired after thawing (ANOVA overall effect, $p < 0.01$). Specifically, INTEM and EXTEM analysis revealed prolonged CT and CFT following cryopreservation compared to Fresh-PLT (Figure 7A,B). Among post- thawed samples, CT further increased significantly after 6 hours compared to 1 and 3hours in INTEM and NATEM assays, respectively (Figure 7A). Cryopreservation also reduced clot strength, as shown by decrease of MCF (Figure 7C) and lower clot amplitude at 20 min from CT (Figure SD1).

To assess platelet activation post-cryopreservation, we performed flow cytometry analysis of CD62P exposure, comparing Cryo-PLT with thrombin-activated and non-activated Fresh-PLT. In non-activated (NA) samples, CD62P-associated median fluorescence channel (MFC) values increased from 296.2 ± 19.4 of Fresh-PLT (Figure 7D, black area) to 405.5 ± 41.7 of Cryo-PLT at 1 h post thaw (Figure 7D, light gray line), alongside an increase of CD62P-positive events in Cryo-PLT at all post-thaw time points analyzed (Figure 7E). However, CD62P exposure in Cryo-PLT was less evident compared to activated Fresh-PLT (Fresh-A) which showed an MFC of 593.0 ± 154.6 (Figure 7D, light blue) and a percentage of 56.1% ± 5.0 (Figure 7E, light blue) of CD62P-positive events. Notably, Cryo-PLT failed to respond to thrombin stimulation post-thaw, showing no additional increase in CD62P expression (Figure SD2).

Cryopreservation resulted in a reduction of CD42b-positive platelets, while the proportion of CD41a-positive PLT increased compared to Fresh-PLT (Figure 7F,G). A slight decrease of CD61-positive PLT was also observed following cryopreservation (see Table SD1), whereas agonist stimulation induced an increase in CD61 expression only in fresh samples.

Intriguingly, the reduction of CD42b-positive platelets after cryopreservation was accompanied by a CD41a-positive/CD42b- negative platelet subpopulation (Figure 7J, fuchsia dots). This subpopulation was also negative for CD62P expression (Figure 7M, fuchsia lines). In contrast, fresh activated PLT expressing both CD41a and CD42b (Figure 7I, L), were positive to CD62P, whereas Fresh- PLT NA (Figure 7H, K) were not. These data indicate that cryopreservation induces significant alterations in the surface marker profile and activation of platelets which may lead to a deterioration of clotting capacity.

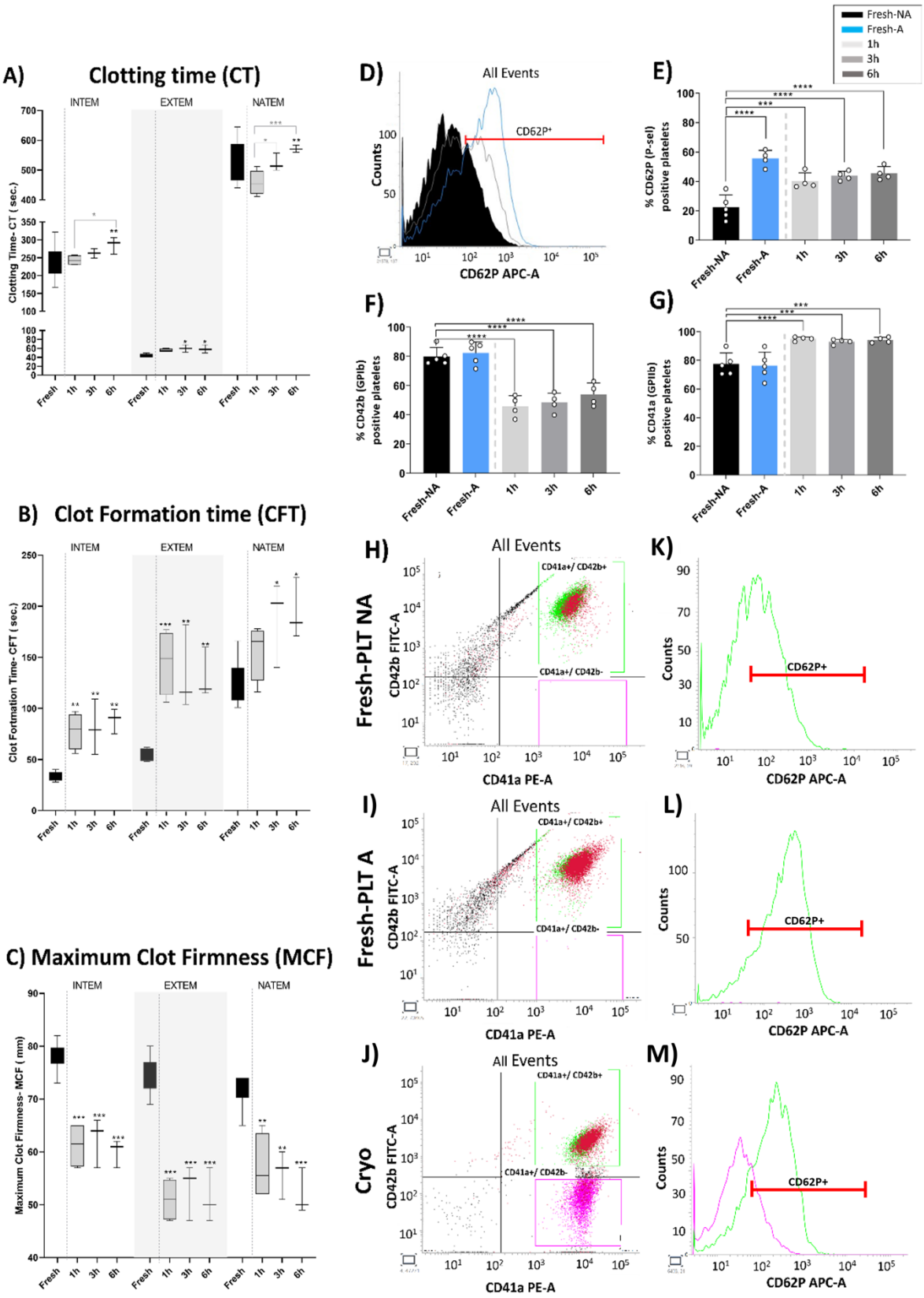
A) Clotting time (CT)
INTEM
EXTEM
NATEM
Clotting Time- CT (sec.)
Fresh
1h
3h
6h
B) Clot Formation time (CFT)
Clot Fortmation Time- CFT (sec.)
C) Maximum Clot Firmness (MCF)
Maximum Clot Firmness- MCF (mm)
D)
All Events
CD62P+
Counts
CD62P APC-A
E)
Fresh-NA
Fresh-A
1h
3h
6h
% CD62P (P-sel) positive platelets
F)
% CD42b (GPIb) positive platelets
G)
% CD41a (GPIIb) positive platelets
H)
All Events
Fresh-PLT NA
CD41a+/ CD42b+
CD41a+/ CD42b-
CD42b FITC-A
CD41a PE-A
K)
Counts
CD62P+
CD62P APC-A
I)
All Events
Fresh-PLT A
CD41a+/ CD42b+
CD41a+/ CD42b-
CD42b FITC-A
CD41a PE-A
L)
Counts
CD62P+
CD62P APC-A
J)
All Events
Cryo
CD41a+/ CD42b+
CD41a+/ CD42b-
CD42b FITC-A
CD41a PE-A
M)
Counts
CD62P+
CD62P APC-A

Figure 7. **Cryopreservation affects coagulation capacity and activation profile of Cryo-PLT vs. Fresh-PLT.** A) clotting time (CT), B) clot formation time (CFT) and C) maximum clot firmness (MCF) for INTEM, EXTEM and NATEM assays in Fresh- and Cryo-PLT analyzed at different time points after reconstitution (1 h, 3 h and 6 h). Data are represented as median with interquartile ranges. D) overlay cytogram of CD62P+ PLT in: fresh non activated samples (Fresh-NA, black), PLT activated with thrombin (Fresh-A, light blue) and Cryo-PLT after 1 h from thawing (1 h, light gray). E) CD62P, F) CD42b, G) and CD41a exposure on Fresh-(NA and A) and Cryo-PLT at different time points after thawing (1 h, 3 h and 6 h). Data are represented as percentage % of positive events and reported as mean ± SD. H, I, J) gating strategy to discriminate CD41a+/CD42b+ (green dots) and CD41a+/CD42b− (fuchsia dots); K, L, M) CD62P expression PLT in Fresh-(NA and A) and Cryo-PLT based on gated population CD41a+/CD42b+ (green curve) and CD41a+/CD42b− (fuchsia curve). Statistical analysis was performed using one-way ANOVA with multiple comparisons *p < .05, **p < .01, ***p < .001, ****p < .0001. Black * and lines indicate significant differences from the Fresh-PLT, while gray * and lines indicate differences among time points after thawing.

3.1.2 PS exposure and EVs shedding are linked to membrane modifications occurring over time after thawing

PS exposure and EVs release were assessed by flow cytometry. As reported in Figure 8A, Cryo-PLT samples 1 h after thawing (1 h, light gray) exhibited an increase of PS-positive platelets (77.0 ± 8.4%) compared to non- activated Fresh-PLT (Fresh-NA, 36.5 ± 4.2), with percentages comparable to fresh activated samples (Fresh-A, 73.0 ± 5.5). Although the increase in PS exposure remained statistically significant, it gradually declined at 3 and 6hours post-thaw. Similar results were obtained with the EVs quantification assay reported in Figure 8B, that showed a 38-fold EVs increase in 1 h post-thaw Cryo-PLT over the non-activated Fresh-PLT (Fresh-NA). Of note, cryopreservation induced a 7-fold increase of EVs also when compared with thrombin-activated Fresh-PLT (Fresh-A). Again, EVs release decreased slightly at 3 and 6 hours after thawing (Figure SD3 and Table SD2) but the differences were not significant. Thrombin-stimulated platelets showed no statistical difference before and after thawing at any of the time points evaluated for both PS exposure (Figure SD3) and EVs formation (Figure SD3 and TableSD2).

FTIR spectroscopy was performed to evaluate the influence of cryopreservation on membrane phospholipids and protein folding. After collection and pre-processing, data were analyzed using both univariate and multivariate approaches. The average absorbance spectra of the data are shown in Figure SD4 of the supplemental data. At a first glance, no major differences could be spotted among the four spectra of Fresh-PLT and Cryo-PLT at 1 h, 3 h and 6 h after thawing. Therefore, specific

bands ratios were calculated (Figure 8C–F). The complete range of CH2-CH3 stretching bands (2800–3000 cm^{-1}) was used to evaluate the lipid content, while the ratio of the single asymmetric stretching bands of CH2 and CH3 was used to evaluate the membrane relative composition, integrity and stiffness[281]. In Figure 8C, the CH2/CH3 ratio increased with time after thawing; Fresh-PLT, 1 h and 3 h Cryo- PLT values were significantly different, whereas 3 h and 6 h were not. Since this ratio is associated to an average membrane composition or stiffness, this trend indicated that the membrane became stiffer at the different time points after thawing.

The proteins/lipids ratio (Figure 8D) was used to evaluate the variation of protein material among the PLT samples with time. In this case, we observed a loss of proteins after thawing, which was noticeable up to 3 h, and then at 6 h became stable.

Figure 8E, F show the lipid and protein peroxidation status by assessing the C=O/proteins and C=O/lipids ratios, respectively. Both values increased with time after thawing, indicating a possible ongoing mild oxidative process. Again, no clear distinction could be made between 3 h and 6 h.

To highlight subtler spectral variations that were not appreciable in the absorbance data, we performed a PCA on the normalized second derivative spectra[282]. In Figure 8G the score values of the acquired spectra on PC1 (x) and PC3 (y) are plotted as a scatterplot. With this representation, Fresh-PLT and Cryo-PLT at 1 h overlap, even though, from the projection representation of the same data on their respective Principal Component (Figure 8H, I), their centroid and distribution are significantly different ($p \leq .001$). Data at 3 h and 6 h after thawing are separated from Fresh-PLT and those at 1 h after thawing along PC1, whereas PC3 separates 3 h (upper quadrant) from 6 h (lower quadrant). In order to identify the spectral features that explain the grouping in different zones of the PCA plane of the data, loading vectors have been plotted in Figure 8J. The PC1 vector that represents 43.5% of the data has the strongest signals in the protein region, one positive at 1655 cm^{-1} and one negative at 1625 cm^{-1}; the first can be assigned to proteins in α- helix conformation, which were found to be higher in Fresh-PLT samples and Cryo-PLT after 1 h from thawing, while the second can be assigned to proteins in β-sheet conformation, higher in Cryo-PLT samples at 3 h and 6 h. Therefore, we can hypothesize that the protein components of the platelets undergo a partial rearrangement of folding already 1 h after thawing, probably due to some oxidative processes (Figure 8E,F)

Spectral features on PC3, that explain 7.4% of the variance within the data, mainly refer to the separation between 3 h and 6 h samples. In this case, the more intense signals are in the range of lipids aliphatic chains (CH2-CH3 stretching bands, 2800–3000 cm^{-1}), and precisely at 2918 and 2848 cm^{-1}. These signals are similar for Fresh-PLT (NA or A) and 1 h samples, whereas at 3 h from thawing are higher and lower at 6 h. Other two strong positive peaks are in the protein region at 1625 cm^{-1} for the Amide I and 1550 cm^{-1} for the amide II. Similarly, to the assignment of this peak for PC1, these

signals can be read as a hint of a lower misfolding of platelets at 3 hours from thawing (3 h) compared to those at 6 hours (6 h).

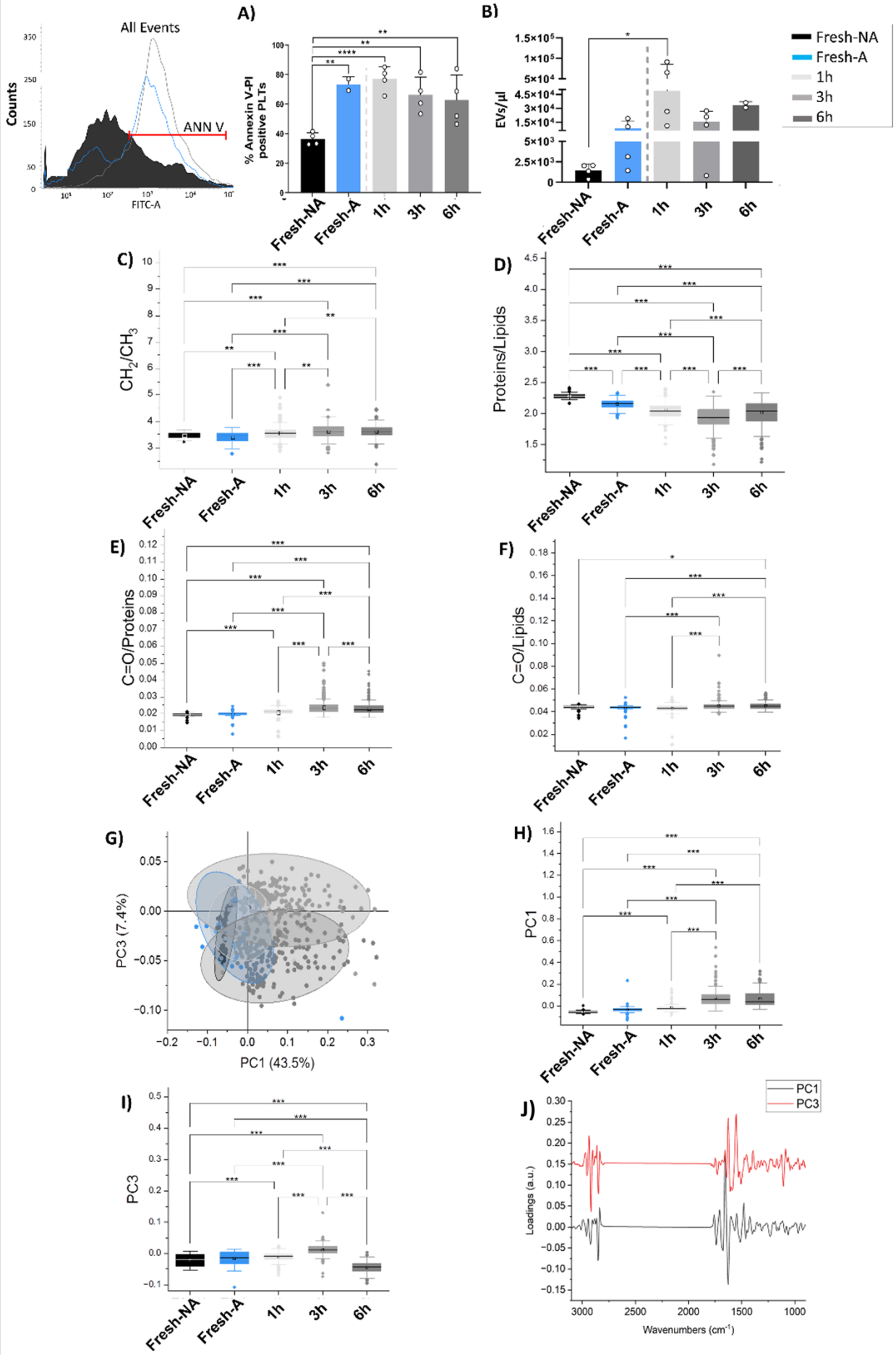
A)
All Events
Counts
ANN V
FITC-A
% Annexin V-PI positive PLTs
Fresh-NA
Fresh-A
1h
3h
6h
B)
EVs/µl
Fresh-NA
Fresh-A
1h
3h
6h
C)
CH2/CH3
D)
Proteins/Lipids
E)
C=O/Proteins
F)
C=O/Lipids
G)
PC3 (7.4%)
PC1 (43.5%)
H)
PC1
I)
PC3
J)
PC1
PC3
Loadings (a.u.)
Wavenumbers (cm-1)

Figure 8. PS exposure and EVs shedding are linked to membrane modifications occurring over time after thawing. A) Annexin-V positive events recorded in Fresh-(NA and A) and Cryo-PLT at different time points after thawing (1 h, 3 h and 6 h) evaluated by flow cytometry and reported as percentage (left panel) mean ± SD (right panel). B) Extracellular vesicles enumeration (EVs/μL) derived from Fresh-PLT (NA and A) and Cryo-PLT analyzed by flow cytometry after thawing (1 h, 3 h and 6 h). One-way ANOVA with multiple comparisons was used to evaluate statistical significance: $**p < .05$; $****p < .0001$. C) CH2/CH3 ratio; D) proteins/lipids (Amide I/CH2-CH3 stretching bands) ratio; E) carbonyl/proteins (C=o/amidei) ratio F) Carbonyl/lipids (C=o/lipids) ratio in Fresh-(NA and A) and Cryo-PLT at different time points after thawing (1 h, 3 h and 6 h) evaluated by FTIR. G) scatter plots of the PCA scores for PC1 and PC3, representing the 43.5% and 7.4% of variance, respectively. Centroid and distribution comparison of H) PC1 and I) PC3 respectively. J) loading vectors of PC1 (black) and PC3 (red). $*p < .05$, $**p < .01$, $***p < .001$, black * and lines indicate significant differences calculated with Tukey method. Data are presented as box 25–75% range of the data, whiskers range within the 1st quartile, line: median line, square: mean, black diamonds: outliers. FTIR unsupervised principal component analysis (PCA).

3.1.3 Cryopreservation induces platelet degranulation

We assessed platelet degranulation by measuring the levels of clinically relevant soluble mediators in PLT supernatant of both Fresh- and Cryo-PLT samples. One hour after thawing, Cryo-PLTs showed a modest but statistically significant increase in several soluble factors (Figure 9A–C), with the most relevant change observed in RANTES which increased by 55%. In contrast, TGF-β levels (Figure 9D) were reduced in Cryo-PLT supernatants compared to those from fresh PLTs, indicating a divergent release pattern. No further changes in soluble factor levels were observed at later time points (data not shown).

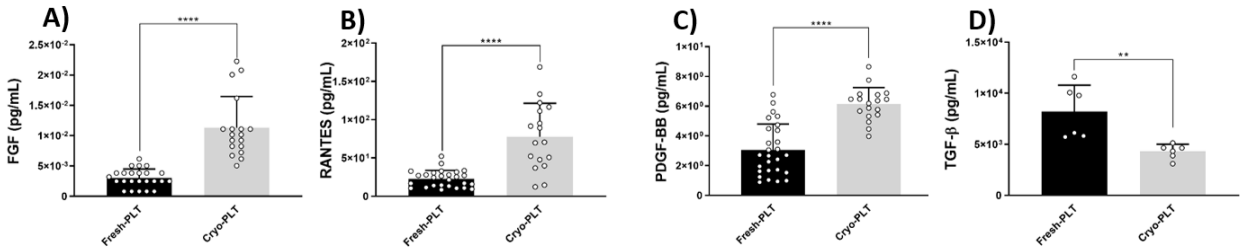

Figure9. **Soluble mediators' levels in PLT supernatants**. ELISA assay was performed on supernatants of Fresh- and Cryo-PLT (after 1 hour from thawing). $^{**}p < .01$ $^{****}p < .0001$.

3.1.4 Cryo-PLT has lower pro-tumoral effect and adhesive capacity compared to Fresh-PLT in MCF-7 and HL-60 cell lines

We used MCF-7 and HL-60 cancer cells to investigate the effect of Fresh and Cryopreserved PLT supernatants on cancer cell proliferation by means of WST1 (see Table 2 for details on culture conditions). For these experiments, we tested only 1 hour after thawing based on soluble mediators' data (Figure 10). Although no statistically significant differences were observed between the conditions, Figure10A shows that MCF-7 cells treated with Fresh- and Cryo-PLT supernatant had a proliferation pattern compared to the negative control (CTRL-). On the other hand, supernatant from Fresh-PLT was able to induce proliferation of HL-60 cells at 72 h, reaching levels comparable to positive control (CTRL+), wherease supernatants from Cryo-PLT had no noticeable effect and remained similar to the negative control (Figure 10B).

To evaluate the impact of PLT supernatants on MCF-7 cells migration, a scratch wound healing assay was performed. As shown in Figure 10C, cells treated with PLT supernatant exhibited a slower overall wound closure rate after 72 hours compared to both positive and negative controls. Although the differences were not statistically significant, a slight difference between Fresh- and Cryo-PLT was found after 72 hours, with the wound closure higher upon treatment with Fresh-PLT.

To assess PLT ability to bind cancer cells, MCF-7 and HL- 60 cells were incubated for 30 minutes with either Fresh or Cryo-PLT, followed by staining with a fluorescently labeled CD41a antibody and analysis by flow cytometry. The percentage of CD41a-positive events, indicative of cancer cells coated with platelets, is reported in Figure 10D. Untreated cells served as CTRL-. Platelets, whether fresh or cryopreserved, were unable to adhere to MCF-7 cells, while the HL-60 displayed a high percentage of CD41a-positive events. Notably, Cryo-PLT demonstrated a reduced capacity to interact with cancer cells, as evidenced by a lower number of CD41a-poisitive events in the HL-60 region (Figure 10D).

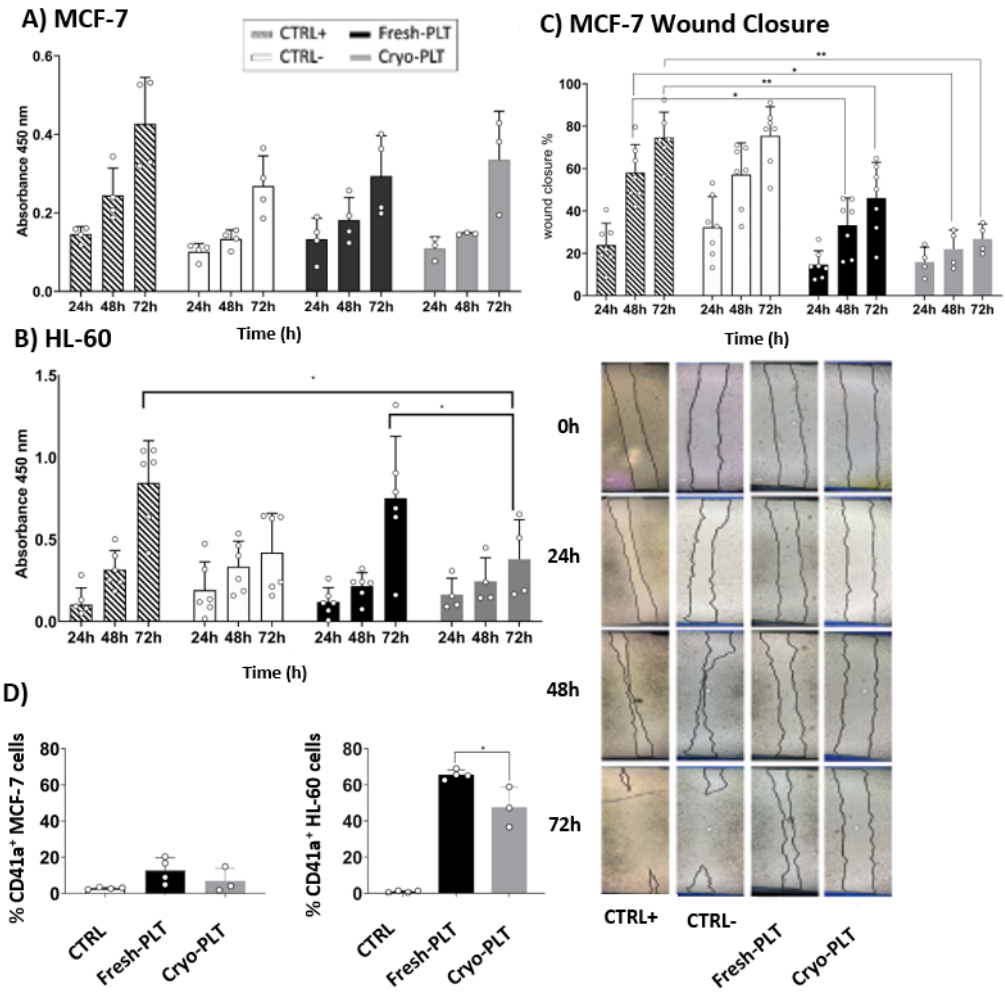

Figure 10. Effect of PLT supernatants on cancer cells behaviour in vitro. Proliferation of A) MCF-7 and B) HL-60 cell lines conditioned with supernatants from Fresh- and Cryo-PLT evaluated by WST1 assay at 24, 48 and 72 hours after seeding. C) Analysis of MCF-7 cells migration by in vitro wound healing assay. Quantification of the wounded area invaded by MCF-7 and time-lapse representative microscopy images of MCF-7 cells after 24, 48 and 72 h of conditioning with PLT supernatants. Data are reported as percentage (%) of wound closure at the baseline (T = 0 h after treatment). Results are reported as mean ± SD of three measurements of the wounded area, obtained in 5 independent experiments (n = 15). Dotted lines outline cell free areas. Scale bars, 100 µm. D) PLT- cancer cells adhesion. Percentage of CD41a-positive cells (MCF-7 or HL-60) following incubation with Fresh- or Cryo- PLT supernatant. Unconditioned cells (CTRL)served as negative controls. Data are expressed as mean ± SD of three independent experiments. Statistical analysis was performed using one-way ANOVA with multiple comparisons *$p < .01$, **$p < .005$.

3.2 Comparison of different PRPs effect on wound healing in vitro

3.2.1 GFs, Calcium, and Citrate quantification in Aphe and BC PRP at T0

GFs are key regulators of tissue regeneration, promoting cell proliferation, migration and differentiation. The concentrations of EGF, FGF2, CTGF, TGF-β1, PDGF-AA and PDGF-AB were measured in both Aphe PRPs and BC PRPs. No statistically significant differences in GF levels were observed between the two PRP preparations (Table 3). Ca^{2+} concentration was slightly higher in Aphe PRP (1.66 mM) compared to BC PRP (1.53 mM). Similarly, citrate concentration in Aphe PRP was 33.3 μM and 28.5 μM in BC PRP.

	Aphe PRP		**BC PRP**		**p-value**
	Mean	**StDev**	**Mean**	**StDev**	
EGF (pg/ml)	429.9	42.3	437.3	20.4	ns
FGF-2 (pg/ml)	92.9	4.4	86.2	2.3	ns
CTGF (ng/ml)	177.8	2612.0	176.9	2217.5	ns
TGF-β1 ng/ml)	195.6	2.3	187.6	3.3	ns
PDGF-AA (ng/ml)	872.4	25	832.7	32	ns
PDGF-AB (ng/ml)	16.9	0.6	18.0	0.9	ns

Table 3. GFs concentrations in Aphe and BC PRPs (n=2).

3.2.2 Release over time of GFs, EVs and Calcium from PRPs

Over time release of GFs, EVs and Ca^{2+} were measured in liquid PRP BC and Aphe over a 7 days period of time. GF concentrations were measured at 24 hours intervals, release values were normalized to the total amount of GF in each PRP type (Table 3) and expressed as a percentage of the total (Figure 11A). Comparative analysis between liquid and gel PRP revealed distinct release dynamics over the 7 days (Figure 11B and Table SD4). FGF2 remained below the detection limit across all conditions. In liquid PRP, EGF and CTGF exhibited rapid initial release, reaching their highest levels at the first time point (day 1), followed by a sharp decline, EGF dropped to below 50%, and CTGF to approximately 30% of their initial values. Conversely, TGF-β1 displayed a more

variable pattern, with fluctuating concentrations over time but an overall increasing trend throughout the 7 days. PDGF-AA and AB showed different release profile between Aphe and BC products: PDGF-AA levels decreased to a 30% of their peak by day 7, with BC PRP peaking at day 1 and Aphe PRP at day 4. PDGF-AB decreased to 50-60% of its maximum concentration at day 7, although Aphe PRP has a releasing peak at day 3 while BC PRP at day 1.

Interestingly, the total GFs released over the 7 days period varied among the different GFs: EGF and CTGF were released at 80-100%, PDGF-AA and AB at 15-25%, while TGF-β1 was released at 27 and 45% respectively for Aphe and BC PRP (Table SD4). In gel PRP relesate, GF concentrations were notably lower than those in liquid PRP, often by an order of magnitude or more. However, GF release from gel PRP followed a slower kinetic profile, with a gradual increase observed primarily during the last 3–4 days. An exception was EGF, which remained relatively constant throughout the 7-day period. Notably, in BC PRP, the release of PDGF-AA and -AB occurred earlier compared to Aphe PRP. TGF-β1 in gel PRPs started to be released after 6 days and at a higher rate in BC PRP.

In parallel, we quantified the release of EVs, which play a critical role in tissue regeneration, transporting GFs and other cellular effectors[283] (Figure 11C). Consistent with the GF release profile, EV release was significantly higher in liquid PRP compared to gel PRP. In gel PRP, EV levels remained close to the detection limit until day 6, with a marked increase occurring only on day 7. In contrast, liquid PRP exhibited a gradual and continuous increase in EV release over the entire 7-day period.

In addition, Ca^{2+} released (Figure 11D) was measured, given its pivotal function in various cellular processes, including those related to cell-cell adhesion and keratinocytes differentiation[284]. The calcium release profile exhibited a peak within the initial two days, followed by a gradual decline over the subsequent five days, displaying a similar pattern in both Aphe and BC PRP. As expected, calcium levels were consistently higher in PRP gel. This is attributed to the use of calcium (in combination with thrombin) during PRP gel preparation, where it facilitates platelet coagulation and gel formation (see Figure 11D and Materials and Methods). In liquid PRP, calcium release predominantly occurred within the first four days. By day 5, calcium levels approached the detection limit, indicating that the majority of calcium release had already taken place.

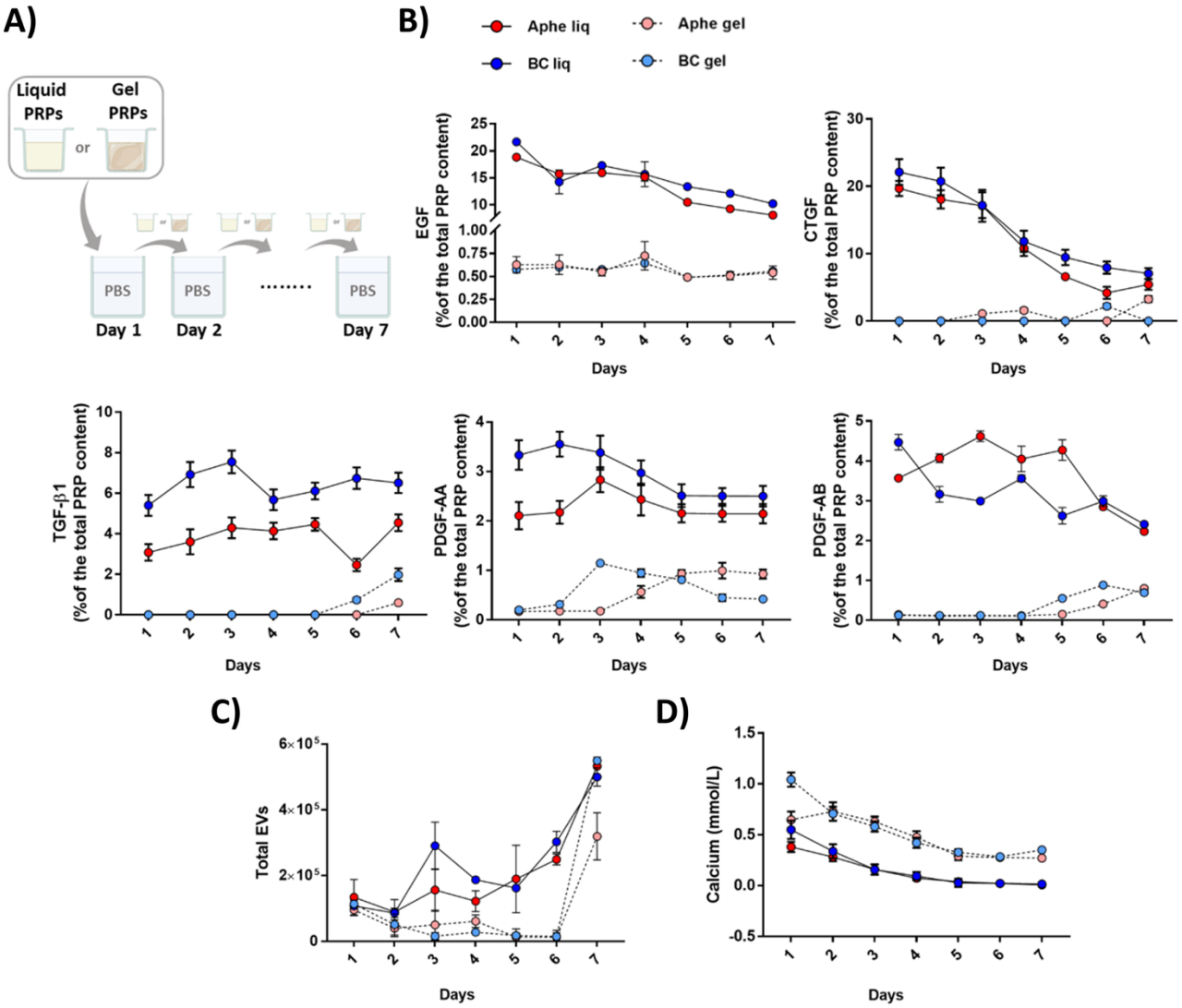

Figure 11. Release of Growth Factors (GFs), Extracellular Vesicles (EVs) and Calcium from Aphe and BC liquid and gel PRP. A) Schematic representation of the experimental design. B) EGF, CTGF, TGF-β1, PDGF-AA, PDGF-AB were normalized for PRPs GFs concentrations and expressed as % of them. C) Number of EVs released. D) Calcium concentration [mM]. Data are shown over 7 time points (days 1-7) for four different PRP preparations: Aphe liquid (red dots), BC liquid (blue dots), Aphe gel (pink dots) and BC gel (light blue dots). GFs were measured with ELISA, EVs release over time was evaluated by EVs quantification kit and flow cytometry, and calcium was quantified with a colorimetric calcium assay. Quantification was carried out on PRP releasate collected from the lower chamber of the Transwell insert every 24 hours over a period of 7-days.

3.2.3 Effect of PRPs on BJ fibroblast cells behaviour

Wound healing is a dynamic, multistage process involving cell proliferation and tissue remodelling. Fibroblasts migrate into the wound in response to various soluble mediators initially released by

platelets. Inflammatory cytokines such as TGF-β and PDGF stimulate fibroblast proliferation, migration to the wound site, and induce phenotypic changes that transform fibroblasts into myofibroblasts[285]. In vitro studies have shown that TGF-β drives fibroblast-to-myofibroblast differentiation within the wound microenvironment[286–288] with increased alpha Smooth Muscle Actin (αSMA) expression serving as a hallmark of this transition[286,289]. Accordingly, a significant increase (Fold change, FC, 9.6 and 6.1) of αSMA expression was observed in BJ cells in the FBS 0.1% condition, used as untreated control, at both 48 and 72 hours after treatment (Figure 12A). Therefore, the subsequent PRPs treatments were performed after 72 h of stimulation with TGF- β. To investigate how soluble mediators released by PRPs influence fibroblast behaviour, BJ cells[290] were used as a model to assess the effects of PRP on fibroblast proliferation, migration, morphology and differentiation (Figure 12B).

WST1 assay was performed to evaluate BJ cell proliferation (n≥3 replicates, Figure 12C). After 24 h of seeding, cells were cultured with or without TGF-β and subsequently treated with PRPs. BJ cells untreated controls showed significantly reduced viability compared to the 10% FBS standard growing control. The absorbance values shown in Figure 16C indicate that PRP treatments significantly enhance BJ cell proliferation compared to untreated controls, with the exception of Aphe PRP gel. Notably, liquid PRP formulations, regardless of their source (Aphe or BC), stimulated significantly higher proliferation than their gel counterparts. The pro-proliferative effect of PRP was further validated in the presence of TGF-β (+TGF-β), where all the tested PRP treatments increased cellular growth. Again, liquid PRPs demonstrated a significantly greater stimulatory effect compared to gel formulations (Figure 12C).

To assess the capacity of different PRP preparations to support fibroblast-mediated wound healing, a scratch wound assay was performed using the same PRP treatments as in the proliferation assay. Migration in FBS 0.1% was not lower than in FBS 10%, suggesting that the effect of FBS supplementation acts mainly on proliferation. After 48 hours, none of the PRP treatments significantly influenced cell migration compared to the controls (Figure 12D). Representative phase-contrast images of the scratch are reported in Figure SD5. Wound closure rates remained similar across all conditions, including the untreated control (≥3 replicates). Similar results were observed for the +TGF-β condition (Figure 12D). Although not statistically significant, BC liquid seemed to promote slightly greater wound closure compared to other PRP formulations (n≥3 replicates).

Given the minimal effect of both TGF-β and PRP on BJ cell migration, we next examined how PRP treatment influences fibroblast morphology, with or without TGF-β co-stimulation. Cellular shape changes were quantified using circularity measurement[279,280] (n≥14 cells for each condition), where low circularity levels indicate more elongated/spindle shape cells. Fibroblast circularity was not

significantly different when comparing the +TGF-β and –TGF-β untreated controls, although both conditions showed a decreased circularity when compared with the FBS10% culture. However, BJ cells became significantly more elongated when PRPs were added in TGF-β treated cells compared to –TGF-β cells, demonstrating a cumulative effect of PRPs and TGF-β (Figure 12E).

Representative phase-contrast images (Figure 12F) showed how liquid PRPs in co-treatment with TGF-β (lower line, +TGF-β) induced BJ to produce vortex-like structures (white row), suggesting an influence on cell polarization and a shift towards apico-basal polarity[291].

Among the key genes identified as marker of the differentiation of fibroblast into myofibroblast, we analysed the expression of αSMA (ACTA2), COL1A1, VIM and MMP1 after 3 days of treatment with PRPs (Figure 12G). Typically, αSMA, COL1A1 and VIM are expected to increase during with myofibroblast differentiation, while MMP1 is expected to decrease[286,289].

Our analysis revealed that in the untreated control (FBS 0.1%), the expression of αSMA, COL1A1 and VIM remained comparable, regardless of pre-treatment with TGF-β. However, MMP1 was significantly downregulated in the +TGF-β untreated condition (FBS 0.1%, Fold change, FC, 1.3, p-value<0.01). Conversely, COL1A1 decreased and MMP1 increased in 0.1% FBS when compared with 10% FBS, in both – and + TGF-β conditions, suggesting that this effect is caused by the FBS concentration and linked to cell viability. VIM increased instead only in the +TGF-β, which might thus be the cause of this gene expression difference (p-value<0.001.).

Interestingly, even in the absence of TGF-β, certain PRP conditions were able to modulate gene expressions associated with myofibroblast differentiation. For example, COL1A1 increased following treatment with PRP gels (both Aphe and BC, p-values<0.001).

Similarly, MMP1 was upregulated in both BC liquid PRP and Aphe gel PRPs (FC= 1.7 for both, p-values<0.01). In contrast, αSMA expression was significantly down regulated in response to Aphe liquid PRP (FC= 1.7, p- value<0.05), a finding that diverges from the typical upregulation associated with myofibroblast differentiation.

Nevertheless, in the presence of TGF-β, PRPs treatment modified gene expression with a pattern consistent with myofibroblast differentiation. In particular, PRP gels (both Aphe and BC) significantly increased the expression of αSMA compared to the untreated control (FBS 0.1%, p-values<0.001). Similarly, COL1A1 expression increased across all PRP conditions, with a more pronounced effect observed in the PRP gels (p-values<0.001). VIM expression was also more elevated in all PRP-treated cells, however, statistical significance relative to the control was achieved only in cells treated with Aphe PRPs (p-values<0.01). Conversely, MMP1 expression was down regulated in all conditions, with the most substantial reductions seen in Aphe liquid and BC gel PRPs (p-values respectively of <0.001, <0.001, <0.05 and <0.001).

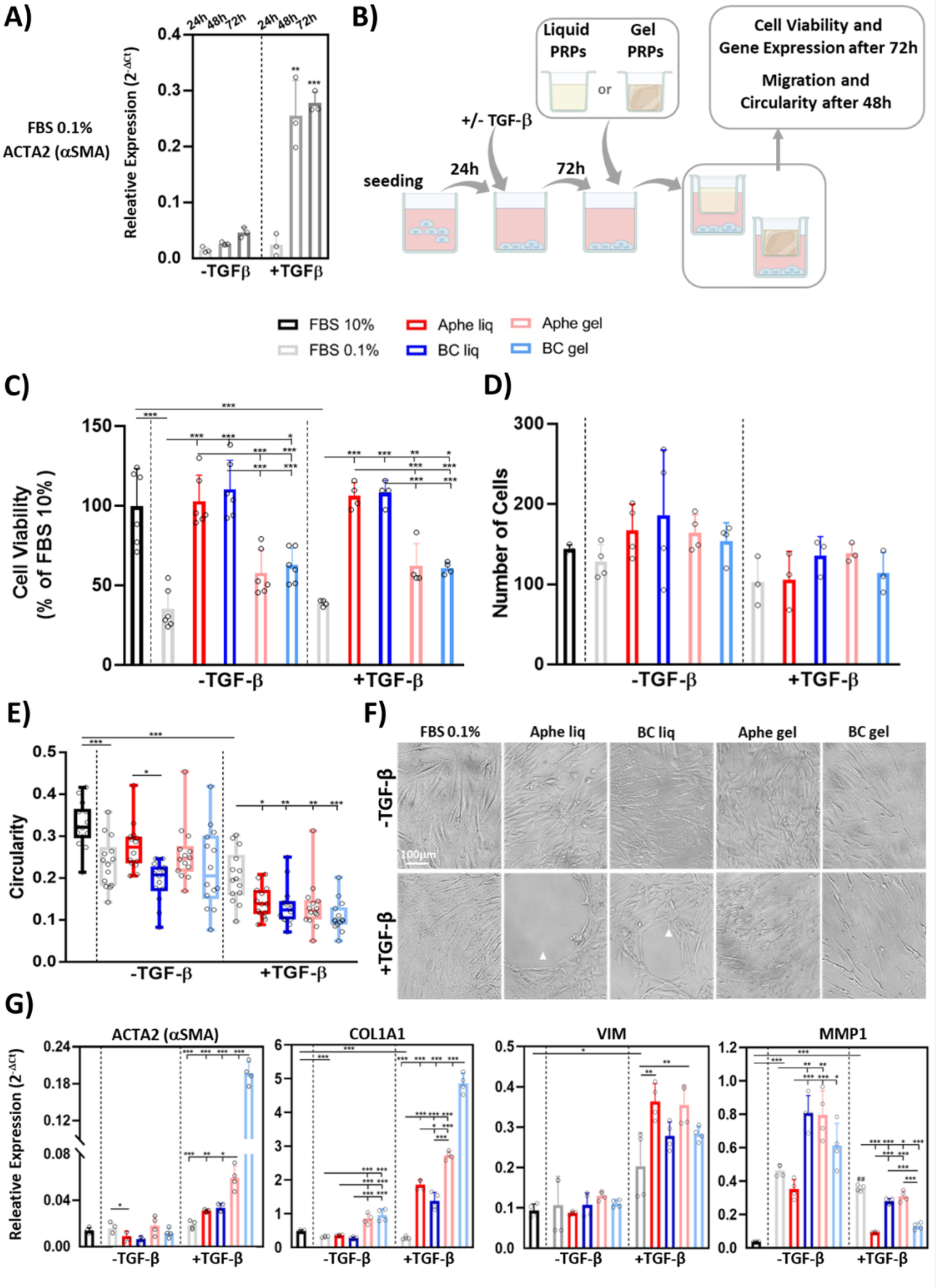
A)
FBS 0.1%
ACTA2 (αSMA)
Releative Expression (2-ΔCt)
24h 48h 72h 24h 48h 72h
-TGFβ
+TGFβ
B)
Liquid PRPs
Gel PRPs
or
+/- TGF-β
seeding
24h
72h
Cell Viability and Gene Expression after 72h
Migration and Circularity after 48h
FBS 10%
FBS 0.1%
Aphe liq
BC liq
Aphe gel
BC gel
C)
Cell Viability (% of FBS 10%)
-TGF-β
+TGF-β
D)
Number of Cells
-TGF-β
+TGF-β
E)
Circularity
-TGF-β
+TGF-β
F)
FBS 0.1%
Aphe liq
BC liq
Aphe gel
BC gel
-TGF-β
+TGF-β
100µm
G)
ACTA2 (αSMA)
COL1A1
VIM
MMP1
Releative Expression (2-ΔCt)
-TGF-β
+TGF-β

Figure 12. Effect of PRPs treatments on BJ cells in the presence (+TGFβ) or absence (-TGFβ) of TGF-β. TGF-β was added to the culture media at a concentration of 10 ng/ml and incubated for 24 hours prior to the addition of PRP treatments to the wells. A) Gene Expression**.** Levels of the myofibroblast differentiation markers ACTA2 (αSMA) was assessed in the presence (+TGFβ) or absence (-TGFβ) at different time points in FBS 0.1%. Significant differences were indicated for the comparison between -TGFβ and +TGFβ at the same time point. B) Schematic representation of the experimental design. C) Proliferation. WST1 assay was performed after 72 hours of PRPs treatment. n≥3 replicates D) Migration. Number of BJ cells migrated into a scratch test after 48 hours of treatment of with PRPs. Data are obtained by constructing a reference area and counting the number of cells migrating within the area over time. n≥3 replicates. E) Circularity. A cellular shape descriptor, circularity, was measured on n=14 cells/condition. Circularity is in a range between 1 and 0, where 1 identifies completely circular cells, and 0 sharp cells. F) Representative phase-contrast images of BJ cellular shape. Images are collected after 72 hours of PRPs treatment. White arrows indicate vortex structures of polarized cells. Scale bar 100μm. G) Gene Expression levels of specific myofibroblast differentiation markers. ACTA2 (αSMA), COL1A1, VIM and MMP1 expression ($2^{-\Delta Ct}$) in BJ fibroblasts evaluated by qPCR after 72 hours of treatment with PRP. n≥3 replicates.
Different bar colours indicate the following conditions: black for 10% FBS, grey for 0.1% FBS, red for liquid Aphe PRP, blue for liquid BC PRP, pink for gelified Aphe PRP and light blue for gelified BC PRP. Data are expressed as mean ± SD. Significance of data differences was established using unpaired two-ways ANOVA test with multiple comparisons. * p-value <0.05, ** p-value<0.01, *** p-value<0.001. ## indicate a p-value<0.01 between the FBS 0.1% untreated conditions of the TGFβ- and TGFβ+ settings.

3.2.4 Effect of PRPs on HaCaT keratinocytes cells behaviour

Keratinocytes proliferation and migration are essential in wound healing, a process partially regulated by growth factors present in PRP, such as EGF and TGF-β[292].
The immortalized human keratinocyte cell line HaCaT is widely used to model keratinocyte responses to various treatments, including PRP[293–295]. HaCaT cells are known to switch between a differentiated and basal state depending on extracellular Ca^{2+} levels[296]. We investigated the effects of PRPs on HaCaT cells cultured in both standard (DMEM) and low Ca^{2+} DMEM with limited proliferative stimuli (FBS 0.1%) to evaluate cellular proliferation, migration, morphology and differentiation (Figure 13A). For proliferation analysis, untreated controls (FBS 0.1%) were compared to cells treated with different PRP preparations (n≥3). FBS 0.1% controls (both in low and high Ca^{2+}) had a decreased viability when compared to 10% FBS. Under standard DMEM culture conditions, PRPs stimulated HaCaT proliferation, although this increase was not significant for BC PRP gel. Liquid

PRPs induced a more pronounced proliferative response than gel formulations. Under low Ca^{2+} conditions, untreated cells displayed significantly lower proliferation compared to standard DMEM cultured cells (#, p-value <0.05, Figure 13B), although PRP treatments significantly increased HaCaT proliferation, with a greater effect measured for gel PRPs. (Figure 13A). While PRPs stimulated cellular grow in low Ca^{2+} conditions, the resulting viability levels remained lower than those observed in standard medium (DMEM). In contrast, cells in high Ca^{2+} medium reached viability levels comparable to the 10% FBS control.

A wound scratch assay was performed to assess the impact of PRPs on wound healing (n≥3) after 72 hours of treatment (Figure 13C). Under low Ca^{2+} conditions, untreated HaCaT cells exhibited reduced wound closure capacity compared to standard DMEM (##, p-value <0.01). Similarly, FBS 0.1% controls showed diminished wound closure when compared to 10% FBS (although this difference was significant only for the low Ca^{2+} condition).

PRP treatments enhanced wound closure across both standard and low-calcium media. In standard DMEM, liquid PRPs significantly promoted wound closure, whereas the effect of PRP gels was less pronounced and did not reach statistical significance. The results demonstrated that liquid PRPs consistently outperformed gel formulations in promoting wound closure (Figure 13C). However, this difference was less evident under low Ca^{2+} conditions and was no longer statistically significant for Aphe gel. Representative phase-contrast images are reported in Figure SD5.

To further investigate cellular behaviour, HaCaT morphology was assessed by measuring cellular circularity (n≥14 cells for each condition, Figure 13D). In standard DMEM, cells exhibited a rounded morphology with no significant differences between conditions. As expected, low Ca^{2+} induced a more elongated morphology in untreated cells[297] compared to high Ca^{2+} FBS 0.1% control and to 10% FBS, while there was not any difference between these two latter conditions. Interestingly, PRPs reversed this effect, partially with liquid PRPs and fully with gel PRPs (Figure 13D).

Phase-contrast images (Figure 13E) after 72 hours of treatment revealed more defined cellular borders in low Ca^{2+} and in HaCaT cells treated with liquid PRPs, probably as a result of altered cell-cell junctions. The observed morphological changes in low calcium conditions induced by PRP gels may be attributed to their elevated calcium content, which is a consequence of their production methodology (see Figure 6B and Materials and Methods).

TGM1 (Transglutaminase 1) gene expression, a marker of keratinocytes and HaCaT differentiation[298–300], was assessed to determine the effect of the low/high Ca^{2+} in combination with the treatment with PRPs. Its expression was significantly lower in low Ca^{2+} compared to both high Ca^{2+} and FBS 10%. All the PRP-treated cells promoted an increase in TGM1 expression compared

to the FBS 0.1% control, in both low and high Ca^{2+}. This effect was slightly higher in liquid PRPs than in gel PRPs and in some cases this increase was significant (Figure 13F).

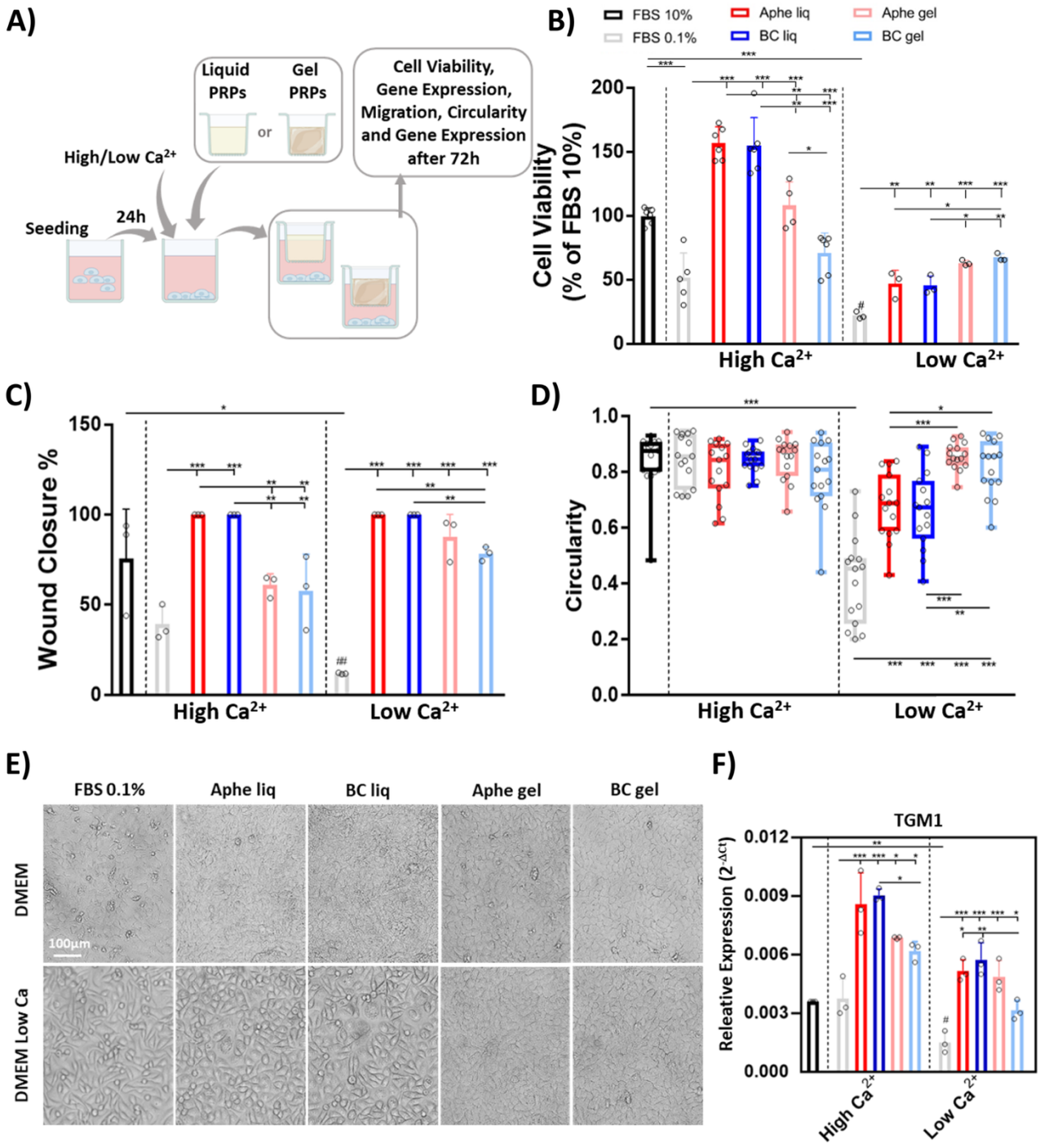

Figure 13. Effect of PRPs treatments on HaCaT cells in normal DMEM and Low Ca^{2+} medium. A) Schematic representation of the experimental design with HaCaT. B) Proliferation. WST1 assay evaluated after 72 hours of PRPs treatment. n≥3 replicates. C) Migration. Number of HaCaT cells migrated into a scratch test after 72 hours of treatment with PRPs. Data are obtained by constructing

a reference area and counting the number of cells migrating within the area over time. n≥3 replicates. D) Circularity. A cellular shape descriptor, circularity, was measured on n≥14 cells/condition. Circularity is in a range between 1 and 0, where 1 identifies completely circular cells, and 0 sharp cells. E) Representative phase-contrast images of HaCaT cellular shape. Images are collected after 72 hours of PRPs treatment. Scale bar 100μm. F) Gene expression levels of TGM1 from HaCaT grown in Low and High Ca^{2+} condition. Cells were treated for 72 hours with PRPs and compared with the untreated control (n=3). Different bar colours indicate the following conditions: black for 10% FBS, grey for 0.1% FBS, red for liquid Aphe PRP, blue for liquid BC PRP, pink for gelified Aphe PRP and light blue for gelified BC PRP. Data are expressed as mean ± SD. Significance of data differences was established using unpaired two-ways ANOVA test with multiple comparisons. * p-value <0.05, ** p-value<0.01, *** p-value<0.001.

3.2.5 Effect of PRPs on HDMEC dermal microvascular endothelial cells behaviour

In addition to keratinocytes and fibroblasts, skin function under both normal and pathological conditions is regulated by microcirculation, which plays a key role in mediating inflammatory responses, cell signalling, and migration[301]. Notably, endothelial cells themselves are often involved in tissue regeneration through tissue micro-vascularization and angiogenesis[302]. Herein we exploited a cellular model of skin microcirculation, specifically human dermal microvascular endothelial cells, HDMEC[303,304], to investigate the effects of PRPs on their cellular behaviour (Figure 14A).

HDMEC proliferation was assessed using the WST1 assay following a 72-hour treatment with four different PRP formulations (n≥3 replicates, Figure 14B). As previously described for BJ and HACAT cell models, HDMEC were cultured in a medium with low concentrations of GFs (0.1% FCS). Cells were treated with PRPs products for 72h and compared with the untreated control (0.1% FCS only) while HDMEC cultured with 5% FCS were used as standard comparative control. Untreated control showed reduced proliferation compared to cells cultured under standard conditions with 5% FCS (p-value<0.001), whereas all PRPs formulations significantly promoted HDMEC proliferation, with liquid PRPs showing a greater effect than gel PRPs.

PRP treatment significantly stimulated the migration ability of HDMECs, as demonstrated by the scratch assay (n≥3 replicates, Figure 14C), with the exception of the BC gel formulation. As observed with cell proliferation, liquid PRPs induced a stronger migratory response than PRP gel. The experiment was conducted over a 64-hour period, during which complete wound closure was observed in several conditions.

To further assess the impact of PRPs on HDMEC morphology, cellular circularity was evaluated after 64 hours of treatment. Cells cultured in FCS 0.1% showed reduced circularity compared to the FCS

5% condition (Figure 14D). Remarkably, treatment with all the PRPs reversed this morphological elongation, causing HDMEC to regain their circularity values. This effect was quantified by measuring circularity in at least n≥15 cells per condition (Figure 14D).

The expression of some key genes involved in vascular endothelial cell regulation (αSMA, COL1A2, SELE, VWF, n≥3 replicates) indicated that PRPs significantly promoted the expression of SELE. Aside from a modest increase in αSMA expression observed in the Aphe liquid PRP condition ($p < 0.05$), no significant changes were detected in the other genes (Figure 14E). SELE is an endothelial-leukocyte adhesion molecule involved in inflammatory responses that plays a critical role also in endothelial cell proliferation[305]. In accordance with proliferation data (Figure 14A) we found an increase of SELE expression after PRP treatments (Figure 14F). PRP treatment restored HDMEC proliferation, migration and their endothelial phenotype compared to the elongated shape of HDMEC in 0.1% FCS condition.

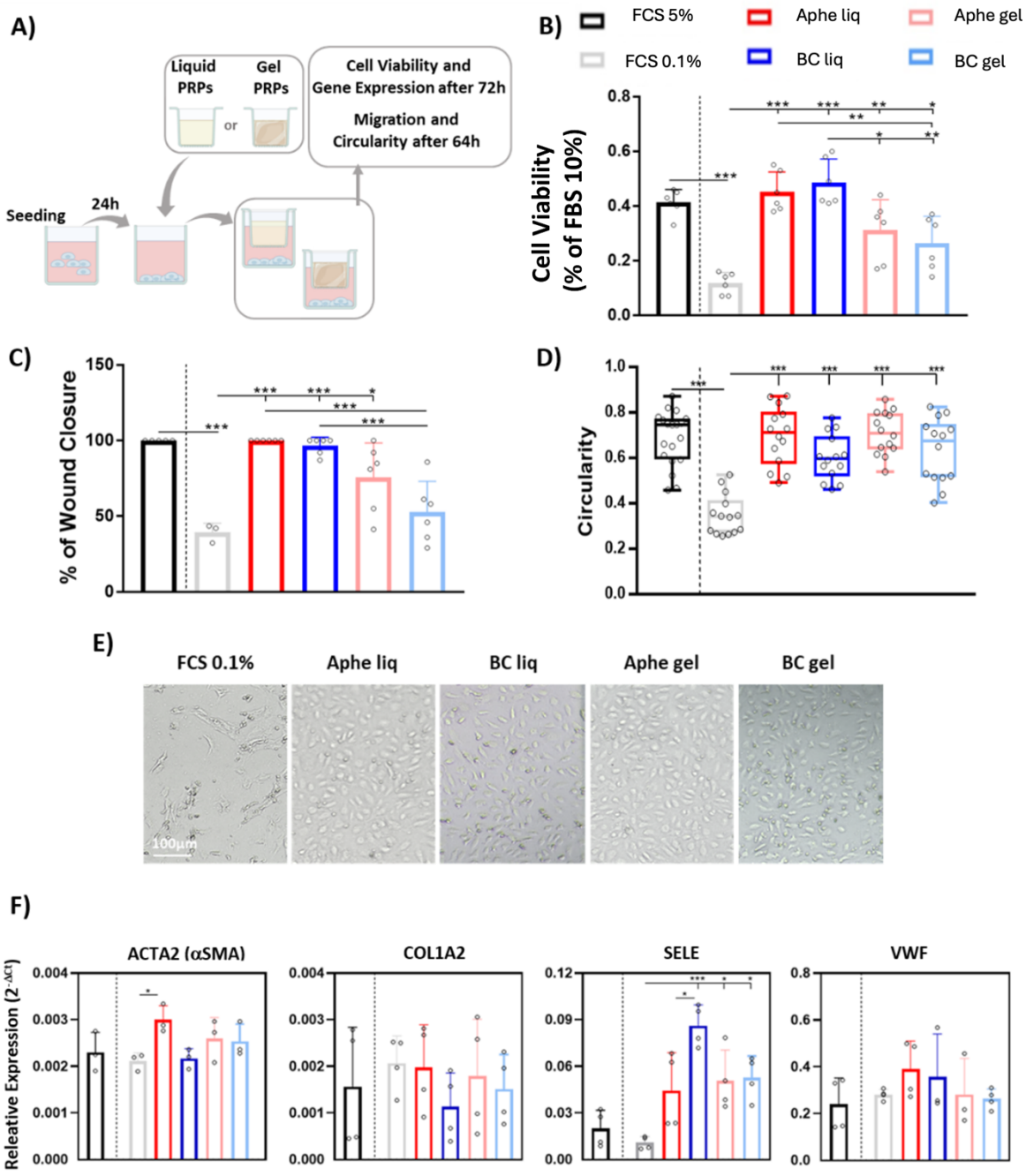

Figure 14. Effect of PRPs treatments on HDMEC investigating: A) Schematic representation of the experimental design with HDMEC. B) Proliferation. WST1 assay evaluated after 72 hours of PRPs treatment. n≥3 replicates. C) Migration. Number of HDMEC cells migrated into a scratch test after 64 hours of treatment with PRPs. Data are obtained by constructing a reference area and counting the number of cells migrating within the area over time. n≥3 replicates. D) Circularity. A cellular shape descriptor, circularity, was measured on n≥15 cells/condition. Circularity is in a range between 1 and 0, where 1 identifies completely circular cells, and 0 sharp cells. E) Representative phase-contrast images of HDMEC cellular shape. Images are collected after 64 hours of PRPs treatment. Scale bar 100µm. F) Gene Expression levels of specific EMT and normal endothelial markers.

ACTA2 (αSMA), VWF, SELE and COL1A1 expression ($2^{-\Delta Ct}$) in HDMEC fibroblasts evaluated by qPCR after 72 hours of treatment with PRP. Different bar colours indicate the following conditions: black for 5% FCS, grey for 0.1% FCS, red for liquid Aphe PRP, blue for liquid BC PRP, pink for gel Aphe PRP and light blue for gel BC PRP. Data are expressed as mean ± SD. Significance of data differences was established using unpaired two-ways ANOVA test with multiple comparisons and simple t-test for the comparison between FCS 5% and FCS 0.1%. * p-value <0.05, ** p-value<0.01, *** p-value<0.001.

3.3 Anticoagulant-Dependent Interaction of Platelet EVs with Monocytes

3.3.1 Evaluation of monocytes subset distribution and their interactions with P-EVs in citrate blood

We compared monocytes subset distribution in whole blood from the same donor but collected with different anticoagulants: citrate and EDTA. Samples were compared right after collection (0hour) and after 3,5 hours of gentle agitation. In Figure 15A, it is explained how the gating strategy was performed, see also Matherials and Method section for further explanation. As Figure 15B shows, the most abundant population in citrate whole blood after collection are the CM (green dots, 66,39%), followed by NCM (brown dots, 12,48%) and IM (orange dots, 7,70%). This did not change after 3.5hours from the collection (Figure 15J), however the only population that increased was the NCM going from 12,48% to 14,76%, while CM and IM decreased in percentage (respectively 58,27% and 6,18%).

EDTA whole blood monocyte distribution was assessed at the same time points (0 and 3,5 hours). CM remains the most abundant in both time points, being respectively 72,47% (green dots, Figure 15F) and 65,69% (green dots, Figure 15N). IM and NCM population increased a little during the 3.5hours agitation, respectively from 5,91% to 6,74% (orange dots, Figure 15F,N) and from 12,18% to 13,31% (brown dots, Figure 15F,N).

When comparing the monocyte distribution of the two different blood collection tubes, the differences are not very significant: at 0hour the percentage of CM ranges from 66.39% in citrate to 72.47% in EDTA, IM decrease from 7.70% in citrate to 5.91% in EDTA, and NCM were very similar. After 3.5 hours of gentle rotation, the percentage of CM decreased in both sample becoming respectively 58.27% in citrate and 65.69% in EDTA while IM remained approximately the same. NCM slightly increased in both tubes.

In Figure 15, from panel C to E and K to M, it can be appreciated the interaction between P-EVs and monocytes whole blood anticoagulated with citrate, right after the collection and 3,5hours after the collection. The gating shows general EVs (LAC+/CD41-), monocytes covered with platelets (LA-

/CD41+), monocytes covered with P-EVs (LA+/CD41+, upper right panel, UR) or monocytes w/o platelets (LA-/CD41-). Notably, the CD41+/LA+ (Figure 15C,K, UR panel) CM population increase from nearly 4% from after the collection to over 30% after 3.5hours. IM mirror this trend going from 5.78% (Figure 15D, UR) to 40.55% (Figure 15L, UR), while NCM increased slightly from 4.61% (Figure 15E, UR) to 10.07% (Figure 15M, UR). This indicates that the longer the sample is left standing, the more P-EVs or platelets with P-EVs adhere to the monocytes, suggesting that blood is not very stable in citrate. Panel from F to I and N to Q, shows P-EVs to monocytes interaction in whole blood anticoagulated with EDTA. CM and IM barely changed in the different time points, going respectively from 0.13% to 0.24% (Figure 15G,O, UR) and from 0.44% to 3.67% (Figure 15H,P, UR) . On the other hand, NCM increase from 2.46% right after collection to 10,21% after 3.5hours agitation (Figure 15I,Q UR), mirroring citrate sample.

Comparing the different tubes at the same time points analayzed it can be seen that at both 0 and 3.5hours from collection there are more P-EVs interacting with CM in citrate sample (Figure 15C,K, UR) than EDTA (Figure 15G,O, UR). The same thing happens with IM (Figure 15 D,H,L,P, UR) while NCM in citrate at 0hour (Figure 15E, UR) are higher than in EDTA (Figure 15M, UR) and reach the same amount (10%) at 3.5hours (Figure15 M,Q, UR).

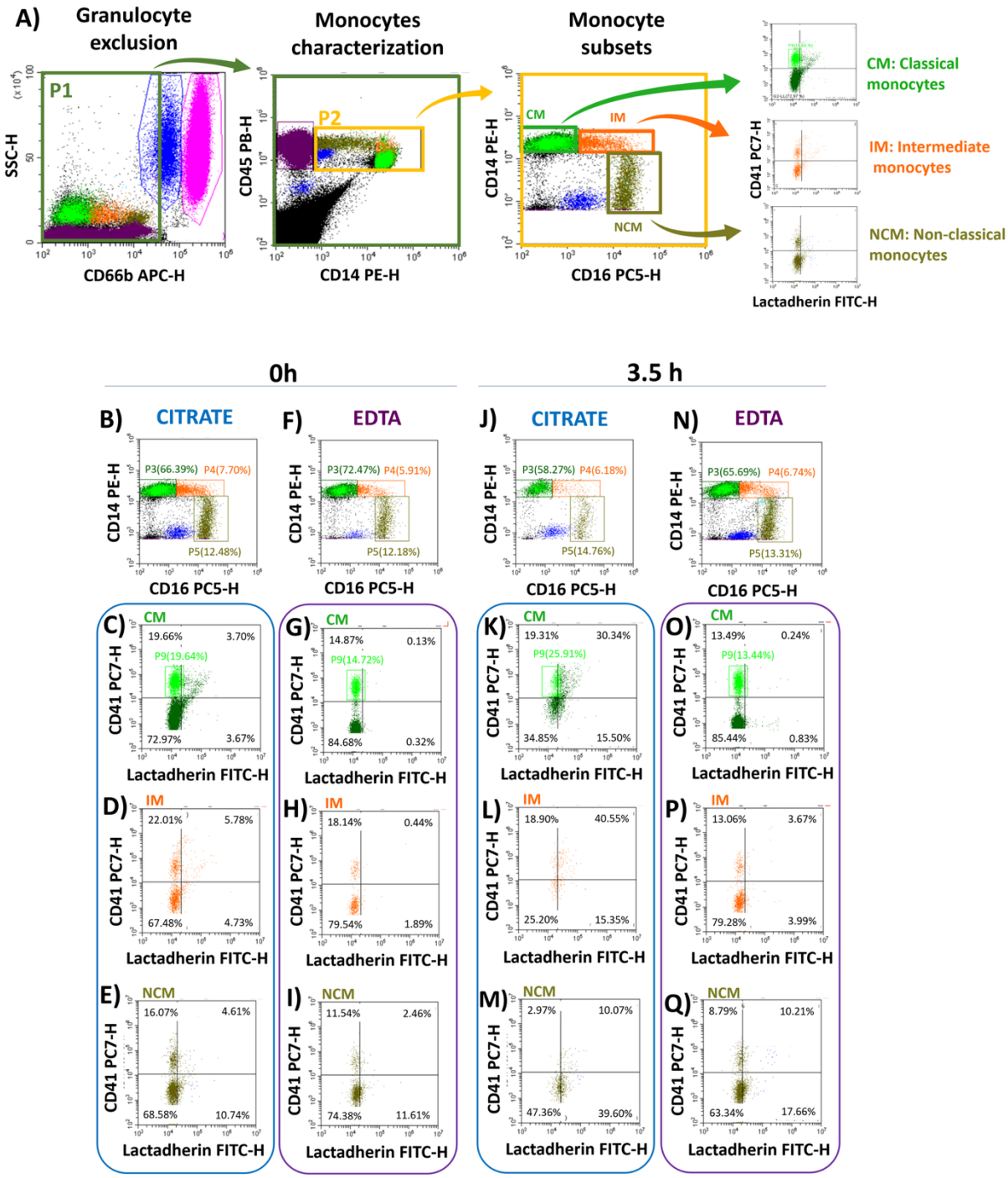

Figure 15. Determination of citrate and EDTA whole blood stability and P-EVs to monocytes interaction. A) Gating strategy used for the determination of monocyte subset distribution and P-EV to monocytes interaction, see Material and Methods, B) Monocytes subpopulation in citrate whole blood right after collection (0hour): classical monocyte (green dots), intermediate monocytes (orange dots) and non-classical monocytes (brown dots), C), D), E) Respectively CM, IM and NCM to P-EVs interaction in citrate at 0hours F) Monocytes subpopulation in EDTA whole blood right after collection (0hour): as explained above, G), H), I) Respectively CM, IM and NCM to P-EVs

interaction in EDTA at 0hours, J) Monocytes subpopulation in citrate whole blood after 3,5hours from collection: as explained above, K), L), M) Respectively CM, IM and NCM to P-EVs interaction in citrate at 3,5hours from collection, N) Monocytes subpopulation in EDTA whole blood after 3,5hours from collection: as explained above, O), P), Q) Respectively CM, IM and NCM to P-EVs interaction in EDTA at 3,5hours from collection. The analysis was conducted using Beckman Coulter CytoFlex LX flow cytometer.

4 DISCUSSION

This section follows the same structure as Material and Methods.

4.1 Characterization of cryopreserved platelets and development of an optimized cryopreservation solution

Platelets are routinely stored in blood banks at RT, limiting the shelf life to just 5–7 days due to the risk of bacterial contamination during storage[211]. Cryopreservation offers a potential alternative to room-stored PLT, with several in vivo studies have demonstrating both safety and efficacy surgical settings[306,307]. However, platelet cryopreservation is associated with storage lesions that can arise from cryoprotectant toxicity, the thawing process, or the resuspension medium, all of which may impair platelet function[200]. Since reduced platelet functionality is strongly linked to increased bleeding risk and shortened platelet survival in recipients, this remains a major concern[308]. Additional issues include the possible uncontrolled release of growth factors and cytokines into circulation, as well as a heightened risk of thrombosis or hypercoagulability[220]. To address these challenges and to explore whether Cryo-PLT could serve as a viable alternative to Fresh-PLT in onco-haematological patients, we conducted an in-depth biochemical characterization of Cryo-PLT. Our study focused on the time-dependent events following thawing that influence platelet morphology, coagulation potential, functional responses to physiological stimuli, and overall activity. Furthermore, we investigated platelet–cancer cell interactions and assessed how platelet supernatants affect cancer cell behaviour *in vitro*[309].

Dynamic insights into coagulation initiation, clot growth kinetics, and clot strength were obtained through ROTEM analysis, which revealed alterations in the coagulation process. In particular, clotting capacity and efficiency were reduced by cryopreservation for all the coagulation pathways investigated (Figure 7A–C). This was reflected by reduced clot strength and stability, along with a prolonged time to achieve stable clot formation, evidenced by increase CFT and decrease clot amplitude. However, the overall clotting capacity did not change over time after reconstitution and always remained within the clinically accepted range[310]. Nevertheless, our data partially diverge from other studies demonstrating faster CT and pro-coagulant phenotype of Cryo-PLT[224,311–313], reporting

that prolonged post-thawed storage only minimally impairs haemostatic function *in vitro*[224,263]. Conflicting results have been published for clot formation time. While some studies observed a reduction in this parameter following cryopreservation, others found no significant differences among different platelet freezing methods[314,315]. Such discrepancies may stem from several factors, including the choice of agonist used in haemostatic assays, e.g. kaolin or tissue factor, variations in preparation methods, platelet concentration[316] and resuspension media[317]. In particular, additive solutions and their components can strongly influence platelet preservation and physicochemical properties[209,317]. Our study focuses on 100% platelet additive solution as a resuspension medium whereas the vast majority of available studies focus on plasma-based solutions[318]. Notably, Johnson et al. demonstrated that Cryo-PLT reconstituted in plasma exhibit a more procoagulant phenotype compared with those reconstituted in additive solution[271,315].

The reduced clotting activity was also accompanied by a glycoprotein pattern modification occurred after thawing (Figure 7). According to what was first reported by Valeri and colleagues[319], our data confirmed that cryopreservation leads to a loss of CD42b expression[313], a key receptor of the haemostatic and coagulation cascade[320]. This decrease is accompanied by a reduced responsiveness to thrombin activation, as shown in Figure SD2. Similar results have been reported in cryopreserved platelet concentrates derived from buffy-coat and resuspended in a solution containing 30% plasma and 70% additive solution[321]. The CD41a+/CD42b− platelet sub-population observed in Cryo-PLT lacked P-selectin expression (Figure 7I,J), supporting the hypothesis that CD42b exposure is necessary to switch to the active phenotype[319]. Based on CD42b/CD62P staining, Johnson and colleagues recently reported that only the 23 ± 7% of cryopreserved platelet would be defined as pro-coagulant[262]. Accordingly, we found only a 25% of CD42b+/CD62P+ activated platelets in the Cryo-PLT at 1 h after thawing. Finally, we saw a higher exposure of CD62P in thawed platelets that, coupled with the ROTEM results discussed earlier, may be explained by an increased degranulation and release of mediators from the α- granules rather than by a higher coagulation activity[322].

It has been reported that platelet morphology is significantly affected after cryopreservation[315,322]. However, most of the evidences regard structural changes and do not investigate how cryopreservation quantitatively alter the biological components of PLT[322,323]. Here, we obtained important clues on the macromolecular changes induced by cryopreservation on membrane lipids, protein content and increasing of peroxidation processes. FTIR analysis revealed that thawing time significantly influences membrane functionality and integrity, with the most pronounced morphological deterioration occurring within the first 3 hours (Figure 8). We found morphological changes in plasma membrane composition, including increased membrane stiffness (CH2/CH3 ratio) and reduced protein content (protein/lipid ratio) after cryopreservation. On the other hand, both

C=O/lipids and C=O/proteins ratios increased over time post thaw possibly because of peroxidation, which may eventually be responsible of impaired platelet function[281]. PCA further demonstrated that thawing disrupts protein folding and membrane phospholipids structure (Figure 8G–J). Within the first hour after thawing, protein structure appeared largely preserved, as indicated by strong α-helix signals in both Fresh and Cryo-PLTs. By 3 hours, however, β-structure signals predominated, consistently with protein misfolding and functional decline[281].

According to previous studies[226,324], we found that cryopreservation increased the secretion of P-EVs and enhanced PS externalization compared with fresh components. Both parameters declined progressively after thawing (Figure 8, 3 h and 6 h). We hypothesize that the reduction in PS-positive platelet and EVs release over time reflects enhanced increased peroxidation and protein misfolding, which compromise membrane integrity and stiffness. These irreversible alterations, evident by 3 hours post-thaw, likely contribute to the diminished clotting capacity of Cryo-PLTs, despite the robust early release of EVs. Although, PS externalization has been largely recognized as a unique marker of pro-coagulant platelets among the subpopulation of activated platelets, recently 3 surface markers have been recommended to be used in order to differentiate pro-coagulant platelets from apoptotic platelets[262]. Accordingly, the higher exposure of PS found in Cryo-PLT is probably caused by the reduced viability as confirmed by the fact that Cryo-PLT are less responsive to physiological agonist treatment (Figure 8B, Fresh-A vs. 1 h)[325].

Several studies suggest that EVs support blood coagulation[319,326], yet more recent findings have challenged this view. For example, Berckmans et al. revisited their previous findings on the coagulant properties of EVs in blood[327] and instead detected fibrinolytic activity, indicating potential anticoagulant functions. These conflicting results may be explained by the existence of different EVs subsets or by numerous subpopulations of EVs (from platelets or other cellular lineages) present in the blood, associated with either pro- or anti-coagulant activity[262]. It can also be hypothesized that it is the plasma rather than the platelets themselves that retain the main effect and that EVs are only effective in the presence of plasma. Thus, although the promotion of coagulation was the first function attributed to EVs, extensive research dedicated to understanding their role is needed.

The membrane damage induced by cryopreservation, together with the observed alterations in glycoprotein exposure, may also account for the changes in soluble mediator release from α-granules. Among all the biomolecules assessed (see Materials and Methods for details), the main differences between Fresh- and Cryo-PLT were detected at 1 h post thaw for FGF, PDGF-BB, RANTES (CCL5) and TGF- β (Figure 9). Subsequently, the residual concentrations of these molecules dropped below the limit of detection (see Material and Methods for details). These findings should be interpreted in light of the resuspension medium and platelet concentration used after thawing. Cardigan and

colleagues reported that markers of platelet activation (e.g., TGF-β, CD62P) and cytokine release (e.g., IL-8) vary according to the composition of PAS and that modification of the quality and concentration of the different components of PAS can improve both the storage and safety profiles of platelet concentrates[328]. In a previous study on cryopreserved platelet concentrates for non-transfusion purposes[261], we observed that the release of growth factors did not correlate with platelet numbers, suggesting that it is more likely dependent on donor variability and specific factors related to the freezing and thawing process. This observation underscores the complexity of the interactions between cryopreservation, platelet concentrations, and the release of soluble mediators. All the evaluated factors[171,306] are involved in cancer progression, although a bidirectional effect on tumour progression has been reported for RANTES and TGF-β[329]. Nevertheless, it has been demonstrated that platelet derived TGF-β is the solely responsible for inducing an invasive epithelial–mesenchymal transition to metastasis[171].

Given the established role of platelets in tumour progression and metastasis[148,171,275], we evaluated the capability of Cryo-PLT to stimulate *in vitro* models of cancer. Compared with Fresh-PLTs, Cryo-PLTs displayed a markedly reduced pro-tumoral effect, as demonstrated by impaired cell migration (Figure 10C), decreased proliferation (Figure 10A, B) and lower ability to interact and aggregate with HL-60 (Figure 10D). In contrast, Fresh-PLTs promoted cell growth more effectively, although their stimulatory effect on proliferation remained modest compared with the positive control (Figure 10B), suggesting that platelet viability is critical for functional platelet–tumour interactions. The lower TGF-β content in Cryo-PLTs may underlie their reduced ability to promote migration relative to Fresh-PLTs. Our data is partially in agreement with those of Pu et al.[227], reporting an inhibitor effect on cell growth by platelet supernatants; an effect attributed to the accumulation of toxic metabolites during storage. Taken together, these findings indicate that Cryo-PLTs are not more likely than Fresh-PLTs to stimulate either solid or haematological tumour cells, and that their releasate does not significantly alter cancer cell behaviour.

With these experiments, we proved that cryopreserved platelets from apheresis donation, collected and resuspended in platelet additive solution, undergo marked morphological changes that impair their integrity. We showed indeed that, after thawing, Cryo-PLT progressively accumulate features ascribable to oxidative stress and PSL with reduced functionality, and increase of PS externalization, peroxidation processes and protein misfolding.

Despite platelets and their soluble factors are known to contribute to tumour progression and metastasis[275], our findings indicate that Cryo-PLTs have limited capacity to enhance proliferation, adhesion, or migration in cancer cell models, supporting their safety for transfusion in onco-haematological patients. Cryo-PLTs can therefore serve as a valuable backup during periods of Fresh-

PLT shortage, helping to prevent bleeding in non-haemorrhagic patients. To preserve their functional performance, it is recommended that cryopreserved platelets be transfused within one hour of thawing.

We acknowledge several limitations of our study. Despite efforts to control for confounding variables, unaccounted or unknown factors may have influenced the observed outcomes beyond the effects of cryopreservation itself. These could include variations in sample collection, processing techniques, and storage conditions that were not directly addressed in our study design. We also acknowledge that the generalizability of our study is limited due to the specific conditions, the small number of test replicates and the parameters used, which may be affected by unidentified confounding factors.

Finally, our investigation is limited to *in-vitro* experiments, lacking of information on the transfusion outcome with Cryo- PLT on patients, such as the determination of the Corrected Count Increment (CCI)[330]. Although the use of the CCI to assess the efficacy of platelet transfusion is controversial[331], we acknowledge that the persistence of platelets after transfusion is a prerequisite for their functionality[308]. The CCI was indeed used as primary outcome to evaluate the efficacy of prophylactic transfusion with buffy coat derived cryo-PLT in three haematological patients[332] and in a small cohort of women with gynecological malignancies treated with autologous cryo-PLT[333]. While existing in vivo studies have demonstrated the haemostatic effectiveness of Cryo-PLT without evidence of an increase in post-transfusion thrombosis[225,334], and clinical trials have been conducted to assess the safety and efficacy of Cryo-PLT in different clinical settings[220,335], we recognize the need for further in vivo studies or clinical trials to determine the clinical relevance of prophylactic Cryo-PLT transfusion in non-actively bleeding thrombocytopenic patients.

4.2 Comparison of different PRPs effect on wound healing in vitro

We compared the effects of different PRP formulations on wound healing aiming to address knowledge gaps regarding various basic PRP products for wound healing to improve clinical decision-making and pave the way for innovative strategies in PRP administration. The heterogeneity of PRP products[246,254] in both preparation and delivery, complicates the establishment of standardized clinical guidelines. PRPs can be produced from both apheresis and BC. Additionally, PRP can be administered as either a liquid or gel, depending on the tissue being treated and clinical judgment[246]. Liquid PRPs can also be delivered via various strategies, such as polymers and hydrogels[336] to increase contact time and enable controlled release of PRP effectors, like growth factors.

In this study, we focused on PRPs produced through a freeze–thaw cycle from both platelet apheresis and buffy coat, in liquid and gel forms. To evaluate differences among these formulations, we quantified the release of growth factors, extracellular vesicles, and calcium ions overtime. We then

assessed their effects on in vitro models of fibroblasts (BJ), keratinocytes (HaCaT), and microvascular endothelial cells (HDMEC). To mitigate donor variability, PRP products were prepared from pooled samples of four donors.

We quantified GFs release from the PRPs at baseline across a seven days period. At baseline, no significant differences in GF content were detected between apheresis-derived and buffy coat-derived PRPs. To mimic GF release from PRPs into wounded tissue, we employed transwells with a permeable barrier. Using this model, we demonstrated that PRP products sustain GF release for up to seven days (Figure 11B).

Notably, liquid PRP exhibited an early and continuous GF release, wherease the gel formulation demonstrated delayed and sensibly lower release. Substantial heterogeneity was observed in the total percentage of GFs released over the entire seven-day period: approximately 100% of EGF and CTGF were released, while TGF-β1 and PDGF releases remained below 50% (Figure 11B). Comparisons between Aphe and BC PRPs revealed no differences in EGF and CTGF release, while higher amounts of TGF-β1 and PDGF-AA were released in liquid BC compared to liquid Aphe. Conversely, previous studies reported that most GFs were released into the supernatant within 24-72 hours[337–339], regardless of freeze-thaw processing. The prolonged release observed may reflect controlled diffusion of GFs from PRP matrix through the transwell membrane.

Emerging evidence highlights the role of EVs as carriers of bioactive molecules that stimulate skin wound healing[340]. Our findings show that EVs release was significantly higher in liquid PRP compared to gel formulations, suggesting greater regenerative potential for the liquid formulation related to it. The delayed release of EVs (Figure 11C) aligns with their nature as byproducts of platelet degradation[341] . Ca2+ is involved in the regulation of keratinocytes function[284,296] and it was predominantly released during the first 72 hours. Increased Ca^{2+} levels in gel PRPs is consistent with its addition during gel preparation (Figure 11D).

To further analyzed how different PRP formulations affect wound healing, we next examined their effects on key cellular processes in culture.

Human fibroblasts (BJ) exposed to different PRP formulations showed differences in cellular proliferation responses. Liquid PRPs demonstrated superior capacity to restore BJ cell proliferation compared gel PRPs (Figure 12C), and this effect was evident both with and without TGF-β pre-treatment. Although less potent, gel PRPs also promoted proliferation, indicating that even lower GFs concentrations can stimulate this response. However, no effects were noted on BJ migration (Figure 12D). With respect to myofibroblast differentiation, TGF-β treatment induced significant changes in expression markers[286,289] without altering cellular morphology (Figure 12 E-G). In contrast, combined treatment with TGF-β and PRPs resulted in more elongated BJ cells and to a sustained dysregulation

of several myofibroblast differentiation markers (Figure 12 E-G). This effect is more pronounced with gel PRPs, suggesting that a difference in GFs balance can finely modulate cell fate between proliferation and/or differentiation. Analysis of MMP1, a marker of ECM remodelling[342], revealed its upregulation in response to PRP treatment and downregulation when PRPs were combined with TGF- β (Figure 12G). Accordingly, a previous research found that MMP1 was upregulated in dermal fibroblast treated with PRP[343]. Our results further suggest that TGF-β pre-treatment may limit the ability of PRP-derived GFs to promote fibroblast-mediated ECM turnover and remodelling. Unlike BJ cells, HaCaT keratinocytes exhibited both stimulated proliferation and migration upon treatment with PRPs (Figure 13B, C); again, liquid formulations outperformed gels without significant differences between apheresis and BC sources. Interestingly, liquid PRPs increased HaCaT cell viability under low calcium conditions, although the effect was less pronounced than under standard DMEM (high Ca^{2+}). Despite this, both high and low calcium conditions resulted in similar wound closure capabilities with liquid PRP treatment (Figure 13C).

These differential effects on proliferation and migration may reflect differences in how quickly PRP releasates restore each function. Calcium concentrations during initial days of treatment were comparable or exceeded those found in normal DMEM (~1-2 mM[344]), suggesting that higher Ca^{2+} concentrations in gel formulations could explain their enhanced effects on cell proliferation and morphology (Figure 13 B-E). Conversely, TGM1 expression, a marker of cellular differentiation[298–300], was slightly higher in liquid than gel formulations, indicating a combined effect from Ca^{2+} and GFs released at higher concentrations from liquid PRPs influencing HaCaT differentiation from basal states (Figure 13F).

The impact of different PRP formulations on microcirculation neoangiogenesis was assessed using HDMEC as an in vitro model. All PRPs tested promoted viability and wound closure along with the typical endothelial morphology, suggesting sustained HDMEC function due to PRP treatment (Figure 14B-E). Additionally, all formulations promoted SELE expression, an adhesion marker correlated with cell growth[305], while EMT markers (αSMA and COL1A2) remained largely unchanged, apart from a slight increase in αSMA following BC liquid treatment (Figure 14F).

Overall, our results demonstrate that all tested PRPs enhance the regenerative capacity of cells involved in wound healing without significant differences between BC-derived and platelet-apheresis-derived products. However, clear distinctions exist between gel and liquid formulations highlighting the importance of GF release kinetics and the need to tailor application strategies for optimal therapeutic outcomes.

For chronic wounds requiring topical application, gel formulations are often preferred; however, liquid PRPs may be advantageous when incorporated into biocompatible carriers such as hydrogel

dressings. In conditioned like lichens sclerosus, where injections are delivered at lesion sites[345], the duration of GFs exposure becomes a critical factor, as rapid clearance may limit effective cellular stimulation.

To better clarify this aspect, further studies quantifying PRP clearance rates at skin and subcutaneous levels are warranted. This work highlights the importance of characterizing GF and EV release kinetics across PRP formulations. Liquid PRP, with its rapid GFs release profile and higher EVs content, may be particularly effective for early wound-healing application, wherease gel-based formulations, providing prolonged GFs release, appear more suitable for sustained tissue repair.

Future research should focus on refine dosing strategies, standardize preparation protocols, and integrate additional bioactive agents to maximize the therapeutic potential of PRP treatments based on specific clinical contexts.

4.3 Anticoagulant-Dependent Interaction of Platelet EVs with Monocytes

P-EVs play a central role in coagulation and immune regulation by interacting with circulating immune cells, particularly monocytes[346]. These interactions are strongly influenced by the anticoagulant used in blood collection. Citrate and EDTA are the most widely employed anticoagulants, and differentially affect both P-EV release and P-EV–monocyte interactions[347].

To assess these effects, we compared citrate and EDTA anticoagulated blood samples at two time points: immediately after collection (0hour) and following 3.5hours of gentle agitation.

Monocyte subset distributions showed minimal differences between the two anticoagulants. However, significant differences were observed when examining P-EVs and platelet–monocyte aggregates (UR quadrant). According to literature[348], P-EV-monocyte interactions occur most commonly with IM. This partially aligns with our data for both samples, since they show that P-EVs similarly interact with CM and IM immediately after collection while after 3.5hour there is a slight preference for IM.

In citrate-anticoagulated samples, aggregates involving CM and IM could increase up to sevenfold after 3.5 h, coinciding with a reduction in measurable monocyte counts. This suggests that monocytes became sequestered within aggregates containing P-EVs or platelets.

On the contrary, EDTA effectively stabilized blood better than citrate, reflecting its superior calcium-chelating capacity and reduced platelet activation and artificial P-EV release during storage[347], impeding calcium-dependent P-EV–immune cell interactions. In citrate samples, platelet activation was evident, as demonstrated by shifts in FSC–SSC dot plots and a higher frequency of P-EV- or platelet-bound monocytes. The P-EV–monocyte interactions are strongly calcium-dependent, and using EDTA as anticoagulants inhibits this associations, becoming a critical step when designing protocols for P-EV studies in coagulation and immune modulation[349].

5 CONCLUSIONS

This research explored the optimization of platelet-based products for both transfusion medicine and regenerative applications, with particular focus on platelet cryopreservation safety and the comparative evaluation of PRP formulations for wound healing. The studies collectively highlight the dual nature of platelets, as both life-saving transfusion components in onco-haematological patients and regenerative tools in tissue repair, and the importance of understanding their biochemical integrity, release dynamics, and clinical suitability.

First, investigations into platelet cryopreservation revealed that while cryopreserved platelets extend shelf life and secure a more stable blood supply, they undergo profound biochemical and structural changes during freezing and thawing. The assessed analysis demonstrated alterations in lipid and protein composition, increased oxidative stress, and premature activation: all of which influencing platelet haemostatic function. Importantly, these changes evolve dynamically within hours after thawing, emphasizing the need to define optimal transfusion timing. Nevertheless, functional assays and in vitro cancer models confirmed that cryopreserved platelets, despite reduced clot strength and altered receptor expression, do not promote tumour growth or migration, supporting their safe use in onco-haematological cancer patients. These insights pave the way for refining cryopreservation protocols, including the exploration of alternative cryoprotectants.

In parallel, the thesis addressed the regenerative dimension of platelet-derived products by characterizing and comparing liquid and gel PRP formulations obtained from both apheresis and buffy coat sources. Over a seven-day period, liquid PRPs consistently released higher amounts of GFs and EVs than gel formulations, while both demonstrated sustained bioactivity. Functional assays in keratinocytes, fibroblasts, and endothelial cells revealed that liquid PRPs promoted stronger proliferative and migratory responses, whereas gel PRPs provided a more gradual release suitable for sustained stimulation. Interestingly, no substantial differences emerged between Aphe- and BC-derived products, underscoring their interchangeability in clinical applications. These findings reinforce the notion that the method of PRP formulation (liquid versus gel) has greater impact on biological performance than the platelet source, and that tailoring the release kinetics to the clinical scenario is critical: liquid PRPs for rapid regenerative needs, gel PRPs for long-term wound support.

New perspective involving clinical settings demonstrate that the choice of anticoagulant profoundly affects P-EV behaviour, particularly their interactions with monocytes. These interactions are strongly calcium-dependent and can be artificially reduced or amplified depending on the anticoagulant used during blood collection. Understanding how anticoagulants modulate P-EV biology is therefore essential for accurate assessment of circulating extracellular vesicles in patient samples, especially in coagulation disorders, cardiovascular disease, or inflammatory conditions

where monocyte–platelet interactions play a central pathophysiological role. Furthermore, in translational applications, such as P-EV-based therapeutics or regenerative medicine strategies, selecting an anticoagulant that preserves vesicle functionality without inducing artificial aggregation is crucial to ensure reproducibility, efficacy, and safety.

Taken together, this body of work underscores the central role of platelets and their derivatives in both transfusion safety and regenerative medicine. This thesis, ultimately, contributes to bridging the difference platelet application in clinical practice, advancing a more precise and evidence-based use of platelet-derived products. Future research should focus on clinical validation of optimized cryopreservation protocols, quantitative assessment of PRP clearance and bioavailability in vivo, and the integration of novel bioactive additives to further enhance safety and efficacy.

6 SUPPLEMENTARY DATA

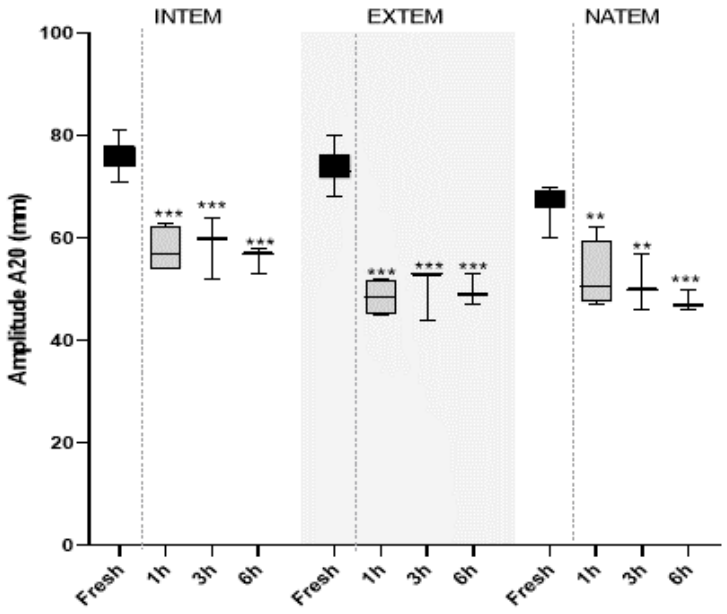

Figure SD1. **Clot Amplitude at 20 min from CT (A20) of Fresh- and Cryo-PLT at different time points after thawing (1h, 3h and 6h).** A20 decreseas significantly after cryopreservation. ANOVA test with multiple comparison was performed against Fresh-PLT. **p<0.05 ****p<0.001.

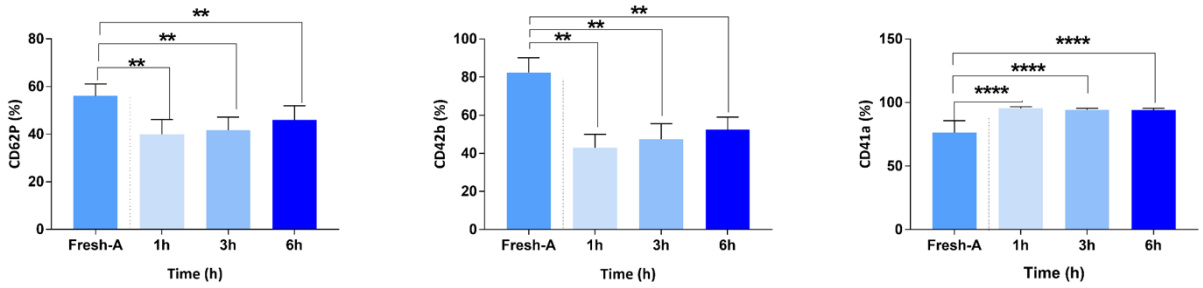

Figure SD2. Glycoprotein exposure on fresh and Cryo-PLTs stimulated with Thrombin (0.5 U/mL). Fresh- and Cryo-PLT at different time points after thawing (1h, 3h and 6h) are represented as percentage % of positive events. ANOVA test with multiple comparison was performed against Fresh-PLT. **p<0.05 ****p<0.001. Trend of CD41a and CD42b glycoprotein is similar to that observed for non activated samples.

State	Sample Type		CD41a		CD42b		CD61	
			Mean	SD	Mean	SD	Mean	SD
NA PLT	Fresh		77.39	7.90	80.07	6.13	48.13	26.13
	Cryo	1h	95.03	1.38	45.90	7.31	36.50	30.01
		3h	92.98	1.77	48.46	6.62	46.44	17.42
		6h	94.14	1.91	54.08	7.85	38.56	15.17
A PLT	Fresh		76.31	9.55	82.44	7.71	59.47	17.20
	Cryo	1h	95.49	1.22	42.95	7.05	40.23	23.60
		3h	94.36	1.12	47.36	8.15	47.22	22.65
		6h	94.22	1.27	52.49	6.55	36.88	19.67

Table SD1. Glycoprotein exposure on cryo-PLTs stimulated with Thrombin (0.5 U/mL).

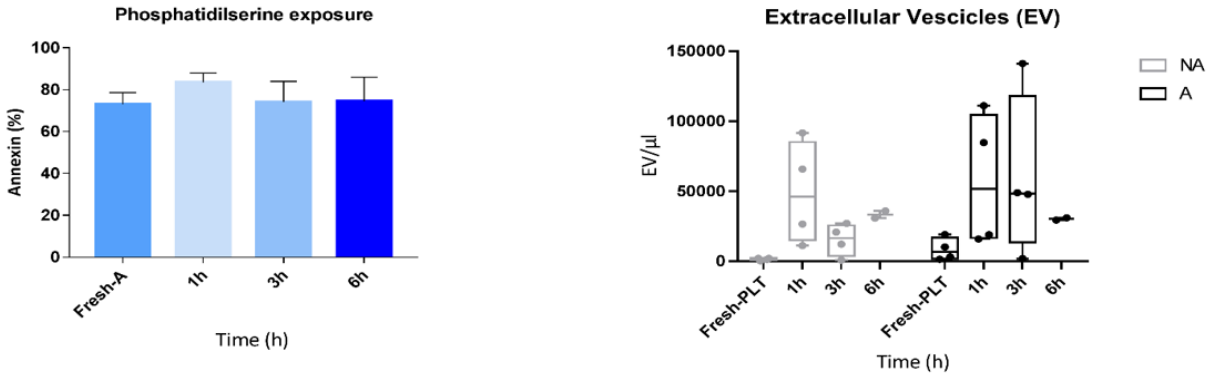

Figure SD3. Phosphatidylserine (PS) exposure in thrombin stimulated (activated)-PLT (Mean ±SD) One-way ANOVA with multiple comparisons was used to evaluate statistical significance with CI 95%; Concentration of EVs (EVs/µL) in fresh and cryo-preserved platelets after 1h, 3h and 6 hours

from thawing (Data are reported as Min to Max). (NA not activated samples. A activated samples with 0.5mU/mL thrombin). Non-parametric one-way ANOVA test with Kruskal-Wallis test was performed (* $p<0.01$).

State	Sample Type		Microparticles	
			Mean	SD
NA PLT	Fresh		$1.29x10^3$	$8.69x10^2$
	Cryo	1h	$4.88x10^4$	$3.67x10^4$
		3h	$1.52x10^4$	$1.14x10^4$
		6h	$3.33x10^4$	$3.65x10^3$
A PLT	Fresh		$6.92x10^3$	$7.74x10^3$
	Cryo	1h	$5.77x10^4$	$4.87x10^4$
		3h	$6.00x10^4$	$5.73x10^4$
		6h	$3.02x10^4$	$1.13x10^3$

Table SD2. Data regarding EV evaluation in Fresh- and Cryo-PLT, not activated and activated samples (induced with 0.5mU/mL trhombin).

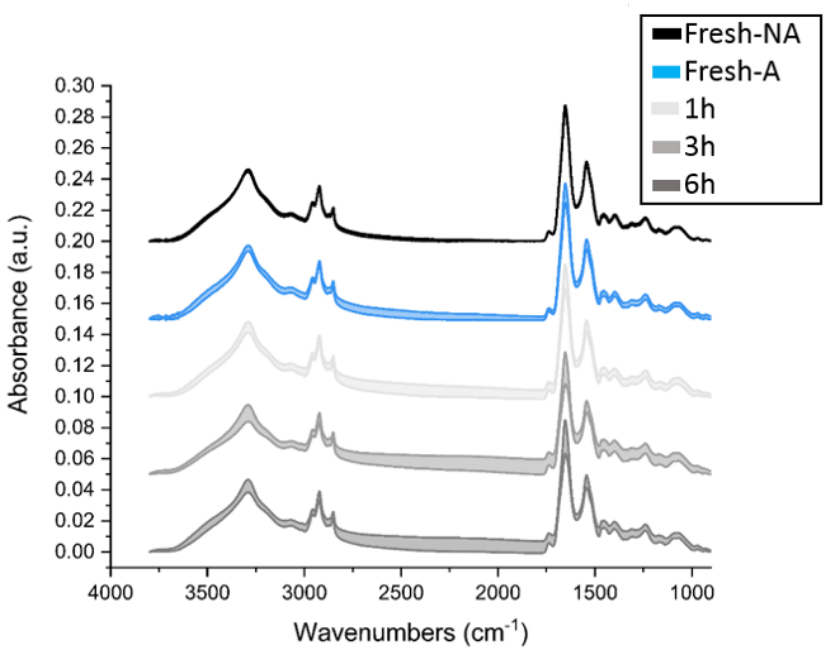

Figure SD4. FTIR average absorbance spectra. The shading represents +/- standard deviation. The averages were calculated from 80 T0-NA spectra, 80 T0-A spectra, 442 1h spectra, 372 3h spectra and 392 6h spectra, respectively.

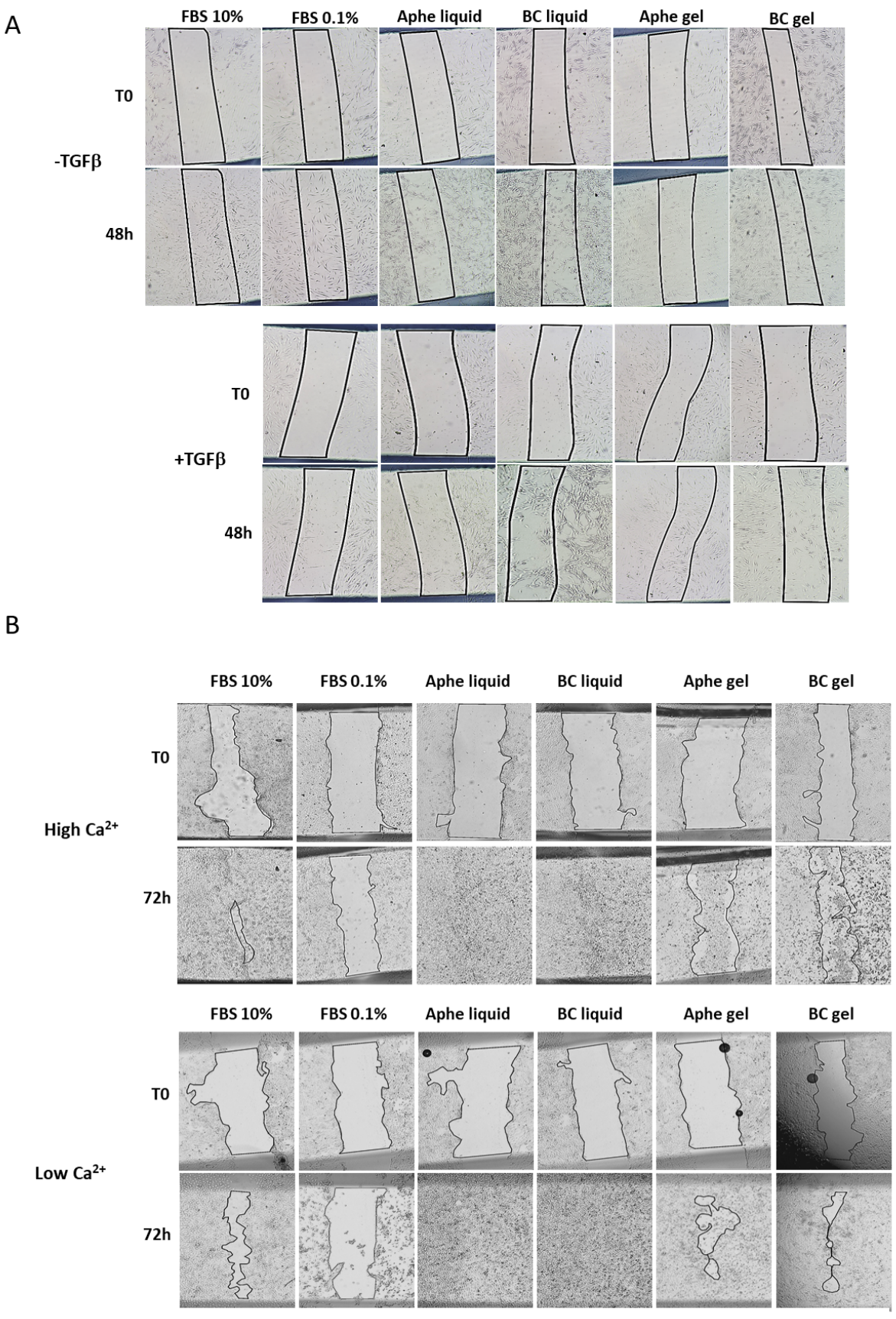
A
FBS 10%
FBS 0.1%
Aphe liquid
BC liquid
Aphe gel
BC gel
T0
-TGFβ
48h
T0
+TGFβ
48h
B
FBS 10%
FBS 0.1%
Aphe liquid
BC liquid
Aphe gel
BC gel
T0
High Ca2+
72h
FBS 10%
FBS 0.1%
Aphe liquid
BC liquid
Aphe gel
BC gel
T0
Low Ca2+
72h

C

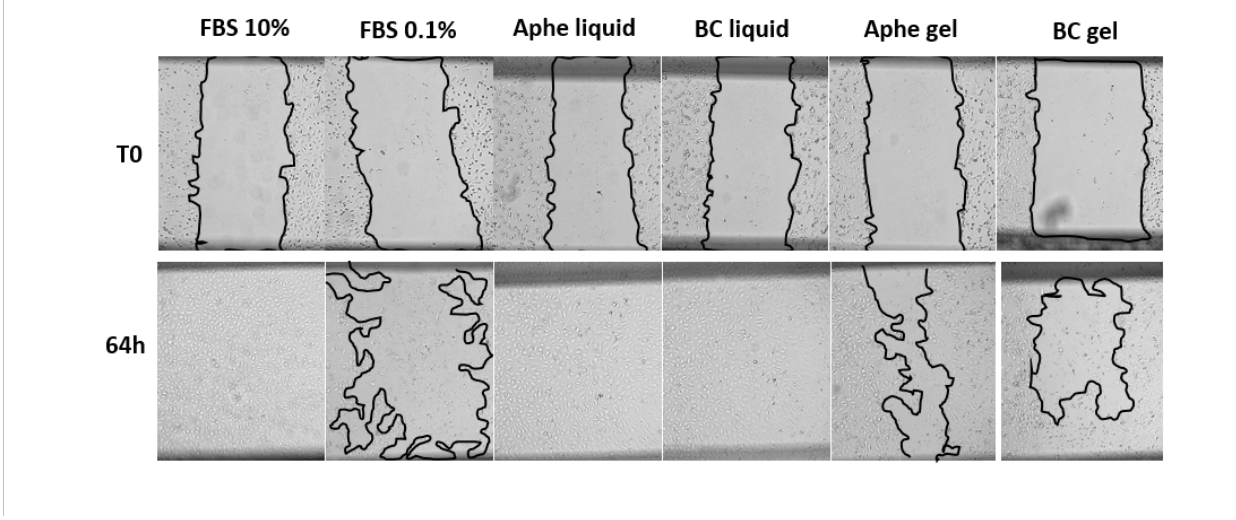

Figure SD5. A) representative phase-contrast images of the scratch assay with BJ with and without pre-treatment with TGFb at T0, beginning of the treatment with PRPs, and after 48 h. **B) representative phase-contrast images of** HaCaT in Low and High Ca^{2+} at T0, beginning of the treatment with PRPs, and after 72 h. **C) representative phase-contrast images of** HDMEC at T0, beginning of the treatment with PRPs, and after 64 h. Black lines indicate the area selected for the scratch measurement.

Gene name (protein name)	Sequences
GAPDH(Glyceraldehyde-3-Phosphate Dehydrogenase)	F: GTCTCCTCTGACTTCAACAGCG R:ACCACCCTGTTGCTGTAGCCAA
VIM (Vimentin)	F: CGAAAACACCCTGCAATCTT R: TTTGGACATGCTGTTCCTGA
ACTA2 (α-SMA)	F: CCGGGAGAAAATGACTCAAA R: GCAAGGCATAGCCCTCATAG
MMP1 (Matrix metallopeptidase 1)	F: TGCTCATGCTTTTCAACCAG R: GGTACATCAAAGCCCCGATA
COL1A1 (Collagen type 1 α 1)	F: TCCAACGAGATCGAGATCC R: AAGCCGAATTCCTGGTCT
TGM1 (Transglutaminase 1)	F: GCACACCTTCCGTCTGCG R: CAATCTGTACTTCACACTCCTGGC

Table SD3. qPCR primers list.

	Aphe							BC						
	Total amount in PRP	Liquid			Gel			Total amount in PRP	Liquid			Gel		
		Conc.	Amount	% Total	Conc.	Amount	% Total		Conc.	Amount	% Total	Conc.	Amount	% Total
EGF	pg	pg/ml	pg		pg/ml	pg			pg/ml	pg		pg/ml	pg	
Day 1		40,46	121,39	18,82	1,35	4,05	0,63		47,40	142,21	21,68	1,26	3,77	0,57
Day 2		33,85	101,55	15,75	1,35	4,05	0,63		31,19	93,56	14,26	1,31	3,94	0,60
Day 3		34,29	102,86	15,95	1,18	3,55	0,55		37,82	113,45	17,29	1,26	3,77	0,57
Day 4		32,66	97,99	15,19	1,56	4,68	0,73		34,29	102,86	15,68	1,41	4,22	0,64
Day 5		22,54	67,61	10,48	1,05	3,16	0,49		29,25	87,76	13,38	1,07	3,22	0,49
Day 6		19,91	59,74	9,26	1,09	3,27	0,51		26,53	79,59	12,13	1,13	3,38	0,52
Day 7		17,43	52,29	8,11	1,16	3,49	0,54		22,36	67,09	10,23	1,22	3,66	0,56
Total	644,90	201,15	603,44	93,57	8,75	26,25	4,07	656,00	228,84	686,53	104,65	8,65	25,96	3,96
PDGF AA	ng	ng/ml	ng		ng/ml	ng			ng/ml	ng		ng/ml	ng	
Day 1		9,19	27,56	2,11	0,75	2,25	0,17		13,86	41,59	3,33	0,84	2,51	0,20
Day 2		9,49	28,46	2,18	0,77	2,32	0,18		14,78	44,34	3,55	1,31	3,94	0,32
Day 3		12,35	37,05	2,83	0,77	2,32	0,18		14,07	42,20	3,38	4,78	14,33	1,15
Day 4		10,61	31,84	2,43	2,47	7,41	0,57		12,37	37,10	2,97	3,94	11,82	0,95
Day 5		9,40	28,20	2,16	4,08	12,25	0,94		10,45	31,35	2,51	3,38	10,14	0,81
Day 6		9,35	28,05	2,14	4,34	13,03	1,00		10,42	31,26	2,50	1,87	5,60	0,45
Day 7		9,36	28,07	2,15	4,05	12,14	0,93		10,40	31,21	2,50	1,76	5,27	0,42
Total	1308,6	69,74	209,22	16,00	17,24	51,73	3,95	1248,05	86,35	259,05	20,76	17,87	53,61	4,30

PDGF AB	ng	ng/ml	ng		ng/ml	ng			ng/ml	ng		ng/ml	ng	
Day 1		297,34	0,89	3,57	11,93	0,04	0,14		402,31	1,21	4,47	11,34	0,03	0,13
Day 2		339,04	1,02	4,07	8,90	0,03	0,11		284,78	0,85	3,16	10,92	0,03	0,12
Day 3		384,81	1,15	4,62	9,54	0,03	0,11		269,59	0,81	3,00	11,17	0,03	0,12
Day 4		337,42	1,01	4,05	9,78	0,03	0,12		320,50	0,96	3,56	9,62	0,03	0,11
Day 5		356,13	1,07	4,27	12,66	0,04	0,15		236,17	0,71	2,62	49,56	0,15	0,55
Day 6		237,39	0,71	2,85	34,18	0,10	0,41		268,94	0,81	2,99	79,59	0,24	0,88
Day 7		185,91	0,56	2,23	66,96	0,20	0,80		216,93	0,65	2,41	62,39	0,19	0,69
Total	25,35	2138,05	6,41	25,66	153,96	0,46	1,85	27,10	1999,22	6,00	22,21	234,58	0,70	2,61

CTGF	ng	ng/ml	ng		ng/ml	ng			ng/ml	ng		ng/ml	ng	
Day 1		17,46	52,37	19,69	0,00	0,00	0,00		19,54	58,62	22,12	0,00	0,00	0,00
Day 2		16,02	48,06	18,07	0,00	0,00	0,00		18,31	54,92	20,73	0,00	0,00	0,00
Day 3		15,16	45,49	17,10	0,98	2,93	1,10		15,19	45,57	17,20	0,00	0,00	0,00
Day 4		9,56	28,69	10,78	1,41	4,24	1,59		10,46	31,38	11,84	0,00	0,00	0,00
Day 5		5,85	17,55	6,60	0,00	0,00	0,00		8,35	25,04	9,45	0,00	0,00	0,00
Day 6		3,71	11,13	4,18	0,00	0,00	0,00		7,02	21,05	7,95	1,96	5,89	2,22
Day 7		4,81	14,44	5,43	2,89	8,66	3,26		6,25	18,74	7,07	0,00	0,00	0,00
Total	266,7	72,58	217,74	81,86	5,28	15,83	5,95	265,40	85,11	255,34	96,35	1,96	5,89	2,22

TGF-β	ng	ng/ml	ng		ng/ml	ng			ng/ml	ng		ng/ml	ng	
Day 1		3,01	9,03	3,08	0,00	0,00	0,00		5,06	15,18	5,40	0,00	0,00	0,00
Day 2		3,52	10,56	3,60	0,00	0,00	0,00		6,48	19,45	6,92	0,00	0,00	0,00
Day 3		4,19	12,58	4,29	0,00	0,00	0,00		7,07	21,21	7,55	0,00	0,00	0,00
Day 4		4,04	12,12	4,14	0,00	0,00	0,00		5,32	15,95	5,68	0,00	0,00	0,00
Day 5		4,36	13,07	4,46	0,00	0,00	0,00		5,72	17,17	6,11	0,00	0,00	0,00
Day 6		2,40	7,20	2,46	0,00	0,00	0,00		6,31	18,94	6,74	0,69	2,07	0,74
Day 7		4,44	13,33	4,55	0,58	1,75	0,60		6,10	18,29	6,51	1,85	5,56	1,98
Total	293,49	25,96	77,89	26,58	0,58	1,75	0,60	281,48	42,06	126,18	44,90	2,55	7,64	2,72

Ca2+	mmoles	mmoles/l	mmoles		mmoles/l	mmoles		mmoles	mmoles/l	mmoles		mmoles/l	mmoles	
Day 1		0,38	1,14	45,98	0,65	1,94	77,93		0,55	1,65	71,93	1,04	3,13	136,59
Day 2		0,28	0,84	33,82	0,73	2,19	87,80		0,34	1,01	44,14	0,71	2,12	92,79
Day 3		0,16	0,48	19,15	0,63	1,89	75,81		0,16	0,47	20,70	0,58	1,74	75,99
Day 4		0,07	0,22	8,70	0,48	1,43	57,37		0,09	0,28	12,38	0,42	1,26	55,11
Day 5		0,04	0,12	4,79	0,29	0,87	34,77		0,03	0,08	3,53	0,33	0,98	42,93
Day 6		0,02	0,06	2,54	0,28	0,83	33,42		0,02	0,07	2,93	0,28	0,85	37,31
Day 7		0,01	0,02	0,99	0,27	0,81	32,60		0,02	0,05	1,98	0,35	1,05	45,89
Total	2,49	0,96	2,89	115,97	3,32	9,95	399,69	2,29	1,20	3,61	157,59	3,71	11,14	486,61

Table SD4. Concentrations, amount and normalized % of GFs and Ca2+ released by PRPs over time and in total over the 7-day period. The total amount of GFs/Ca2+ in the tested PRPs (both Aphe and BC) was obtained using the concentrations measured for the volume of PRPs in the transwell (i.e. 1.5 ml). Amount of GFs/Ca2+ in the PBS (releasate) was obtained multiplying the concentrations measured for the volume (i.e. 3 ml). % Total was obtained dividing the amount in the releasate for the total amount in the PRPs. Total values in the in the releasate are obtained by summing the values in the 7 days.

7 ABBREVIATIONS LIST

A: Activated

A20: Amplitude 20minutes after CT

ACD-A: Acid Citrate Dextrose Solution A

ACS: Autologous Conditioned Serum

ADP: Adenosine Diphosphate

ALR: AIM2-Like Receptors

AMR: Ashwell-Morell Receptor

Aphe PRP: Apheresis-derived PRP

aPTT: activated Partial Thromboplastin Time

AT: Antithrombin

ATP: Adenosine Triphosphate

BC PRP: Buffy Coat-derived PRP

Ca2+: Calcium

CFT: Clot Formation Time

cGAS: cyclic GMP-AMP Synthase

CM: Classical Monocytes

c-MPL: Thrombopoietin receptor

COL1A: Collagen type I Alpha

CPA: Cryoprotective Agents

Cryo-PLT: Cryopreserved Platelets

CT: Clotting Time

CTRL-: Negative control

CTRL+: Positive control

DIC: Disseminated Intravascular Coagulation

DMEM: Dulbecco's Modified Eagle's Medium

DMSO: Dimetilsulfoxyde

ECGF: Endothelial Cell Growth Factor

ECM: Extracellular Matrix

EDQM: European Directorate for the Quality of Medicine & Healthcare

EGF: Epidemic Growth Factors

EMT: Epithelial–Mesenchymal Transition

EU: European

FBS: Fetal Bovine Serum

FCS: Fetal Calf Serum

FDP: Fibrin Degradation Products

Fresh-PLT: Fresh platelet

FTIR: Fourier Transform Infrared

FV: Coagulation Factor V

GF: Growth Factors

GMP: Good Manufacturing Practice

GP: Platelet Glycoprotein

GPIbα: Glycoprotein Ibα

HDMEC: Human Dermal Microvascular Endothelial Cells

HMGB1: High-Mobility Group Box 1

HSC: Haematopoietic Stem Cells

ICAM: Intercellular Adhesion Molecules

IGF: Insulin-like Growth Factor

IL-6: Interleukin 6

IM: Intermediate Monocytes

INR: International Normalized Ratio

IPD: Inherited Platelet Disorders

ITP: Immune Thrombocytopenia

JAM: Junctional Adhesion Molecules

LA: Lactadherin

L-PRF: Leukocyte- and Platelet-Rich Fibrin

L-PRP: Leukocyte- and PRP

MCF: Maximum Clot Firmness

MCT: Mercury Cadmium Telluride

MFC: Median Fluorescence Channel

MMP: Matrix Metalloproteinase

MPO: Myeloperoxidase

NA: Non-Activated

NCM: Non-classical Monocytes

NE: Neutrophil Elastase

NET: Neutrophil Extracellular Traps

NLRP3: Nod-Like Receptor Protein 3

NSF: N-ethylmaleimide Sensitive Fusion protein

PAF: Platelet-Activating Factor

PAI-1: Plasminogen Activator Inhibitor-1

PAS: Platelet Additive Solution

PCA: Principal Component Analysis

PDGF: Platelet Derived Growth Factor

PDPN: Podoplanin

PECAM-1: Platelet Endothelial Cell Adhesion Molecule-1

Pen-Strep: Penicillin-Streptomycin

P-EVs: Platelet derived Extracellular vesicles

PLA: Platelet–Leukocyte Aggregates

PLT: Platelet

P-PRF: Pure Platelet-Rich Fibrin

PRP: Platelet Rich Plasma

PS: Phosphatidylserine

PSGL-1: P-Selectin Glycoprotein Ligand-1

PSL: Platelet Storage Lesions

PT: Prothrombin Time

RANTES: Regulated on Activation, Normal T cell Expressed and Secreted

ROS: Reactive Oxygen Species

ROTEM: Thromboelastometry

RT: Room Temperature

SD: Standard Deviation

SELE: Selectin E

SNAREs: Soluble N-ethylmaleimide-sensitive factor Attachment protein Receptors

SVN: Standard Vector Normalization

TACO: Transfusion-Associated Circulatory Overload

TEG: Thromboelastography

TF: Tissue Factor

TFPI: Factor Pathway Inhibitor

TGF- β: Transforming Growth Factor

TGM1: Transglutaminase 1

TLR: Toll-Like Receptors

TME: Tumour Microenvironment

t-PA: tissue Plasminogen Activator

T-PAS: Platelet Additive Solution

TPO: Thrombopoitein

TRALI: Transfusion-Related Acute Lung Injury

TT: Thrombin Time

UFH: Unfractionated Heparin

UR: Upper Right

VEGF: Vascular Endothelial Growth Factor

VIM: Vimentin

VWD: Von Willebrand Disease

VWF: Von Willebrand Factor

WHO: World Health Organization

αSMA: alpha Smooth Muscle Actin

8 AKNOWLEDGMENTS

First and foremost, I would like to express my deepest gratitude to my supervisor, Dr. Lucia Merolle, for her invaluable guidance, continuous support, and insightful feedback throughout my PhD journey. I am equally grateful to Dr. Chiara Marraccini and Dr. Davide Schiroli for their mentorship and encouragement, which have been fundamental in shaping both this research and my development as a scientist.

I am also sincerely thankful to all my colleagues at the Transfusion Medicine Unit of AUSL-IRCCS of Reggio Emilia, led by Dr. Roberto Baricchi, for creating a welcoming and supportive environment where I always felt at home. A special thanks to Dr. Agnese Razzoli and Margherita Genitoni, who have been not only pillars of my daily lab life but also true friends outside of work.

I would also like to acknowledge the Department of Biomedical, Metabolic and Neural Sciences of the University of Modena and Reggio Emilia, the EVIta society and the Berlucchi Foundation for providing the financial support that allowed me to conduct part of my research as a visiting PhD student at the University of Continuing Education in Krems, Austria. In this regard, I am especially grateful to Dr. Viktoria Weber, Dr. Tanja Eichhorn, Dr. Marwa Mostageer, Dr. Vladislav Semak and Dr. Susanne Krenn for their kindness, guidance and for making me feel welcome in their lab since day one.

I am deeply thankful to my family for their unwavering belief in me, for encouraging me to chase my dreams, and teaching me the value of perseverance. Your guidance, sacrifices, and constant reassurance have been my foundation.

Finally, to Davide. Your love, patience, and constant support made even the toughest days feel manageable. Thank you for celebrating the small victories, for comforting me through the setbacks, and for being my rock throughout this entire journey. I could not have achieved this milestone without you.

This thesis is not only the result of my own work but also a reflection of the support, encouragement, and inspiration I have received from all of you.

9 REFERENCES

1. Van Der Meijden PEJ, Heemskerk JWM. Platelet biology and functions: new concepts and clinical perspectives. *Nat Rev Cardiol*. 2019;16(3):166-179. doi:10.1038/s41569-018-0110-0

2. Holinstat M. Normal platelet function. *Cancer Metastasis Rev*. 2017;36(2):195-198. doi:10.1007/s10555-017-9677-x

3. Quach ME, Chen W, Li R. Mechanisms of platelet clearance and translation to improve platelet storage. *Blood*. 2018;131(14):1512-1521. doi:10.1182/blood-2017-08-743229

4. White JG. Current Concepts of Platelet Structure. *Am J Clin Pathol*. 1979;71(4):363-378. doi:10.1093/ajcp/71.4.363

5. White G. Further Studies of the Secretory Pathway in.

6. Escolar G, Leistikow E, White J. The fate of the open canalicular system in surface and suspension-activated platelets. *Blood*. 1989;74(6):1983-1988. doi:10.1182/blood.V74.6.1983.1983

7. Gremmel T, Frelinger A, Michelson A. Platelet Physiology. *Semin Thromb Hemost*. 2016;42(03):191-204. doi:10.1055/s-0035-1564835

8. Ostrowska M, Kubica J, Adamski P, et al. Stratified Approaches to Antiplatelet Therapies Based on Platelet Reactivity Testing. *Front Cardiovasc Med*. 2019;6:176. doi:10.3389/fcvm.2019.00176

9. King SM, Reed GL. Development of platelet secretory granules. *Semin Cell Dev Biol*. 2002;13(4):293-302. doi:10.1016/S1084952102000599

10. Chen CH, Lo RW, Urban D, Pluthero FG, Kahr WHA. α-granule biogenesis: from disease to discovery. *Platelets*. 2017;28(2):147-154. doi:10.1080/09537104.2017.1280599

11. Zhou Y, Dong J, Wang M, Liu Y. New insights of platelet endocytosis and its implication for platelet function. *Front Cardiovasc Med*. 2024;10:1308170. doi:10.3389/fcvm.2023.1308170

12. Italiano Jr. JE, Battinelli EM. Selective sorting of alpha-granule proteins. *J Thromb Haemost*. 2009;7:173-176. doi:10.1111/j.1538-7836.2009.03387.x

13. Maynard DM, Heijnen HFG, Horne MK, White JG, Gahl WA. Proteomic analysis of platelet α-granules using mass spectrometry. *J Thromb Haemost*. 2007;5(9):1945-1955. doi:10.1111/j.1538-7836.2007.02690.x

14. Michelson A. Flow cytometry: a clinical test of platelet function. *Blood*. 1996;87(12):4925-4936. doi:10.1182/blood.V87.12.4925.bloodjournal87124925

15. Berger G, Masse J, Cramer E. Alpha-granule membrane mirrors the platelet plasma membrane and contains the glycoproteins Ib, IX, and V. *Blood*. 1996;87(4):1385-1395. doi:10.1182/blood.V87.4.1385.bloodjournal8741385

16. Suzuki H, Murasaki K, Kodama K, Takayama H. Intracellular localization of glycoprotein VI in human platelets and its surface expression upon activation. *Br J Haematol*. 2003;121(6):904-912. doi:10.1046/j.1365-2141.2003.04373.x

17. Kasper B, Brandt E, Bulfone-Paus S, Petersen F. Platelet factor 4 (PF-4)–induced neutrophil adhesion is controlled by src-kinases, whereas PF-4–mediated exocytosis requires the additional activation of p38

MAP kinase and phosphatidylinositol 3-kinase. *Blood*. 2004;103(5):1602-1610. doi:10.1182/blood-2003-08-2802

18. Gleissner CA, Von Hundelshausen P, Ley K. Platelet Chemokines in Vascular Disease. *Arterioscler Thromb Vasc Biol*. 2008;28(11):1920-1927. doi:10.1161/ATVBAHA.108.169417

19. Devine DV, Rosse WF. Regulation of the activity of platelet-bound C3 convertase of the alternative pathway of complement by platelet factor H. *Proc Natl Acad Sci*. 1987;84(16):5873-5877. doi:10.1073/pnas.84.16.5873

20. Licht C, Pluthero FG, Li L, et al. Platelet-associated complement factor H in healthy persons and patients with atypical HUS. *Blood*. 2009;114(20):4538-4545. doi:10.1182/blood-2009-03-205096

21. Schmaier AH, Smith PM, Colman RW. Platelet C1- inhibitor. A secreted alpha-granule protein. *J Clin Invest*. 1985;75(1):242-250. doi:10.1172/JCI111680

22. Schmaier AH, Amenta S, Xiong T, Gewirtz AM. Expression of Platelet C1 Inhibitor.

23. Rendu F, Brohard-Bohn B. The platelet release reaction: granules' constituents, secretion and functions. *Platelets*. 2001;12(5):261-273. doi:10.1080/09537100120068170

24. Brill A. Differential role of platelet granular mediators in angiogenesis. *Cardiovasc Res*. 2004;63(2):226-235. doi:10.1016/j.cardiores.2004.04.012

25. Battinelli EM, Markens BA, Italiano JE. Release of angiogenesis regulatory proteins from platelet alpha granules: modulation of physiologic and pathologic angiogenesis. *Blood*. 2011;118(5):1359-1369. doi:10.1182/blood-2011-02-334524

26. Slater M, Patava J, Kingham K, Mason RS. Involvement of platelets in stimulating osteogenic activity. *J Orthop Res*. 1995;13(5):655-663. doi:10.1002/jor.1100130504

27. Eppley BL, Woodell JE, Higgins J. Platelet Quantification and Growth Factor Analysis from Platelet-Rich Plasma: Implications for Wound Healing: *Plast Reconstr Surg*. Published online November 2004:1502-1508. doi:10.1097/01.PRS.0000138251.07040.51

28. Ambrosio AL, Di Pietro SM. Storage pool diseases illuminate platelet dense granule biogenesis. *Platelets*. 2017;28(2):138-146. doi:10.1080/09537104.2016.1243789

29. Meyers KM, Holmsen H, Seachord CL. Comparative study of platelet dense granule constituents. *Am J Physiol-Regul Integr Comp Physiol*. 1982;243(3):R454-R461. doi:10.1152/ajpregu.1982.243.3.R454

30. Chen Y, Yuan Y, Li W. Sorting machineries: how platelet-dense granules differ from α-granules. *Biosci Rep*. 2018;38(5):BSR20180458. doi:10.1042/BSR20180458

31. Golebiewska EM, Poole AW. Platelet secretion: From haemostasis to wound healing and beyond. *Blood Rev*. 2015;29(3):153-162. doi:10.1016/j.blre.2014.10.003

32. Duerschmied D, Suidan GL, Demers M, et al. Platelet serotonin promotes the recruitment of neutrophils to sites of acute inflammation in mice. *Blood*. 2013;121(6):1008-1015. doi:10.1182/blood-2012-06-437392

33. Ginsberg M, Taylor L, Painter R. The mechanism of thrombin-induced platelet factor 4 secretion. *Blood*. 1980;55(4):661-668. doi:10.1182/blood.V55.4.661.661

34. Stenberg PE, Shuman MA, Levine SP, Bainton DF. http://www.jstor.org Redistribution of Alpha-Granules and Their Contents in Thrombin-Stimulated Platelets. *J Cell Biol*. 1984;98(2):748-760.

35. Feng D, Crane K, Rozenvayn N, Dvorak AM, Flaumenhaft R. Subcellular distribution of 3 functional platelet SNARE proteins: human cellubrevin, SNAP-23, and syntaxin 2. *Blood*. 2002;99(11):4006-4014. doi:10.1182/blood.V99.11.4006

36. Polgár J, Reed GL. A Critical Role for N-ethylmaleimide–Sensitive Fusion Protein (NSF) in Platelet Granule Secretion. *Blood*. 1999;94(4):1313-1318. doi:10.1182/blood.V94.4.1313

37. Lemons PP, Chen D, Whiteheart SW. Molecular Mechanisms of Platelet Exocytosis: Requirements for α-Granule Release. *Biochem Biophys Res Commun*. 2000;267(3):875-880. doi:10.1006/bbrc.1999.2039

38. Machlus KR, Italiano JE. The incredible journey: From megakaryocyte development to platelet formation. *J Cell Biol*. 2013;201(6):785-796. doi:10.1083/jcb.201304054

39. Ivanovna Gabrilchak A, Anatolievna Gusyakova O, Aleksandrovich Antipov V, Alekseevna Medvedeva E, Leonidovna Tukshumskaya L. A modern overview of the process of platelet formation (thrombocytopoiesis) and its dependence on several factors. *Biochem Medica*. 2024;34(3). doi:10.11613/BM.2024.030503

40. Pease DC. An Electron Microscopic Study of Red Bone Marrow. *Blood*. 1956;11(6):501-526. doi:10.1182/blood.V11.6.501.501

41. Ogawa M. Differentiation and Proliferation of Hematopoietic Stem Cells.

42. Kaushansky K, Lok S, Holly RD, et al. Promotion of megakaryocyte progenitor expansion and differentiation by the c-Mpl ligand thrombopoietin. *Nature*. 1994;369(6481):568-571. doi:10.1038/369568a0

43. Vitrat N, Cohen-Solal K, Pique C, et al. Endomitosis of Human Megakaryocytes Are Due to Abortive Mitosis.

44. Zimmet J, Ravid K. Polyploidy: Occurrence in nature, mechanisms, and significance for the megakaryocyte-platelet system.

45. Lecine P, Jr JEI, Kim SW, Villeval JL, Shivdasani RA. Hematopoietic-specific b1 tubulin participates in a pathway of platelet biogenesis dependent on the transcription factor NF-E2.

46. Patel SR, Richardson JL, Schulze H, et al. Differential roles of microtubule assembly and sliding in proplatelet formation by megakaryocytes. *Blood*. 2005;106(13):4076-4085. doi:10.1182/blood-2005-06-2204

47. Kunishima S, Kobayashi R, Itoh TJ, Hamaguchi M, Saito H. Mutation of the 1-tubulin gene associated with congenital macrothrombocytopenia affecting microtubule assembly.

48. Richardson JL, Shivdasani RA, Boers C, Hartwig JH, Italiano JE. Mechanisms of organelle transport and capture along proplatelets during platelet production. *Blood*. 2005;106(13):4066-4075. doi:10.1182/blood-2005-06-2206

49. Moujalled D, Gangatirkar P, Kauppi M, et al. The necroptotic cell death pathway operates in megakaryocytes, but not in platelet synthesis. *Cell Death Dis*. 2021;12(1):133. doi:10.1038/s41419-021-03418-z

50. Rasche H. Haemostasis and thrombosis: an overview. *Eur Heart J Suppl*. 2001;3:Q3-Q7. doi:10.1016/S1520-765X(01)90034-3

51. Palta S, Saroa R, Palta A. Overview of the coagulation system. *Indian J Anaesth*. 2014;58(5):515. doi:10.4103/0019-5049.144643

52. Zaidi A, Green L. Physiology of haemostasis. *Anaesth Intensive Care Med*. 2019;20(3):152-158. doi:10.1016/j.mpaic.2019.01.005

53. Hoffman M, Monroe D. A Cell-based Model of Hemostasis. *Thromb Haemost*. 2001;85(06):958-965. doi:10.1055/s-0037-1615947

54. Mackman N. Role of Tissue Factor in Hemostasis, Thrombosis, and Vascular Development. *Arterioscler Thromb Vasc Biol*. 2004;24(6):1015-1022. doi:10.1161/01.ATV.0000130465.23430.74

55. Hoffman M. A cell-based model of coagulation and the role of factor VIIa. *Blood Rev*. 2003;17:S1-S5. doi:10.1016/S0268-960X(03)90000-2

56. Hoffman M, Monroe DM. Coagulation 2006: A Modern View of Hemostasis. *Hematol Oncol Clin North Am*. 2007;21(1):1-11. doi:10.1016/j.hoc.2006.11.004

57. Oliver JA, Monroe DM, Roberts HR, Hoffman M. Thrombin Activates Factor XI on Activated Platelets in the Absence of Factor XII. *Arterioscler Thromb Vasc Biol*. 1999;19(1):170-177. doi:10.1161/01.ATV.19.1.170

58. Andrews RK, Berndt MC. Platelet physiology and thrombosis. *Thromb Res*. 2004;114(5-6):447-453. doi:10.1016/j.thromres.2004.07.020

59. Sira J, Eyre L. Physiology of haemostasis. *Anaesth Intensive Care Med*. 2016;17(2):79-82. doi:10.1016/j.mpaic.2015.11.004

60. Laurens N, Koolwijk P, De Maat MPM. Fibrin structure and wound healing. *J Thromb Haemost*. 2006;4(5):932-939. doi:10.1111/j.1538-7836.2006.01861.x

61. Stalker TJ, Traxler EA, Wu J, et al. Hierarchical organization in the hemostatic response and its relationship to the platelet-signaling network. *Blood*. 2013;121(10):1875-1885. doi:10.1182/blood-2012-09-457739

62. Cesarman-Maus G, Hajjar KA. Molecular mechanisms of fibrinolysis. *Br J Haematol*. 2005;129(3):307-321. doi:10.1111/j.1365-2141.2005.05444.x

63. ES04.01 Physiology of haemostasis. Published online 2004.

64. Vaughan DE. PAI-1 and atherothrombosis. *J Thromb Haemost*. 2005;3(8):1879-1883. doi:10.1111/j.1538-7836.2005.01420.x

65. Olson ST, Richard B, Izaguirre G, Schedin-Weiss S, Gettins PGW. Molecular mechanisms of antithrombin–heparin regulation of blood clotting proteinases. A paradigm for understanding proteinase regulation by serpin family protein proteinase inhibitors. *Biochimie*. 2010;92(11):1587-1596. doi:10.1016/j.biochi.2010.05.011

66. Rezaie AR, Giri H. Anticoagulant and signaling functions of antithrombin. *J Thromb Haemost*. 2020;18(12):3142-3153. doi:10.1111/jth.15052

67. Wood JP, Ellery PER, Maroney SA, Mast AE. Biology of tissue factor pathway inhibitor. *Blood*. 2014;123(19):2934-2943. doi:10.1182/blood-2013-11-512764

68. Levy JH, Szlam F, Wolberg AS, Winkler A. Clinical Use of the Activated Partial Thromboplastin Time and Prothrombin Time for Screening. *Clin Lab Med*. 2014;34(3):453-477. doi:10.1016/j.cll.2014.06.005

69. Poller L. International Normalized Ratios (INR): the first 20 years. *J Thromb Haemost*. 2004;2(6):849-860. doi:10.1111/j.1538-7836.2004.00775.x

70. Arachchillage DRJ, Kamani F, Deplano S, Banya W, Laffan M. Should we abandon the APTT for monitoring unfractionated heparin? *Thromb Res*. 2017;157:157-161. doi:10.1016/j.thromres.2017.07.006

71. Johansson PI, Stissing T, Bochsen L, Ostrowski SR. Thrombelastography and tromboelastometry in assessing coagulopathy in trauma. *Scand J Trauma Resusc Emerg Med*. 2009;17(1):45. doi:10.1186/1757-7241-17-45

72. Nielsen VG. A comparison of the Thrombelastograph and the ROTEM. *Blood Coagul Fibrinolysis*. 2007;18(3):247-252. doi:10.1097/MBC.0b013e328092ee05

73. Whiting D, DiNardo JA. TEG and ROTEM: Technology and clinical applications. *Am J Hematol*. 2014;89(2):228-232. doi:10.1002/ajh.23599

74. Schenk B, Görlinger K, Treml B, et al. A comparison of the new ROTEM® *sigma* with its predecessor, the ROTEM *delta*. *Anaesthesia*. 2019;74(3):348-356. doi:10.1111/anae.14542

75. Veigas PV, Callum J, Rizoli S, Nascimento B, Da Luz LT. A systematic review on the rotational thrombelastometry (ROTEM®) values for the diagnosis of coagulopathy, prediction and guidance of blood transfusion and prediction of mortality in trauma patients. *Scand J Trauma Resusc Emerg Med*. 2016;24(1):114. doi:10.1186/s13049-016-0308-2

76. Peyvandi F, Garagiola I, Young G. The past and future of haemophilia: diagnosis, treatments, and its complications. *The Lancet*. 2016;388(10040):187-197. doi:10.1016/S0140-6736(15)01123-X

77. Seidizadeh O, Eikenboom JCJ, Denis CV, et al. von Willebrand disease. *Nat Rev Dis Primer*. 2024;10(1):51. doi:10.1038/s41572-024-00536-8

78. Casini A. Dysfibrinogenemia: from molecular anomalies to clinical manifestations and management. Published online 2015.

79. Kodama T, Takehara T, Hikita H, et al. BH3-only Activator Proteins Bid and Bim Are Dispensable for Bak/Bax-dependent Thrombocyte Apoptosis Induced by Bcl-xL Deficiency. *J Biol Chem*. 2011;286(16):13905-13913. doi:10.1074/jbc.M110.195370

80. Mason KD, Carpinelli MR, Fletcher JI, et al. Programmed Anuclear Cell Death Delimits Platelet Life Span. *Cell*. 2007;128(6):1173-1186. doi:10.1016/j.cell.2007.01.037

81. Schoenwaelder SM, Yuan Y, Josefsson EC, et al. Two distinct pathways regulate platelet phosphatidylserine exposure and procoagulant function. *Blood*. 2009;114(3):663-666. doi:10.1182/blood-2009-01-200345

82. Van Kruchten R, Mattheij NJA, Saunders C, et al. Both TMEM16F-dependent and TMEM16F-independent pathways contribute to phosphatidylserine exposure in platelet apoptosis and platelet activation. *Blood*. 2013;121(10):1850-1857. doi:10.1182/blood-2012-09-454314

83. Suzuki J, Umeda M, Sims PJ, Nagata S. Calcium-dependent phospholipid scrambling by TMEM16F. *Nature*. 2010;468(7325):834-838. doi:10.1038/nature09583

84. Quach ME, Chen W, Li R. Mechanisms of platelet clearance and translation to improve platelet storage. *Blood*. 2018;131(14):1512-1521. doi:10.1182/blood-2017-08-743229

85. Soslau G, Giles J. THE LOSS OF SIALIC ACID AND ITS PREVENTIONIN SXWEDHUMANPIATEIZTS.

86. Li Y, Fu J, Ling Y, et al. Sialylation on O-glycans protects platelets from clearance by liver Kupffer cells. *Proc Natl Acad Sci*. 2017;114(31):8360-8365. doi:10.1073/pnas.1707662114

87. Rivadeneyra L, Falet H, Hoffmeister KM. Circulating platelet count and glycans. *Curr Opin Hematol*. 2021;28(6):431-437. doi:10.1097/MOH.0000000000000682

88. Ballem PJ, Segal GM, Stratton JR, Gernsheimer T, Adamson JW, Slichter SJ. Mechanisms of thrombocytopenia in chronic autoimmune thrombocytopenic purpura. Evidence of both impaired platelet production and increased platelet clearance. *J Clin Invest*. 1987;80(1):33-40. doi:10.1172/JCI113060

89. Casari C, Du V, Wu YP, et al. Accelerated uptake of VWF/platelet complexes in macrophages contributes to VWD type 2B–associated thrombocytopenia. *Blood*. 2013;122(16):2893-2902. doi:10.1182/blood-2013-03-493312

90. Sørensen AL, Rumjantseva V, Nayeb-Hashemi S, et al. Role of sialic acid for platelet life span: exposure of β-galactose results in the rapid clearance of platelets from the circulation by asialoglycoprotein receptor–expressing liver macrophages and hepatocytes. *Blood*. 2009;114(8):1645-1654. doi:10.1182/blood-2009-01-199414

91. Chen W, Liang X, Syed AK, et al. Inhibiting GPIbα Shedding Preserves Post-Transfusion Recovery and Hemostatic Function of Platelets After Prolonged Storage. *Arterioscler Thromb Vasc Biol*. 2016;36(9):1821-1828. doi:10.1161/ATVBAHA.116.307639

92. Gauer RL. Thrombocytopenia.

93. Cines DB, Blanchette VS. Immune Thrombocytopenic Purpura. Published online 2002.

94. Veneri D, Franchini M, Randon F, Nichele I, Pizzolo G, Ambrosetti A. Thrombocytopenias: a clinical point of view. *Blood Transfus*. Published online 2008. doi:10.2450/2008.0012-08

95. Buss DH, Cashell AW, O'Connor ML, Richards F, Case LD. Occurence, etiology, and clinical significance of extreme thrombocytosis: A study of 280 cases. *Am J Med*. 1994;96(3):247-253. doi:10.1016/0002-9343(94)90150-3

96. Schafer AI. Thrombocytosis and thrombocythemia. *Blood Rev*. 2001;15(4):159-166. doi:10.1054/blre.2001.0162

97. Palma-Barqueros V, Revilla N, Sánchez A, et al. Inherited Platelet Disorders: An Updated Overview. *Int J Mol Sci*. 2021;22(9):4521. doi:10.3390/ijms22094521

98. Bastida JM, Benito R, Lozano ML, et al. Molecular Diagnosis of Inherited Coagulation and Bleeding Disorders. *Semin Thromb Hemost*. 2019;45(07):695-707. doi:10.1055/s-0039-1687889

99. Nurden P, Stritt S, Favier R, Nurden AT. Inherited platelet diseases with normal platelet count: phenotypes, genotypes and diagnostic strategy. *Haematologica*. 2020;106(2):337-350. doi:10.3324/haematol.2020.248153

100. Bolton-Maggs PHB, Chalmers EA, Collins PW, et al. A review of inherited platelet disorders with guidelines for their management on behalf of the UKHCDO. *Br J Haematol*. 2006;135(5):603-633. doi:10.1111/j.1365-2141.2006.06343.x

101. Andonegui G, Kerfoot SM, McNagny K, Ebbert KVJ, Patel KD, Kubes P. Platelets express functional Toll-like receptor-4. *Blood*. 2005;106(7):2417-2423. doi:10.1182/blood-2005-03-0916

102. Semple JW, Italiano JE, Freedman J. Platelets and the immune continuum. *Nat Rev Immunol*. 2011;11(4):264-274. doi:10.1038/nri2956

103. Semple JW, Freedman J. Platelets and innate immunity. *Cell Mol Life Sci*. 2010;67(4):499-511. doi:10.1007/s00018-009-0205-1

104. Von Hundelshausen P, Weber C. Platelets as Immune Cells: Bridging Inflammation and Cardiovascular Disease. *Circ Res*. 2007;100(1):27-40. doi:10.1161/01.RES.0000252802.25497.b7

105. Ruggeri ZM, Mendolicchio GL. Adhesion Mechanisms in Platelet Function. *Circ Res*. 2007;100(12):1673-1685. doi:10.1161/01.RES.0000267878.97021.ab

106. Van Gils JM, Zwaginga JJ, Hordijk PL. Molecular and functional interactions among monocytes, platelets, and endothelial cells and their relevance for cardiovascular diseases. *J Leukoc Biol*. 2009;85(2):195-204. doi:10.1189/jlb.0708400

107. Hui P, Cook DJ, Lim W, Fraser GA, Arnold DM. The Frequency and Clinical Significance of Thrombocytopenia Complicating Critical Illness. *Chest*. 2011;139(2):271-278. doi:10.1378/chest.10-2243

108. Gawaz M, Fateh-Moghadam S, Pilz G, Gurland H -J., Werdan K. Platelet activation and interaction with leucocytes in patients with sepsis or multiple organ failure. *Eur J Clin Invest*. 1995;25(11):843-851. doi:10.1111/j.1365-2362.1995.tb01694.x

109. Clark SR, Ma AC, Tavener SA, et al. Platelet TLR4 activates neutrophil extracellular traps to ensnare bacteria in septic blood. *Nat Med*. 2007;13(4):463-469. doi:10.1038/nm1565

110. Assinger A, Laky M, Schabbauer G, et al. Efficient phagocytosis of periodontopathogens by neutrophils requires plasma factors, platelets and TLR2. *J Thromb Haemost*. 2011;9(4):799-809. doi:10.1111/j.1538-7836.2011.04193.x

111. Elzey BD, Ratliff TL, Sowa JM, Crist SA. Platelet CD40L at the interface of adaptive immunity. *Thromb Res*. 2011;127(3):180-183. doi:10.1016/j.thromres.2010.10.011

112. Henn V, Slupsky JR, Gräfe M, et al. CD40 ligand on activated platelets triggers an inflammatory reaction of endothelial cells. *Nature*. 1998;391(6667):591-594. doi:10.1038/35393

113. Yang H, Biermann MH, Brauner JM, Liu Y, Zhao Y, Herrmann M. New Insights into Neutrophil Extracellular Traps: Mechanisms of Formation and Role in Inflammation. *Front Immunol*. 2016;7. doi:10.3389/fimmu.2016.00302

114. Papayannopoulos V. Neutrophil extracellular traps in immunity and disease. *Nat Rev Immunol*. 2018;18(2):134-147. doi:10.1038/nri.2017.105

115. Brinkmann V, Reichard U, Goosmann C, et al. Neutrophil Extracellular Traps Kill Bacteria. *Science*. 2004;303(5663):1532-1535. doi:10.1126/science.1092385

116. Etulain J, Martinod K, Wong SL, Cifuni SM, Schattner M, Wagner DD. P-selectin promotes neutrophil extracellular trap formation in mice. *Blood*. 2015;126(2):242-246. doi:10.1182/blood-2015-01-624023

117. Takei H, Araki A, Watanabe H, Ichinose A, Sendo F. Rapid killing of human neutrophils by the potent activator phorbol 12-myristate 13-acetate (PMA) accompanied by changes different from typical apoptosis or necrosis. *J Leukoc Biol*. 1996;59(2):229-240. doi:10.1002/jlb.59.2.229

118. Desai J, Mulay SR, Nakazawa D, Anders HJ. Matters of life and death. How neutrophils die or survive along NET release and is "NETosis" = necroptosis? *Cell Mol Life Sci*. 2016;73(11-12):2211-2219. doi:10.1007/s00018-016-2195-0

119. Yipp BG, Kubes P. NETosis: how vital is it? *Blood*. 2013;122(16):2784-2794. doi:10.1182/blood-2013-04-457671

120. Galluzzi L, Vitale I, Aaronson SA, et al. Molecular mechanisms of cell death: recommendations of the Nomenclature Committee on Cell Death 2018. *Cell Death Differ*. 2018;25(3):486-541. doi:10.1038/s41418-017-0012-4

121. Maugeri N, Campana L, Gavina M, et al. Activated platelets present high mobility group box 1 to neutrophils, inducing autophagy and promoting the extrusion of neutrophil extracellular traps. *J Thromb Haemost*. 2014;12(12):2074-2088. doi:10.1111/jth.12710

122. Zhan Y, Ling Y, Deng Q, et al. HMGB1-Mediated Neutrophil Extracellular Trap Formation Exacerbates Intestinal Ischemia/Reperfusion-Induced Acute Lung Injury. *J Immunol*. 2022;208(4):968-978. doi:10.4049/jimmunol.2100593

123. Wienkamp AK, Erpenbeck L, Rossaint J. Platelets in the NETworks interweaving inflammation and thrombosis. *Front Immunol*. 2022;13:953129. doi:10.3389/fimmu.2022.953129

124. Tsourouktsoglou TD, Warnatsch A, Ioannou M, Hoving D, Wang Q, Papayannopoulos V. Histones, DNA, and Citrullination Promote Neutrophil Extracellular Trap Inflammation by Regulating the Localization and Activation of TLR4. *Cell Rep*. 2020;31(5):107602. doi:10.1016/j.celrep.2020.107602

125. Semeraro F, Ammollo CT, Morrissey JH, et al. Extracellular histones promote thrombin generation through platelet-dependent mechanisms: involvement of platelet TLR2 and TLR4. *Blood*. 2011;118(7):1952-1961. doi:10.1182/blood-2011-03-343061

126. Campos J, Ponomaryov T, De Prendergast A, et al. Neutrophil extracellular traps and inflammasomes cooperatively promote venous thrombosis in mice. *Blood Adv*. 2021;5(9):2319-2324. doi:10.1182/bloodadvances.2020003377

127. Aubé FA, Bidias A, Pépin G. Who and how, DNA sensors in NETs-driven inflammation. *Front Immunol*. 2023;14:1190177. doi:10.3389/fimmu.2023.1190177

128. Zhang W, Zhang Y, Han L, et al. Double-stranded DNA enhances platelet activation, thrombosis, and myocardial injury via cyclic GMP-AMP synthase. *Cardiovasc Res*. 2025;121(2):353-366. doi:10.1093/cvr/cvae218

129. Sennett C, Pula G. Trapped in the NETs: Multiple Roles of Platelets in the Vascular Complications Associated with Neutrophil Extracellular Traps. *Cells*. 2025;14(5):335. doi:10.3390/cells14050335

130. Zhang Y, Ye J, Sun S, et al. Role of platelets and NETs in arterial thrombosis. *Naunyn Schmiedebergs Arch Pharmacol*. Published online February 24, 2025. doi:10.1007/s00210-025-03921-6

131. Li W, Chi D, Ju S, et al. Platelet factor 4 promotes deep venous thrombosis by regulating the formation of neutrophil extracellular traps. *Thromb Res*. 2024;237:52-63. doi:10.1016/j.thromres.2024.03.005

132. Kastrup CJ, Boedicker JQ, Pomerantsev AP, et al. Spatial localization of bacteria controls coagulation of human blood by "quorum acting." *Nat Chem Biol*. 2008;4(12):742-750. doi:10.1038/nchembio.124

133. Kraemer BF, Campbell RA, Schwertz H, et al. Novel Anti-bacterial Activities of β-defensin 1 in Human Platelets: Suppression of Pathogen Growth and Signaling of Neutrophil Extracellular Trap Formation. DeLeo FR, ed. *PLoS Pathog*. 2011;7(11):e1002355. doi:10.1371/journal.ppat.1002355

134. Youssefian T, Drouin A, Massé JM, Guichard J, Cramer EM. Host defense role of platelets: engulfment of HIV andStaphylococcus aureus occurs in a specific subcellular compartment and is enhanced by platelet activation. *Blood*. 2002;99(11):4021-4029. doi:10.1182/blood-2001-12-0191

135. White JG. Why human platelets fail to kill bacteria. *Platelets*. 2006;17(3):191-200. doi:10.1080/09537100500441234

136. Pak S, Kondo T, Nakano Y, et al. Platelet adhesion in the sinusoid caused hepatic injury by neutrophils after hepatic ischemia reperfusion. *Platelets*. 2010;21(4):282-288. doi:10.3109/09537101003637265

137. Varki A. Trousseau's syndrome: multiple definitions and multiple mechanisms. *Blood*. 2007;110(6):1723-1729. doi:10.1182/blood-2006-10-053736

138. Gasic GJ, Gasic TB, Galanti N, Johnson T, Murphy S. Platelet—tumor-cell interactions in mice. The role of platelets in the spread of malignant disease. *Int J Cancer*. 1973;11(3):704-718. doi:10.1002/ijc.2910110322

139. Karpatkin S, Pearlstein E, Ambrogio C, Coller BS. Role of adhesive proteins in platelet tumor interaction in vitro and metastasis formation in vivo. *J Clin Invest*. 1988;81(4):1012-1019. doi:10.1172/JCI113411

140. Kim YJ, Borsig L, Varki NM, Varki A. P-selectin deficiency attenuates tumor growth and metastasis. *Proc Natl Acad Sci*. 1998;95(16):9325-9330. doi:10.1073/pnas.95.16.9325

141. Bakewell SJ, Nestor P, Prasad S, et al. Platelet and osteoclast β_3 integrins are critical for bone metastasis. *Proc Natl Acad Sci*. 2003;100(24):14205-14210. doi:10.1073/pnas.2234372100

142. Palumbo JS, Degen JL. Mechanisms linking tumor cell-associated procoagulant function to tumor metastasis. *Thromb Res*. 2007;120:S22-S28. doi:10.1016/S0049-3848(07)70127-5

143. Labelle M, Hynes RO. The Initial Hours of Metastasis: The Importance of Cooperative Host–Tumor Cell Interactions during Hematogenous Dissemination. *Cancer Discov*. 2012;2(12):1091-1099. doi:10.1158/2159-8290.CD-12-0329

144. Jain S, Harris J, Ware J. Platelets: Linking Hemostasis and Cancer. *Arterioscler Thromb Vasc Biol*. 2010;30(12):2362-2367. doi:10.1161/ATVBAHA.110.207514

145. Hanahan D, Weinberg RA. Hallmarks of Cancer: The Next Generation. *Cell*. 2011;144(5):646-674. doi:10.1016/j.cell.2011.02.013

146. Hanahan D, Weinberg RA. The Hallmarks of Cancer Review.

147. Zhang S, Xiao X, Yi Y, et al. Tumor initiation and early tumorigenesis: molecular mechanisms and interventional targets. *Signal Transduct Target Ther*. 2024;9(1):149. doi:10.1038/s41392-024-01848-7

148. Gay LJ, Felding-Habermann B. Contribution of platelets to tumour metastasis. *Nat Rev Cancer*. 2011;11(2):123-134. doi:10.1038/nrc3004

149. Khorana AA, Francis CW, Culakova E, Kuderer NM, Lyman GH. Thromboembolism is a leading cause of death in cancer patients receiving outpatient chemotherapy. *J Thromb Haemost*. 2007;5(3):632-634. doi:10.1111/j.1538-7836.2007.02374.x

150. Nichetti F, Ligorio F, Montelatici G, et al. Risk assessment of thromboembolic events in hospitalized cancer patients. *Sci Rep*. 2021;11(1):18200. doi:10.1038/s41598-021-97659-9

151. Abdel-Razeq H, Mansour A, Saadeh SS, et al. The Application of Current Proposed Venous Thromboembolism Risk Assessment Model for Ambulatory Patients With Cancer. *Clin Appl Thromb*. 2018;24(3):429-433. doi:10.1177/1076029617692880

152. Patell R, Rybicki L, McCrae KR, Khorana AA. Predicting risk of venous thromboembolism in hospitalized cancer patients: Utility of a risk assessment tool. *Am J Hematol*. 2017;92(6):501-507. doi:10.1002/ajh.24700

153. Stone RL, Nick AM, McNeish IA, et al. Paraneoplastic Thrombocytosis in Ovarian Cancer. *N Engl J Med*. 2012;366(7):610-618. doi:10.1056/NEJMoa1110352

154. Cerutti A, Custodi P, Duranti M, Noris P, Balduini CL. Thrombopoietin levels in patients with primary and reactive thrombocytosis. *Br J Haematol*. 1997;99(2):281-284. doi:10.1046/j.1365-2141.1997.3823196.x

155. Besbes S, Shah S, Al-dybiat I, et al. Thrombopoietin Secretion by Human Ovarian Cancer Cells. *Int J Cell Biol*. 2017;2017:1-10. doi:10.1155/2017/1873834

156. Kaser A, Brandacher G, Steurer W, et al. Interleukin-6 stimulates thrombopoiesis through thrombopoietin: role in inflammatory thrombocytosis. *Blood*. 2001;98(9):2720-2725. doi:10.1182/blood.V98.9.2720

157. Riedl J, Hell L, Kaider A, et al. Association of platelet activation markers with cancer-associated venous thromboembolism. *Platelets*. 2016;27(1):80-85. doi:10.3109/09537104.2015.1041901

158. Rank A, Liebhardt S, Zwirner J, Burges A, Nieuwland R, Toth B. Circulating Microparticles in Patients with Benign and Malignant Ovarian Tumors. *ANTICANCER Res*. Published online 2012.

159. Jurasz P, Alonso-Escolano D, Radomski MW. Platelet–cancer interactions: mechanisms and pharmacology of tumour cell-induced platelet aggregation. *Br J Pharmacol*. 2004;143(7):819-826. doi:10.1038/sj.bjp.0706013

160. Suzuki-Inoue K. Roles of the CLEC-2–podoplanin interaction in tumor progression. *Platelets*. 2018;29(8):786-792. doi:10.1080/09537104.2018.1478401

161. Kasthuri RS, Taubman MB, Mackman N. Role of Tissue Factor in Cancer. *J Clin Oncol*. 2009;27(29):4834-4838. doi:10.1200/JCO.2009.22.6324

162. Eelen G, Treps L, Li X, Carmeliet P. Basic and Therapeutic Aspects of Angiogenesis Updated. *Circ Res*. 2020;127(2):310-329. doi:10.1161/CIRCRESAHA.120.316851

163. Janowska-Wieczorek A, Wysoczynski M, Kijowski J, et al. Microvesicles derived from activated platelets induce metastasis and angiogenesis in lung cancer. *Int J Cancer*. 2005;113(5):752-760. doi:10.1002/ijc.20657

164. Lakka Klement G, Yip TT, Cassiola F, et al. Platelets actively sequester angiogenesis regulators. *Blood*. 2009;113(12):2835-2842. doi:10.1182/blood-2008-06-159541

165. Guan X. Cancer metastases: challenges and opportunities. *Acta Pharm Sin B*. 2015;5(5):402-418. doi:10.1016/j.apsb.2015.07.005

166. Strilic B, Offermanns S. Intravascular Survival and Extravasation of Tumor Cells. *Cancer Cell*. 2017;32(3):282-293. doi:10.1016/j.ccell.2017.07.001

167. Camerer E, Qazi AA, Duong DN, Cornelissen I, Advincula R, Coughlin SR. Platelets, protease-activated receptors, and fibrinogen in hematogenous metastasis. *Blood*. 2004;104(2):397-401. doi:10.1182/blood-2004-02-0434

168. Gasic GJ, Gasic TB, Stewart CC. Antimetastatic effects associated with platelet reduction. *Proc Natl Acad Sci*. 1968;61(1):46-52. doi:10.1073/pnas.61.1.46

169. Palumbo JS, Talmage KE, Massari JV, et al. Platelets and fibrin(ogen) increase metastatic potential by impeding natural killer cell–mediated elimination of tumor cells. *Blood*. 2005;105(1):178-185. doi:10.1182/blood-2004-06-2272

170. Yang J, Antin P, Berx G, et al. Guidelines and definitions for research on epithelial–mesenchymal transition. *Nat Rev Mol Cell Biol*. 2020;21(6):341-352. doi:10.1038/s41580-020-0237-9

171. Labelle M, Begum S, Hynes RO. Direct Signaling between Platelets and Cancer Cells Induces an Epithelial-Mesenchymal-Like Transition and Promotes Metastasis. *Cancer Cell*. 2011;20(5):576-590. doi:10.1016/j.ccr.2011.09.009

172. McCarty OJT, Mousa SA, Bray PF, Konstantopoulos K. Immobilized platelets support human colon carcinoma cell tethering, rolling, and firm adhesion under dynamic flow conditions. 2000;96(5).

173. Zimmerman GA. Two by two: The pairings of P-selectin and P-selectin glycoprotein ligand 1. *Proc Natl Acad Sci*. 2001;98(18):10023-10024. doi:10.1073/pnas.191367898

174. Kim YJ, Borsig L, Han HL, Varki NM, Varki A. Distinct Selectin Ligands on Colon Carcinoma Mucins Can Mediate Pathological Interactions among Platelets, Leukocytes, and Endothelium. *Am J Pathol*. 1999;155(2):461-472. doi:10.1016/S0002-9440(10)65142-5

175. Wojtukiewicz MZ, Sierko E, Hempel D, Tucker SC, Honn KV. Platelets and cancer angiogenesis nexus. *Cancer Metastasis Rev*. 2017;36(2):249-262. doi:10.1007/s10555-017-9673-1

176. Tkach M, Théry C. Communication by Extracellular Vesicles: Where We Are and Where We Need to Go. *Cell*. 2016;164(6):1226-1232. doi:10.1016/j.cell.2016.01.043

177. Kibria G, Ramos EK, Lee KE, et al. A rapid, automated surface protein profiling of single circulating exosomes in human blood. *Sci Rep*. 2016;6(1):36502. doi:10.1038/srep36502

178. Zhang J, Li S, Li L, et al. Exosome and Exosomal MicroRNA: Trafficking, Sorting, and Function. *Genomics Proteomics Bioinformatics*. 2015;13(1):17-24. doi:10.1016/j.gpb.2015.02.001

179. Nawaz M, Camussi G, Valadi H, et al. The emerging role of extracellular vesicles as biomarkers for urogenital cancers. *Nat Rev Urol*. 2014;11(12):688-701. doi:10.1038/nrurol.2014.301

180. Flaumenhaft R, Mairuhu A, Italiano J. Platelet- and Megakaryocyte-Derived Microparticles. *Semin Thromb Hemost*. 2010;36(08):881-887. doi:10.1055/s-0030-1267042

181. Abels ER, Breakefield XO. Introduction to Extracellular Vesicles: Biogenesis, RNA Cargo Selection, Content, Release, and Uptake. *Cell Mol Neurobiol*. 2016;36(3):301-312. doi:10.1007/s10571-016-0366-z

182. Antwi-Baffour S, Adjei J, Aryeh C, Kyeremeh R, Kyei F, Seidu MA. Understanding the biosynthesis of platelets-derived extracellular vesicles. *Immun Inflamm Dis*. 2015;3(3):133-140. doi:10.1002/iid3.66

183. Boilard E, Nigrovic PA, Larabee K, et al. Platelets Amplify Inflammation in Arthritis via Collagen-Dependent Microparticle Production. *Science*. 2010;327(5965):580-583. doi:10.1126/science.1181928

184. Żmigrodzka M, Witkowska-Piłaszewicz O, Winnicka A. Platelets Extracellular Vesicles as Regulators of Cancer Progression—An Updated Perspective. *Int J Mol Sci*. 2020;21(15):5195. doi:10.3390/ijms21155195

185. Mause SF, Ritzel E, Liehn EA, et al. Platelet Microparticles Enhance the Vasoregenerative Potential of Angiogenic Early Outgrowth Cells After Vascular Injury. *Circulation*. 2010;122(5):495-506. doi:10.1161/CIRCULATIONAHA.109.909473

186. Ogata N, Imaizumi M, Nomura S, et al. Increased levels of platelet-derived microparticles in patients with diabetic retinopathy. *Diabetes Res Clin Pract*. 2005;68(3):193-201. doi:10.1016/j.diabres.2004.10.010

187. Nomura S. Platelet-derived microparticles may influence the development of atherosclerosis in diabetes mellitus. *Atherosclerosis*. 1995;116(2):235-240. doi:10.1016/0021-9150(95)05551-7

188. Feng B, Chen Y, Luo Y, Chen M, Li X, Ni Y. Circulating level of microparticles and their correlation with arterial elasticity and endothelium-dependent dilation in patients with type 2 diabetes mellitus. *Atherosclerosis*. 2010;208(1):264-269. doi:10.1016/j.atherosclerosis.2009.06.037

189. Biasucci LM, Porto I, Di Vito L, et al. Differences in Microparticle Release in Patients With Acute Coronary Syndrome and Stable Angina. *Circ J*. 2012;76(9):2174-2182. doi:10.1253/circj.CJ-12-0068

190. Chimen M, Evryviadou A, Box CL, et al. Appropriation of GPIbα from platelet-derived extracellular vesicles supports monocyte recruitment in systemic inflammation. *Haematologica*. 2020;105(5):1248-1261. doi:10.3324/haematol.2018.215145

191. BCSH platelet guideline 08 08 16 Changes accepted.

192. Solves Alcaina P. Platelet Transfusion: And Update on Challenges and Outcomes. *J Blood Med*. 2020;Volume 11:19-26. doi:10.2147/JBM.S234374

193. European Directorate for the Quality of Medicines & HealthCare (EDQM). *Guide to the Preparation, Use and Quality Assurance of Blood Components (Blood Guide)*. 22nd ed. Strasbourg: Council of Europe https://www.edqm.eu/en/blood-guide

194. Siebert H. Platelet-rich plasma in clinical practice. *South Afr Fam Pract*. 2016;58(1):4. doi:10.4102/safp.v58i1.4440

195. Aljefri AM, Brien CO, Tan TJ, Sheikh AM, Ouellette H, Bauones S. Clinical Applications of PRP: Musculoskeletal Applications, Current Practices and Update. *Cardiovasc Intervent Radiol*. 2023;46(11):1504-1516. doi:10.1007/s00270-023-03567-y

196. Geerling G, MacLennan S, Hartwig D. Autologous serum eye drops for ocular surface disorders. *Br J Ophthalmol*. Published online 2025.

197. Spotnitz WD. Fibrin Sealant: Past, Present, and Future: A Brief Review. *World J Surg*. 2010;34(4):632-634. doi:10.1007/s00268-009-0252-7

198. Li S, Lu Z, Wu S, et al. The dynamic role of platelets in cancer progression and their therapeutic implications. *Nat Rev Cancer*. 2024;24(1):72-87. doi:10.1038/s41568-023-00639-6

199. Humbrecht C, Kientz D, Gachet C. Platelet transfusion: Current challenges. *Transfus Clin Biol*. 2018;25(3):151-164. doi:10.1016/j.tracli.2018.06.004

200. Schiffer CA, Bohlke K, Delaney M, et al. Platelet Transfusion for Patients With Cancer: American Society of Clinical Oncology Clinical Practice Guideline Update. *J Clin Oncol*. 2018;36(3):283-299. doi:10.1200/JCO.2017.76.1734

201. Estcourt LJ. Why has demand for platelet components increased? A review. *Transfus Med*. 2014;24(5):260-268. doi:10.1111/tme.12155

202. Wandt H, Schäfer-Eckart K, Greinacher A. Platelet Transfusion in Hematology, Oncology and Surgery. *Dtsch Ärztebl Int*. Published online November 28, 2014. doi:10.3238/arztebl.2014.0809

203. Slichter SJ. Platelet Transfusion Therapy. *Hematol Oncol Clin North Am*. 2007;21(4):697-729. doi:10.1016/j.hoc.2007.06.010

204. Schiroli D, Merolle L, Quartieri E, et al. Comparison of Two Alternative Procedures to Obtain Packed Red Blood Cells for β-Thalassemia Major Transfusion Therapy. *Biomolecules*. 2021;11(11):1638. doi:10.3390/biom11111638

205. Heddle NM, Arnold DM, Boye D, Webert KE, Resz I, Dumont LJ. Comparing the efficacy and safety of apheresis and whole blood–derived platelet transfusions: a systematic review. *Transfusion (Paris)*. 2008;48(7):1447-1458. doi:10.1111/j.1537-2995.2008.01731.x

206. Thomas S. Platelets: handle with care. *Transfus Med*. 2016;26(5):330-338. doi:10.1111/tme.12327

207. Ng MSY, Tung JP, Fraser JF. Platelet Storage Lesions: What More Do We Know Now? *Transfus Med Rev*. 2018;32(3):144-154. doi:10.1016/j.tmrv.2018.04.001

208. Paglia G, Sigurjónsson ÓE, Rolfsson Ó, et al. Comprehensive metabolomic study of platelets reveals the expression of discrete metabolic phenotypes during storage. *Transfusion (Paris)*. 2014;54(11):2911-2923. doi:10.1111/trf.12710

209. Vit G, Klüter H, Wuchter P. Platelet storage and functional integrity. *J Lab Med*. 2020;44(5):285-293. doi:10.1515/labmed-2020-0067

210. Rinder HM, Murphy M, Mitchell JG, Stocks J, Ault KA, Hillman RS. Progressive platelet activation with storage: evidence for shortened survival of activated platelets after transfusion. *Transfusion (Paris)*. 1991;31(5):409-414. doi:10.1046/j.1537-2995.1991.31591263195.x

211. Kogler VJ, Stolla M. There and back again: the once and current developments in donor-derived platelet products for hemostatic therapy. *Blood*. 2022;139(26):3688-3698. doi:10.1182/blood.2021014889

212. Soutar R, McSporran W, Tomlinson T, Booth C, Grey S. Guideline on the investigation and management of acute transfusion reactions. *Br J Haematol*. 2023;201(5):832-844. doi:10.1111/bjh.18789

213. Pavenski K, Freedman J, Semple JW. HLA alloimmunization against platelet transfusions: pathophysiology, significance, prevention and management. *Tissue Antigens*. 2012;79(4):237-245. doi:10.1111/j.1399-0039.2012.01852.x

214. Forest SK, Hod EA. Management of the Platelet Refractory Patient. *Hematol Oncol Clin North Am*. 2016;30(3):665-677. doi:10.1016/j.hoc.2016.01.008

215. Schiroli D, Merolle L, Molinari G, et al. The impact of COVID -19 outbreak on the Transfusion Medicine Unit of a Northern Italy Hospital and Cancer Centre. *Vox Sang*. 2022;117(2):235-242. doi:10.1111/vox.13174

216. Noorman F, Rijnhout TWH, De Kort B, Hoencamp R. Frozen for combat: Quality of deep-frozen thrombocytes, produced and used by The Netherlands Armed Forces 2001–2021. *Transfusion (Paris)*. 2023;63(1):203-216. doi:10.1111/trf.17166

217. Valeri C, Ragno G, Khuri S. Freezing human platelets with 6 percent dimethyl sulfoxide with removal of the supernatant solution before freezing and storage at −80°C without postthaw processing. *Transfusion (Paris)*. 2006;46(2):313-313. doi:10.1111/j.1537-2995.2006.00754.x

218. Valeri CR, Feingold H, Marchionni LD. A Simple Method for Freezing Human Platelets Using 6% Dimethylsulfoxide and Storage at -80°C. *Blood*. 1974;43(1):131-136. doi:10.1182/blood.V43.1.131.131

219. Kelly K, Cancelas JA, Szczepiorkowski ZM, Dumont DF, Rugg N, Dumont LJ. Frozen Platelets—Development and Future Directions. *Transfus Med Rev*. 2020;34(4):286-293. doi:10.1016/j.tmrv.2020.09.008

220. Slichter SJ, Dumont LJ, Cancelas JA, et al. Safety and efficacy of cryopreserved platelets in bleeding patients with thrombocytopenia. *Transfusion (Paris)*. 2018;58(9):2129-2138. doi:10.1111/trf.14780

221. Rajashekaraiah V, Rajanand MC. Platelet storage: Progress so far. *J Thromb Thrombolysis*. 2022;55(1):9-17. doi:10.1007/s11239-022-02716-3

222. Dumont LJ, Slichter SJ, Reade MC. Cryopreserved platelets: frozen in a logjam? *Transfusion (Paris)*. 2014;54(8):1907-1910. doi:10.1111/trf.12758

223. Valeri CR, Srey R, Lane JP, Ragno G. Effect of WBC reduction and storage temperature on PLTs frozen with 6 percent DMSO for as long as 3 years. *Transfusion (Paris)*. 2003;43(8):1162-1167. doi:10.1046/j.1537-2995.2003.00468.x

224. Johnson L, Vekariya S, Tan S, Padula MP, Marks DC. Extended storage of thawed platelets: Refrigeration supports postthaw quality for 10 days. *Transfusion (Paris)*. 2020;60(12):2969-2981. doi:10.1111/trf.16127

225. Gerber B, Alberio L, Rochat S, et al. Safety and efficacy of cryopreserved autologous platelet concentrates in HLA-alloimmunized patients with hematologic malignancies. *Transfusion (Paris)*. 2016;56(10):2426-2437. doi:10.1111/trf.13690

226. Johnson L, Tan S, Jenkins E, Wood B, Marks DC. Characterization of biologic response modifiers in the supernatant of conventional, refrigerated, and cryopreserved platelets. *Transfusion (Paris)*. 2018;58(4):927-937. doi:10.1111/trf.14475

227. Pu F, Li X, Wang S, Huang Y, Wang D. Platelet supernatant with longer storage inhibits tumor cell growth. *Transfus Apher Sci*. 2021;60(2):103042. doi:10.1016/j.transci.2020.103042

228. Palacios-Acedo AL, Mège D, Crescence L, Dignat-George F, Dubois C, Panicot-Dubois L. Platelets, Thrombo-Inflammation, and Cancer: Collaborating With the Enemy. *Front Immunol*. 2019;10:1805. doi:10.3389/fimmu.2019.01805

229. Best BP. Cryoprotectant Toxicity: Facts, Issues, and Questions. *Rejuvenation Res*. 2015;18(5):422-436. doi:10.1089/rej.2014.1656

230. Whaley D, Damyar K, Witek RP, Mendoza A, Alexander M, Lakey JR. Cryopreservation: An Overview of Principles and Cell-Specific Considerations. *Cell Transplant*. 2021;30:0963689721999617. doi:10.1177/0963689721999617

231. Awan M, Buriak I, Fleck R, et al. Dimethyl Sulfoxide: A Central Player Since the Dawn of Cryobiology, is Efficacy Balanced by Toxicity? *Regen Med*. 2020;15(3):1463-1491. doi:10.2217/rme-2019-0145

232. Johnson L, Lei P, Roan C, Marks DC. Development of a simplified platelet cryopreservation method: An in vitro investigation of reducing the DMSO concentration to allow administration without its pre-transfusion removal. *Vox Sang*. Published online January 6, 2025:vox.13789. doi:10.1111/vox.13789

233. Ehn K, Wikman A, Uhlin M, Sandgren P. Cryopreserved Platelets in a Non-Toxic DMSO-Free Solution Maintain Hemostatic Function In Vitro. *Int J Mol Sci*. 2023;24(17):13097. doi:10.3390/ijms241713097

234. Alves R, Grimalt R. A Review of Platelet-Rich Plasma: History, Biology, Mechanism of Action, and Classification. *Skin Appendage Disord*. 2018;4(1):18-24. doi:10.1159/000477353

235. Dohan Ehrenfest DM, Rasmusson L, Albrektsson T. Classification of platelet concentrates: from pure platelet-rich plasma (P-PRP) to leucocyte- and platelet-rich fibrin (L-PRF). *Trends Biotechnol*. 2009;27(3):158-167. doi:10.1016/j.tibtech.2008.11.009

236. M. Dohan Ehrenfest D, Bielecki T, Jimbo R, et al. Do the Fibrin Architecture and Leukocyte Content Influence the Growth Factor Release of Platelet Concentrates? An Evidence-based Answer Comparing a Pure Platelet-Rich Plasma (P-PRP) Gel and a Leukocyte- and Platelet-Rich Fibrin (L-PRF). *Curr Pharm Biotechnol*. 2012;13(7):1145-1152. doi:10.2174/138920112800624382

237. Saqlain N, Mazher N, Fateen T, Siddique A. Comparison of single and double centrifugation methods for preparation of Platelet-Rich Plasma (PRP). *Pak J Med Sci*. 2023;39(3). doi:10.12669/pjms.39.3.7264

238. Dhurat R, Sukesh M. Principles and methods of preparation of platelet-rich plasma: A review and author's perspective. *J Cutan Aesthetic Surg*. 2014;7(4):189. doi:10.4103/0974-2077.150734

239. Anitua E, Sánchez M, Orive G. The importance of understanding what is platelet-rich growth factor (PRGF) and what is not. *J Shoulder Elbow Surg*. 2011;20(1):e23-e24. doi:10.1016/j.jse.2010.07.005

240. Ehrenfest DMD, Sammartino G, Shibli JA, Wang HL, Zou DR, Bernard JP. Guidelines for the publication of articles related to platelet concentrates (Platelet-Rich Plasma - PRP, or Platelet-Rich Fibrin - PRF): the international classification of the.

241. Merolle L, Iotti B, Berni P, et al. Platelet-Rich Plasma Lysate for Treatment of Eye Surface Diseases. *J Vis Exp*. 2022;(186):63772. doi:10.3791/63772

242. Henschler R, Gabriel C, Schallmoser K, Burnouf T, Koh MBC. Human platelet lysate current standards and future developments. *Transfusion (Paris)*. 2019;59(4):1407-1413. doi:10.1111/trf.15174

243. Boero V, Cetera GE, Caia C, et al. Is there a role for platelet rich plasma injection in vulvar lichen sclerosus? A self-controlled pilot study. *Arch Gynecol Obstet*. 2024;309(6):2719-2726. doi:10.1007/s00404-024-07424-2

244. Coombes BK, Bisset L, Vicenzino B. Efficacy and safety of corticosteroid injections and other injections for management of tendinopathy: a systematic review of randomised controlled trials. *The Lancet*. 2010;376(9754):1751-1767. doi:10.1016/S0140-6736(10)61160-9

245. Rutgers M, Saris DB, Dhert WJ, Creemers LB. Cytokine profile of autologous conditioned serum for treatment of osteoarthritis, in vitroeffects on cartilage metabolism and intra-articular levels after injection. *Arthritis Res Ther*. 2010;12(3):R114. doi:10.1186/ar3050

246. Oneto P, Etulain J. PRP in wound healing applications. *Platelets*. 2021;32(2):189-199. doi:10.1080/09537104.2020.1849605

247. Menchisheva Y, Mirzakulova U, Yui R. Use of platelet-rich plasma to facilitate wound healing. *Int Wound J*. 2019;16(2):343-353. doi:10.1111/iwj.13034

248. Anitua E, Fernández-de-Retana S, Alkhraisat MH. Platelet rich plasma in oral and maxillofacial surgery from the perspective of composition. *Platelets*. 2021;32(2):174-182. doi:10.1080/09537104.2020.1856361

249. Everts PA, Van Erp A, DeSimone A, Cohen DS, Gardner RD. Platelet Rich Plasma in Orthopedic Surgical Medicine. *Platelets*. 2021;32(2):163-174. doi:10.1080/09537104.2020.1869717

250. Giannaccare G, Versura P, Buzzi M, Primavera L, Pellegrini M, Campos EC. Blood derived eye drops for the treatment of cornea and ocular surface diseases. *Transfus Apher Sci*. 2017;56(4):595-604. doi:10.1016/j.transci.2017.07.023

251. Yessirkepov M, Fedorchenko Y, Zimba O, Mukanova U. Use of platelet-rich plasma in rheumatic diseases. *Rheumatol Int*. 2024;45(1):13. doi:10.1007/s00296-024-05776-1

252. Guberti M, Schiroli D, Marraccini C, et al. Homologous platelet gel on radiation-induced dermatitis in a patient receiving head and neck radiotherapy plus cetuximab: A case report. *Medicine (Baltimore)*. 2023;102(34):e34779. doi:10.1097/MD.0000000000034779

253. Condorelli AG, Paganelli A, Marraccini C, et al. Platelet-rich plasma for the treatment of scleroderma-associated ulcers: a single-center experience and literature review. *Dermatol Rep*. Published online February 21, 2024. doi:10.4081/dr.2024.9878

254. Verma R, Kumar S, Garg P, Verma YK. Platelet-rich plasma: a comparative and economical therapy for wound healing and tissue regeneration. *Cell Tissue Bank*. 2023;24(2):285-306. doi:10.1007/s10561-022-10039-z

255. Everts PAM, Knape JTA, Weibrich G, et al. Platelet-Rich Plasma and Platelet Gel: A Review. *J Extracorpor Technol*. 2006;38(2):174-187. doi:10.1051/ject/200638174

256. Vladulescu D, Scurtu LG, Simionescu AA, Scurtu F, Popescu MI, Simionescu O. Platelet-Rich Plasma (PRP) in Dermatology: Cellular and Molecular Mechanisms of Action. *Biomedicines*. 2023;12(1):7. doi:10.3390/biomedicines12010007

257. Manole CG, Soare C, Ceafalan LC, Voiculescu VM. Platelet-Rich Plasma in Dermatology: New Insights on the Cellular Mechanism of Skin Repair and Regeneration. *Life*. 2023;14(1):40. doi:10.3390/life14010040

258. Qu W, Wang Z, Hunt C, et al. The Effectiveness and Safety of Platelet-Rich Plasma for Chronic Wounds. *Mayo Clin Proc*. 2021;96(9):2407-2417. doi:10.1016/j.mayocp.2021.01.030

259. Roubelakis MG, Trohatou O, Roubelakis A, et al. Platelet-Rich Plasma (PRP) Promotes Fetal Mesenchymal Stem/Stromal Cell Migration and Wound Healing Process. *Stem Cell Rev Rep*. 2014;10(3):417-428. doi:10.1007/s12015-013-9494-8

260. Hesseler MJ, Shyam N. Platelet-rich plasma and its utility in medical dermatology: A systematic review. *J Am Acad Dermatol*. 2019;81(3):834-846. doi:10.1016/j.jaad.2019.04.037

261. Pulcini S, Merolle L, Marraccini C, et al. Apheresis Platelet Rich-Plasma for Regenerative Medicine: An In Vitro Study on Osteogenic Potential. *Int J Mol Sci*. 2021;22(16):8764. doi:10.3390/ijms22168764

262. Johnson L, Lei P, Waters L, Padula MP, Marks DC. Identification of platelet subpopulations in cryopreserved platelet components using multi-colour imaging flow cytometry. *Sci Rep*. 2023;13(1):1221. doi:10.1038/s41598-023-28352-2

263. Johnson LN, Winter KM, Reid S, Hartkopf-Theis T, Marks DC. Cryopreservation of buffy-coat-derived platelet concentrates in dimethyl sulfoxide and platelet additive solution. *Cryobiology*. 2011;62(2):100-106. doi:10.1016/j.cryobiol.2011.01.003

264. Italiano JE, Mairuhu AT, Flaumenhaft R. Clinical relevance of microparticles from platelets and megakaryocytes: *Curr Opin Hematol*. 2010;17(6):578-584. doi:10.1097/MOH.0b013e32833e77ee

265. Kireev D, Popenko N, Pichugin A, et al. Platelet microparticle membranes have 50- to 100-fold higher specific procoagulant activity than activated platelets. *Thromb Haemost*. 2007;97(03):425-434. doi:10.1160/th06-06-0313

266. Ebeyer-Masotta M, Eichhorn T, Weiss R, Lauková L, Weber V. Activated Platelets and Platelet-Derived Extracellular Vesicles Mediate COVID-19-Associated Immunothrombosis. *Front Cell Dev Biol*. 2022;10. doi:10.3389/fcell.2022.914891

267. Weiss R, Gröger M, Rauscher S, et al. Differential Interaction of Platelet-Derived Extracellular Vesicles with Leukocyte Subsets in Human Whole Blood. *Sci Rep*. 2018;8(1). doi:10.1038/s41598-018-25047-x

268. Fendl B, Weiss R, Fischer MB, Spittler A, Weber V. Characterization of extracellular vesicles in whole blood: Influence of pre-analytical parameters and visualization of vesicle-cell interactions using imaging flow cytometry. *Biochem Biophys Res Commun*. 2016;478(1):168-173. doi:10.1016/j.bbrc.2016.07.073

269. Liumbruno GM, Bennardello F, Lattanzio A, Piccoli PL, Rossetti G. Recommendations for the transfusion of plasma and platelets. *Blood Transfus*. Published online 2009. doi:10.2450/2009.0005-09

270. Valeri CR, Ragno G, Khuri S. Freezing human platelets with 6 percent dimethyl sulfoxide with removal of the supernatant solution before freezing and storage at −80°C without postthaw processing. *Transfusion (Paris)*. 2005;45(12):1890-1898. doi:10.1111/j.1537-2995.2005.00647.x

271. Marks DC, Johnson L. Assays for phenotypic and functional characterization of cryopreserved platelets. *Platelets*. 2019;30(1):48-55. doi:10.1080/09537104.2018.1514108

272. Marchisio M, Simeone P, Bologna G, et al. Flow Cytometry Analysis of Circulating Extracellular Vesicle Subtypes from Fresh Peripheral Blood Samples. *Int J Mol Sci*. 2020;22(1):48. doi:10.3390/ijms22010048

273. Birarda G, Bedolla DE, Piccirilli F, Stani C, Vondracek H, Vaccari L. Chemical analyses at micro and nano scale at SISSI-Bio beamline at elettra-sincrotrone trieste. *Biomedical vibrational spectroscopy 2022: advances in research and industry*. 2022:27-39.

274. Toplak M, Read ST, Sandt C, Borondics F. Quasar: Easy Machine Learning for Biospectroscopy. *Cells*. 2021;10(9):2300. doi:10.3390/cells10092300

275. Zuo X xiao, Yang Y, Zhang Y, Zhang Z gang, Wang X fei, Shi Y gang. Platelets promote breast cancer cell MCF-7 metastasis by direct interaction: surface integrin α2β1-contacting-mediated activation of Wnt-β-catenin pathway. *Cell Commun Signal*. 2019;17(1). doi:10.1186/s12964-019-0464-x

276. Comşa Ş, Cîmpean AM, Raica M. The Story of MCF-7 Breast Cancer Cell Line: 40 years of Experience in Research. *ANTICANCER Res*. Published online 2015.

277. Schneider CA, Rasband WS, Eliceiri KW. NIH Image to ImageJ: 25 years of image analysis. *Nature methods*. 10.1038/nmeth.2089. 2012.

278. Shou LM, Zhang QY, Li W, et al. Cantharidin and norcantharidin inhibit the ability of MCF-7 cells to adhere to platelets via protein kinase C pathway-dependent downregulation of α2 integrin. *Oncol Rep*. 2013;30(3):1059-1066. doi:10.3892/or.2013.2601

279. Maurizi E, Merra A, Macaluso C, Schiroli D, Pellegrini G. GSK-3 inhibition reverts mesenchymal transition in primary human corneal endothelial cells. *Eur J Cell Biol*. 2023;102(2):151302. doi:10.1016/j.ejcb.2023.151302

280. Lustig M, Feng Q, Payan Y, Gefen A, Benayahu D. Noninvasive Continuous Monitoring of Adipocyte Differentiation: From Macro to Micro Scales. *Microsc Microanal*. 2019;25(1):119-128. doi:10.1017/s1431927618015520

281. Pachetti M, Zupin L, Venturin I, et al. FTIR Spectroscopy to Reveal Lipid and Protein Changes Induced on Sperm by Capacitation: Bases for an Improvement of Sample Selection in ART. *Int J Mol Sci*. 2020;21(22):8659. doi:10.3390/ijms21228659

282. Baker MJ, Trevisan J, Bassan P, et al. Using Fourier transform IR spectroscopy to analyze biological materials. *Nat Protoc*. 2014;9(8):1771-1791. doi:10.1038/nprot.2014.110

283. Johnson J, Wu YW, Blyth C, Lichtfuss G, Goubran H, Burnouf T. Prospective Therapeutic Applications of Platelet Extracellular Vesicles. *Trends Biotechnol*. 2021;39(6):598-612. doi:10.1016/j.tibtech.2020.10.004

284. Bikle DD, Xie Z, Tu CL. Calcium regulation of keratinocyte differentiation. *Expert Rev Endocrinol Metab*. 2012;7(4):461-472. doi:10.1586/eem.12.34

285. Fibroblast Differentiation in Wound Healing and Fibrosis. In: *International Review of Cytology*. Elsevier; 2007:143-179. doi:10.1016/s0074-7696(07)57004-x

286. Garrett SM, Baker Frost D, Feghali-Bostwick C. The Mighty Fibroblast and Its Utility in Scleroderma Research. *J Scleroderma Relat Disord*. 2017;2(2):100-107. doi:10.5301/jsrd.5000240

287. Phan SH. Genesis of the Myofibroblast in Lung Injury and Fibrosis. *Proc Am Thorac Soc*. 2012;9(3):148-152. doi:10.1513/pats.201201-011aw

288. Sonnylal S, Denton CP, Zheng B, et al. Postnatal induction of transforming growth factor β signaling in fibroblasts of mice recapitulates clinical, histologic, and biochemical features of scleroderma. *Arthritis Rheum*. 2007;56(1):334-344. doi:10.1002/art.22328

289. Yuan W, Varga J. Transforming Growth Factor-β Repression of Matrix Metalloproteinase-1 in Dermal Fibroblasts Involves Smad3. *J Biol Chem*. 2001;276(42):38502-38510. doi:10.1074/jbc.m107081200

290. Gnani D, Crippa S, Della Volpe L, et al. An early-senescence state in aged mesenchymal stromal cells contributes to hematopoietic stem and progenitor cell clonogenic impairment through the activation of a pro-inflammatory program. *Aging Cell*. 2019;18(3). doi:10.1111/acel.12933

291. Berndt S, Turzi A, Pittet-Cuénod B, Modarressi A. Autologous Platelet-Rich Plasma (CuteCell PRP) Safely Boosts*In Vitro*Human Fibroblast Expansion. *Tissue Eng Part A*. 2019;25(21-22):1550-1563. doi:10.1089/ten.tea.2018.0335

292. Hashimoto K. Regulation of keratinocyte function by growth factors. *J Dermatol Sci*. 2000;24:S46-S50. doi:10.1016/s0923-1811(00)00141-9

293. Baik SY, Lim YA, Kang SJ, Ahn SH, Lee WG, Kim CH. Effects of Platelet Lysate Preparations on the Proliferation of HaCaT Cells. *Ann Lab Med*. 2014;34(1):43-50. doi:10.3343/alm.2014.34.1.43

294. Park HB, Yang JH, Chung KH. Characterization of the cytokine profile of platelet rich plasma (PRP) and PRP-induced cell proliferation and migration: Upregulation of matrix metalloproteinase-1 and -9 in HaCaT cells. *Korean J Hematol*. 2011;46(4):265. doi:10.5045/kjh.2011.46.4.265

295. Cui X, Ma Y, Wang H, et al. The Anti-photoaging Effects of Pre- and Post-treatment of Platelet-rich Plasma on UVB-damaged HaCaT Keratinocytes. *Photochem Photobiol*. 2021;97(3):589-599. doi:10.1111/php.13354

296. Colombo I, Sangiovanni E, Maggio R, et al. HaCaT Cells as a Reliable In Vitro Differentiation Model to Dissect the Inflammatory/Repair Response of Human Keratinocytes. *Mediators Inflamm*. 2017;2017:1-12. doi:10.1155/2017/7435621

297. Wilson VG. Growth and differentiation of HaCaT keratinocytes. In: *Epidermal Cells: Methods and Protocols*. 2014:33-41. https://doi.org/10.1007/7651_2013_42

298. Pleguezuelos O, Kapas S. Differentiation of the HaCaT keratinocyte cell line: modulation by adrenomedullin: Adrenomedullin and keratinocyte differentiation. *Br J Dermatol*. 2006;154(4):602-608. doi:10.1111/j.1365-2133.2005.07117.x

299. Polito MP, Romaldini A, Rinaldo S, Enzo E. Coordinating energy metabolism and signaling pathways in epithelial self-renewal and differentiation. *Biol Direct*. 2024;19(1). doi:10.1186/s13062-024-00510-0

300. Sercia L, Romano O, Marini G, et al. A cellular disease model toward gene therapy of TGM1-dependent lamellar ichthyosis. *Mol Ther - Methods Clin Dev*. 2024;32(3):101311. doi:10.1016/j.omtm.2024.101311

301. Oberringer M, Meins C, Bubel M, Pohlemann T. A new *in vitro* wound model based on the co-culture of human dermal microvascular endothelial cells and human dermal fibroblasts. *Biol Cell*. 2007;99(4):197-207. doi:10.1042/bc20060116

302. Tonnesen MG, Feng X, Clark RAF. Angiogenesis in Wound Healing. *J Investig Dermatol Symp Proc*. 2000;5(1):40-46. doi:10.1046/j.1087-0024.2000.00014.x

303. Ades EW, Candal FJ, Swerlick RA, et al. HMEC-1: Establishment of an Immortalized Human Microvascular Endothelial Cell Line. *J Invest Dermatol*. 1992;99(6):683-690. doi:10.1111/1523-1747.ep12613748

304. Sanchez B, Li L, Dulong J, et al. Impact of Human Dermal Microvascular Endothelial Cells on Primary Dermal Fibroblasts in Response to Inflammatory Stress. *Front Cell Dev Biol*. 2019;7. doi:10.3389/fcell.2019.00044

305. Luo J, Paranya G, Bischoff J. Noninflammatory Expression of E-Selectin Is Regulated by Cell Growth. *Blood*. 1999;93(11):3785-3791. doi:10.1182/blood.v93.11.3785

306. Slichter SJ, Jones M, Ransom J, et al. Review of In Vivo Studies of Dimethyl Sulfoxide Cryopreserved Platelets. *Transfus Med Rev*. 2014;28(4):212-225. doi:10.1016/j.tmrv.2014.09.001

307. McGuinness S, Charlewood R, Gilder E, et al. A pilot randomized clinical trial of cryopreserved versus liquid-stored platelet transfusion for bleeding in cardiac surgery: The cryopreserved versus liquid platelet - New Zealand pilot trial. *Vox Sang*. 2022;117(3):337-345. doi:10.1111/vox.13203

308. Larsen JB, Hojbjerg JA, Hvas AM. The Role of Platelets in Cancer-Related Bleeding Risk: A Systematic Review. *Semin Thromb Hemost*. 2020;46(03):328-341. doi:10.1055/s-0039-3402429

309. Gavioli G, Razzoli A, Bedolla DE, et al. Cryopreservation affects platelet macromolecular composition over time after thawing and differently impacts on cancer cells behavior in vitro. *Platelets*. 2023;34(1):2281943. doi:10.1080/09537104.2023.2281943

310. Lang T, Bauters A, Braun SL, et al. Multi-centre investigation on reference ranges for ROTEM thromboelastometry. *Blood Coagul Fibrinolysis*. 2005;16(4):301-310. doi:10.1097/01.mbc.0000169225.31173.19

311. Johnson L, Reade MC, Hyland RA, Tan S, Marks DC. In vitro comparison of cryopreserved and liquid platelets: potential clinical implications. *Transfusion (Paris)*. 2015;55(4):838-847. doi:10.1111/trf.12915

312. Cid J, Escolar G, Galan A, et al. In vitro evaluation of the hemostatic effectiveness of cryopreserved platelets. *Transfusion (Paris)*. 2016;56(3):580-586. doi:10.1111/trf.13371

313. Kwan PSL, Kirwan S, Tuinukuafe A, Morley S. Temporal dynamics of in vitro hemostatic function in platelets cryopreserved using a novel approach for rapid issuance. *Transfusion (Paris)*. 2024;64(7):1287-1295. doi:10.1111/trf.17871

314. Meinke S, Wikman A, Gryfelt G, et al. Cryopreservation of buffy coat–derived platelet concentrates photochemically treated with amotosalen and UVA light. *Transfusion (Paris)*. 2018;58(11):2657-2668. doi:10.1111/trf.14905

315. Johnson L, Coorey CP, Marks DC. The hemostatic activity of cryopreserved platelets is mediated by phosphatidylserine-expressing platelets and platelet microparticles. *Transfusion (Paris)*. 2014;54(8):1917-1926. doi:10.1111/trf.12578

316. Nagler M, Kathriner S, Bachmann LM, Wuillemin WA. Impact of changes in haematocrit level and platelet count on thromboelastometry parameters. *Thromb Res*. 2013;131(3):249-253. doi:10.1016/j.thromres.2013.01.009

317. Noorman F, Hess JR. The contribution of the individual blood elements to the variability of thromboelastographic measures. *Transfusion (Paris)*. 2018;58(10):2430-2436. doi:10.1111/trf.14884

318. Waters L, Padula MP, Marks DC, Johnson L. Cryopreserved platelets demonstrate reduced activation responses and impaired signaling after agonist stimulation. *Transfusion (Paris)*. 2017;57(12):2845-2857. doi:10.1111/trf.14310

319. Barnard MR, MacGregor H, Ragno G, et al. Fresh, liquid-preserved, and cryopreserved platelets: adhesive surface receptors and membrane procoagulant activity. *Transfusion (Paris)*. 1999;39(8):880-888. doi:10.1046/j.1537-2995.1999.39080880.x

320. Springer TA. von Willebrand factor, Jedi knight of the bloodstream. *Blood*. 2014;124(9):1412-1425. doi:10.1182/blood-2014-05-378638

321. Winskel-Wood B, Padula MP, Marks DC, Johnson L. The phenotype of cryopreserved platelets influences the formation of platelet-leukocyte aggregates in an *in vitro* model. *Platelets*. 2023;34(1):2206916. doi:10.1080/09537104.2023.2206916

322. Six KR, Compernolle V, Feys HB. Platelet Biochemistry and Morphology after Cryopreservation. *Int J Mol Sci*. 2020;21(3):935. doi:10.3390/ijms21030935

323. Gläfke C, Akhoondi M, Oldenhof H, Sieme H, Wolkers WF. Cryopreservation of platelets using trehalose: The role of membrane phase behavior during freezing. *Biotechnol Prog*. 2012;28(5):1347-1354. doi:10.1002/btpr.1600

324. Six KR, Delabie W, Devreese KMJ, et al. Comparison between manufacturing sites shows differential adhesion, activation, and GPIbα expression of cryopreserved platelets. *Transfusion (Paris)*. 2018;58(11):2645-2656. doi:10.1111/trf.14828

325. Żmigrodzka M, Guzera M, Miśkiewicz A, Jagielski D, Winnicka A. The biology of extracellular vesicles with focus on platelet microparticles and their role in cancer development and progression. *Tumor Biol*. 2016;37(11):14391-14401. doi:10.1007/s13277-016-5358-6

326. Tegegn TZ, De Paoli SH, Orecna M, et al. Characterization of procoagulant extracellular vesicles and platelet membrane disintegration in DMSO-cryopreserved platelets. *J Extracell Vesicles*. 2016;5(1):30422. doi:10.3402/jev.v5.30422

327. Berckmans RJ, Lacroix R, Hau CM, Sturk A, Nieuwland R. Extracellular vesicles and coagulation in blood from healthy humans revisited. *J Extracell Vesicles*. 2019;8(1):1688936. doi:10.1080/20013078.2019.1688936

328. Cardigan R, Sutherland J, Wadhwa M, Dilger P, Thorpe R. The influence of platelet additive solutions on cytokine levels and complement activation in platelet concentrates during storage. *Vox Sang*. 2003;84(1):28-35. doi:10.1046/j.1423-0410.2003.00257.x

329. Morikawa M, Derynck R, Miyazono K. TGF-β and the TGF-β Family: Context-Dependent Roles in Cell and Tissue Physiology. *Cold Spring Harb Perspect Biol*. 2016;8(5):a021873. doi:10.1101/cshperspect.a021873

330. Jaime-Pérez JC, Vázquez-Hernández KE, Jiménez-Castillo RA, Fernández LT, Salazar-Riojas R, Gómez-Almaguer D. Platelet Survival in Hematology Patients Assessed by the Corrected Count Increment and Other Formulas. *Am J Clin Pathol*. 2018;150(3):267-272. doi:10.1093/ajcp/aqy052

331. Davis KB, Slichter SJ, Corash L. Corrected count increment and percent platelet recovery as measures of posttransfusion platelet response: problems and a solution. *Transfusion (Paris)*. 1999;39(6):586-592. doi:10.1046/j.1537-2995.1999.39060586.x

332. Napolitano M, Mancuso S, Lo Coco L, et al. Buffy coat-derived platelets cryopreserved using a new method: Results from in vitro studies. *Transfus Apher Sci*. 2018;57(4):578-581. doi:10.1016/j.transci.2018.07.020

333. Vadhan-Raj S, Kavanagh JJ, Freedman RS, et al. Safety and efficacy of transfusions of autologous cryopreserved platelets derived from recombinant human thrombopoietin to support chemotherapy-associated severe thrombocytopenia: a randomised cross-over study. *The Lancet*. 2002;359(9324):2145-2152. doi:10.1016/S0140-6736(02)09090-6

334. Khuri SF, Healey N, MacGregor H, et al. Comparison of the effects of transfusions of cryopreserved and liquid-preserved platelets on hemostasis and blood loss after cardiopulmonary bypass. *J Thorac Cardiovasc Surg*. 1999;117(1):172-184. doi:10.1016/S0022-5223(99)70483-6

335. Reade MC, Marks DC, Bellomo R, et al. A randomized, controlled pilot clinical trial of cryopreserved platelets for perioperative surgical bleeding: the CLIP-I trial *(Editorial, p. 2759)*. *Transfusion (Paris)*. 2019;59(9):2794-2804. doi:10.1111/trf.15423

336. Zhang Y, Wang ZL, Deng ZP, Wang ZL, Song F, Zhu LL. Emerging Delivery Strategies of Platelet-Rich Plasma with Hydrogels for Wound Healing. Baldino L, ed. *Adv Polym Technol*. 2022;2022:1-11. doi:10.1155/2022/5446291

337. Oh JH, Kim W, Park KU, Roh YH. Comparison of the Cellular Composition and Cytokine-Release Kinetics of Various Platelet-Rich Plasma Preparations. *Am J Sports Med*. 2015;43(12):3062-3070. doi:10.1177/0363546515608481

338. Su R, Sun L, Ding YF, et al. In vitro studies on the effects of cryopreserved platelet-rich plasma on cells related to wound healing. *Platelets*. 2024;35(1):2347331. doi:10.1080/09537104.2024.2347331

339. Yang HS, Shin J, Bhang SH, et al. Enhanced skin wound healing by a sustained release of growth factors contained in platelet-rich plasma. *Exp Mol Med*. 2011;43(11):622. doi:10.3858/emm.2011.43.11.070

340. Narauskaitė D, Vydmantaitė G, Rusteikaitė J, et al. Extracellular Vesicles in Skin Wound Healing. *Pharmaceuticals*. 2021;14(8):811. doi:10.3390/ph14080811

341. Nash J, Davies A, Saunders CV, George CE, Williams JO, James PE. Quantitative increases of extracellular vesicles in prolonged cold storage of platelets increases the potential to enhance fibrin clot formation. *Transfus Med*. 2023;33(6):467-477. doi:10.1111/tme.12989

342. Rohani MG. Matrix remodeling by MMPs during wound repair.

343. Shin MK, Lee JW, Kim YI, Kim YO, Seok H, Kim NI. The effects of platelet-rich clot releasate on the expression of MMP-1 and type I collagen in human adult dermal fibroblasts: PRP is a stronger MMP-1 stimulator. *Mol Biol Rep*. 2014;41(1):3-8. doi:10.1007/s11033-013-2718-9

344. Fujisaki H, Futaki S, Yamada M, et al. Respective optimal calcium concentrations for proliferation on type I collagen fibrils in two keratinocyte line cells, HaCaT and FEPE1L-8. *Regen Ther*. 2018;8:73-79. doi:10.1016/j.reth.2018.04.001

345. Paganelli A, Contu L, Condorelli A, et al. Platelet-Rich Plasma (PRP) and Adipose-Derived Stem Cell (ADSC) Therapy in the Treatment of Genital Lichen Sclerosus: A Comprehensive Review. *Int J Mol Sci*. 2023;24(22):16107. doi:10.3390/ijms242216107

346. Chimen M, Evryviadou A, Box CL, et al. Appropriation of GPIbα from platelet-derived extracellular vesicles supports monocyte recruitment in systemic inflammation. *Haematologica*. 2020;105(5):1248-1261. doi:10.3324/haematol.2018.215145

347. Buntsma NC, Gąsecka A, Roos YBWEM, Van Leeuwen TG, Van Der Pol E, Nieuwland R. EDTA stabilizes the concentration of platelet-derived extracellular vesicles during blood collection and handling. *Platelets*. 2022;33(5):764-771. doi:10.1080/09537104.2021.1991569

348. Weiss R, Gröger M, Rauscher S, et al. Differential Interaction of Platelet-Derived Extracellular Vesicles with Leukocyte Subsets in Human Whole Blood. *Sci Rep*. 2018;8(1):6598. doi:10.1038/s41598-018-25047-x

349. Shantsila E, Montoro-Garcia S, Lip GYH. Monocytes circulate in constant reversible interaction with platelets in a [Ca2+]-dependent manner. *Platelets*. 2014;25(3):197-201. doi:10.3109/09537104.2013.784248